# On the Multiplicity of Solutions of Boundary-Layer Flows due to Stretching/Shrinking Surfaces



By:

Ghulam Dastgir Tabassum Reg. No. 44-FBAS/PHDMA/F14

Supervised By:

Dr. Ahmer Mehmood

Department of Mathematics and Statistics
Faculty of Basic and Applied Sciences
International Islamic University, Islamabad
Pakistan
2022

PhD 531.11 GHM

TH-26041

Soundary layer the distribution of the dindividual distribution of the distribution of the distribution of

# On the Multiplicity of Solutions of Boundary-Layer Flows due to Stretching/Shrinking Surfaces

By:

Ghulam Dastgir Tabassum Reg. No. 44-FBAS/PHDMA/F14

A DISSERTATION
SUBMITTED IN THE PARTIAL FULFILLMENT
OF THE REQUIREMENTS FOR THE DEGREE OF
DOCTOR OF PHILOSOPHY

IN
MATHEMATICS

Supervised By:

Dr. Ahmer Mehmood

Department of Mathematics and Statistics
Faculty of Basic and Applied Sciences
International Islamic University, Islamabad
Pakistan
2022

# **Author's Declaration**

I, Ghulam Dastgir Tabassum Reg. No. 44-FBAS/PHDMA/F14 hereby state that my Ph.D. thesis titled: On the Multiplicity of Solutions of Boundary-Layer Flows due to Stretching/Shrinking Surfaces is my own work and has not been submitted previously by me for taking any degree from this university, International Islamic University, Sector H-10, Islamabad, Pakistan or anywhere else in the country/world.

At any time if my statement is found to be incorrect even after my Graduation the university has the right to withdraw my Ph.D. degree.

Name of Student: (Ghulam Dastgir Tabassum)

Reg. No. 44-FBAS/PAIDMA/F14

Dated: 19/05/2022

Plagiarism Undertaking

I solemnly declare that research work presented in the thesis titled: On

Multiplicity of Solutions of Boundary-Layer Flows due to

Stretching/Shrinking Surfaces is solely my research work with no significant

contribution from any other person. Small contribution/help wherever taken has

been duly acknowledged and that complete thesis has been written by me.

I understand the zero tolerance policy of the HEC and University,

International Islamic University, Sector H-10, Islamabad, Pakistan towards

plagiarism. Therefore, I as an Author of the above titled thesis declare that no

portion of my thesis has been plagiarized and any material used as reference is

properly referred/cited.

I undertake that if I am found guilty of any formal plagiarism in the

above titled thesis even after award of Ph.D. degree, the university reserves the

rights to withdraw/revoke my Ph.D. degree and that HEC and the University

has the right to publish my name on the HEC/University Website on which

names of students are placed who submitted plagiarized thesis.

Student/Author Signature:

Name: (Ghulam Dastgir Tabassum)

## **Certificate of Approval**

This is to certify that the research work presented in this thesis, entitled: On the Multiplicity of Solutions of Boundary-Layer Flows due to Stretching/Shrinking Surfaces was conducted by Mr. Ghulam Dastgir Tabassum, Reg. No. 44-FBAS/PHDMA/F14 under the supervision of Dr. Ahmer Mehmood no part of this thesis has been submitted anywhere else for any other degree. This thesis is submitted to the Department of Mathematics & Statistics, FBAS, IIU, Islamabad in partial fulfillment of the requirements for the degree of Doctor of Philosophy in Mathematics, Department of Mathematics & Statistics, Faculty of Basic & Applied Science, International Islamic University, Sector H-10, Islamabad, Pakistan.

Student Name: Ghulam Dastgir Tabassum Signature:

### **Examination Committee:**

a) External Examiner 1:
Name/Designation/Office Address Signature:
Prof. Dr. Mazhar Hussain
Professor of Mathematics,
National University of Computer & Emerging Sciences,
Lahore, Pakistan.

b) External Examiner 2:
Name/Designation/Office Address) Signature:

Dr. Muhammad Asad Zaigham
Associate Professor

Department of Mathematics and Statistics, Riphah International

Department of Mathematics and Statistics, Riphah International University, I-14, Islamabad.

c) Internal Examiner:
Name/Designation/Office Address) Signature:
Prof. Dr. Muhammad Sajid T.I

Professor

Supervisor Name:

Dr. Ahmer Mehmood Signature:

<u>Name of HOD:</u>

Prof. Dr. Tariq Javed Signature:

Name of Dean:
Prof. Dr. Muhammad Irfan Khan Signature:

## **Dedicated**

To

My Tenderhearted Parents (late)

My Beloved Wife

My Lovely Daughters

Arfa Jahan

Zartashia Tabassum

&

Miral Tabassum

who are the source of my physical and spiritual motivations in the accomplishment of my PhD thesis.

## Acknowledgement

All the praises to the Allah Almighty Who is the Cherisher, the Most Gracious and the Most Merciful. I am grateful to Almighty Allah for enabling me to complete the research presented in this thesis. Indeed, it is only His unending mercy that the task has successfully accomplished. I feel honour to offer my humblest and sincerest thanks to the Last Holy Prophet Hazrat Muhammad (\*) who is forever a torch of guidance and knowledge for humanity because he was designated as City of Knowledge.

I express my humble gratitude to my kind nature and devoted supervisor Dr. Ahmer Mehmood for his valuable guidance and assistance to complete this task. Definitely, his sincere efforts, motivations, painstaking attitude and valuable contributions are served as major part in the completion of my thesis. He is one of the best teachers who has strong grip in his research-field, and always remains involve with his research students till the completion of their tasks.

I am extremely thankful to Prof. Dr. Nasir Ali, Chairman, Department of Mathematics and Statistics (IIUI) for his motivation and administrative support. I express my sincere thanks to external examiners Prof. Dr. Muhammad Mazhar Hussain and Dr. Muhammad Asad Zaigham for valuable comments and encouragement.

I am grateful to the faculty members and staff of Mathematics Department (IIUI) especially Prof. Dr. Muhammad Sajid (T.I) and Prof. Dr. Tahir Mehmood for their cooperation and moral support. I desire to extend the acknowledgement to my seniors Dr. Muhammad Saleem Iqbal and Dr. Muhammad Usman for their help and cooperation.

I would like to express my thanks to all my friends Dr. Sajid Khan, Mr. Babar Shah and Mr. Muhammad Usman Javed for their encouragement and moral support. Special thanks to Mr. Iqrar Raza, and Mr. Muhammad Awais, for their extraordinary support in all affairs throughout my research work.

In the end, I am extremely grateful to my wife, brothers, sisters and my well-wishers for their prayers and motivations. The completion of my education was not possible without their prayers and supports. I am also thankful to my little princesses Arfa Jahan, Zartashia Tabassum and Miral Tabassum for their innocent love and sacrifices as well as sincere prayers.

#### **Preface**

Among the diverse class of the self-similar boundary-layer flows, the flows due to stretching/shrinking surfaces have become more familiar on account of their vast practical applications that are frequently experienced in various industrial and engineering arenas. The flow phenomenon, caused by the motion of shrinking continuous surfaces has provided a great deal of work to the researchers to explore its various hidden aspects, particularly the existence of non-unique solution. A lot of attempts have been materialized to figure out the multiple solutions under different situations and impressive conclusions have been drawn regarding the physical richness of these flows. A thorough analysis of such kind of findings reveals that "non-uniqueness of solution"; "physical richness"; and "more non-linear phenomenon" are unanimously accepted integral features of the shrinking surface flows. Moreover, some baseless facts such as the nonexistence of solution; and necessity of sufficient wall suction for the existence of solution have also been attributed to these flows. Unfortunately, the above mentioned facts are not particular to a group of studies rather they have been established as widely admitted truths about the shrinking surface flows. This can immediately be verified from the recent literature on this topic. On the other hand the stretching surface flows are treated as an infertile topic with regard to the above mentioned "important" facts. However, the reality is quite opposite because the existing facts about the shrinking surface flows have not been drawn due to a correct analysis. Infact, it is the retarded nature of the flow that provides the opportunity of the appearance of non-unique solution. Accidently, the first ever study on the shrinking surface flows, was conducted by considering a retarded shrinking wall velocity. Consequently, the absence of any solution and the occurrence of

non-unique solution due to the provision of sufficient wall suction was an ultimate. In actual, this was not a specialty or uniqueness of the shrinking surface flows, rather an already observed and understood fact that a retarded boundary-layer is vulnerable of the occurrence of non-unique solution. But, unfortunately, the findings of this first study were assumed to be valid to all shrinking surface flows. Interestingly, the involved authors always considered the retarded shrinking wall velocities and the accelerated stretching wall velocities in their studies because of which they ever obtained a non-unique solution for the shrinking surfaces while a unique solution for the stretching surfaces. Unfortunately, the stretching/shrinking surface flows have rarely been investigated in complete with regard to their accelerated/decelerated nature. On behalf of the authentic outcomes of current study, it is humbly argued that the multiplicity is not confined to the family of shrinking surface flows only but the similar kind of outcomes can also be obtained for the stretching surface flows, equally.

The present thesis is presented to elaborate the correct and true understanding of the multiple/dual nature of solution that has been observed during the analysis of self-similar boundary-layer flows caused by the stretching/shrinking surfaces. In the presence of a bulk of confusing literature regarding the existence of non-unique solution, the currents efforts to present the real causes behind the existence of non-unique solution is like a hard neck to crack. Chapter 1 covers the historical developments of the subject, relevant literature, and essential description of the basic terminology for the better understanding of the readers. Since, now it has become a crystal clear reality that the duality of solution can be sighted for stretching continuous surfaces too and the non-uniqueness of solution cannot be attributed to shrinking surfaces, only. In this context

Chapter 2 is devoted to present the non-uniqueness of solution steady/unsteady viscous flow caused by a flat stretching sheet. Valuable outcomes have been reported regarding the presence of non-unique solution. The existence of dual solutions for steady as well as for unsteady situations is shown to happen in the retarded flow situations while in the accelerated flow the solution is observed to be unique. Indeed, the outcomes reported in Chapter 2 have countered the admitted myths regarding the existence of non-unique solutions. The contents of this chapter are under consideration for publication. It is a reality that the shrinking surface flows have enjoyed a unique popularity due to the existence of non-uniqueness of solution, though erroneously, linked to them. The reality is that, in this case too, the existence of non-unique solution is not associated to the shrinking nature of the wall velocity; instead the duality of solution in a shrinking surface flow is observed only when the decelerated shrinking wall velocity is considered. Therefore, Chapter 3 of this dissertation aims to present the true facts regarding the occurrence of non-unique solution in steady/unsteady shrinking sheet flow. It is explained that the duality of solution in both, the steady and unsteady, flow situations is strictly associated with the retarded nature of the shrinking wall velocity. The contents presented in this chapter have been published in International Journal of Nonlinear Sciences and Numerical Simulation, in 2020. In previous two chapters i.e., Ch. 2 and Ch. 3 the planner cases of stretching/shrinking surfaces have been considered. The axisymmetric flow situations due to the stretching/shrinking surfaces have been considered in next four Chapters.

Particular to the axisymmetric case of stretching/shrinking cylinder important results have been reported in the next couple of chapters. Since, the transverse curvature

is an additional factor attached with the axisymmetric surfaces of cylindrical shape. It's important and interesting role regarding the existence of duality of solution, not only in the shrinking cylinder case but also in the stretching cylinder case, has been explored in detail which are novel findings of its own nature. For this purpose, steady/unsteady flow situations due to stretching cylinder are investigated for the possibility of multiple solutions in Chapter 4. The steady flow due to a stretching cylinder is examined by considering the power-law form of stretching wall velocity and the dual solutions are captured not only for the suction/injection effects but also in the absence of any of these. Such types of findings are actually due to the presence of surface transverse curvature and are a consequence of the supportive role of transverse curvature in the retarded flow situations. The flow situation induced by the unsteady stretching cylinder is studied for a linearly varying wall velocity, wherein the similar type of results, as in the case of steady stretching cylinder, are noticed for a retarded flow situation. The results figured out for unsteady stretching cylinder have been published in Journal of Applied Mechanics and Technical Physics, in 2020, whereas the outcomes reported for steady case of stretching cylinder are in the review process for possible publication. Steady and unsteady cases of shrinking cylinder flow have also been considered to analyze the duality of solution. In this case too, a power-law form (of shrinking wall velocity) has been considered in the steady case. The shrinking wall velocity in the unsteady case has been considered of linear nature. It is figured out that the non-uniqueness of solution is observed for the retarded wall velocity whereas a unique solution is observed for the accelerated case of shrinking cylinder. The results of unsteady shrinking cylinder flow have been published

in European Journal of Mechanics / B Fluids, in 2020, while the outcomes regarding steady shrinking cylinder flow are under review for possible publication.

Another interesting axisymmetric flow situation occurs on a flat circular disk of infinite radius. In this regard, the existing literature is mostly comprised of the study of rotating disk boundary-layer whereas the non-rotating features have hardly been investigated and the existence of dual solutions is rarely reported. Chapter 6 consists of the analysis of steady/unsteady flow phenomenon stimulated by the stretching disk surface, wherein the duality of solution is scrutinized successfully. The outcomes, traced out for a stretching disk flow, are under consideration for possible publication. The nonrotating disk flow is further extended towards the shrinking disk flow, wherein the almost similar information is noticed as prescribed in the case of stretching disk flow. It is important to reiterate that the shrinking disk flow is not observed any interesting than the stretching disk flow. In both situations the duality of solution is simply associated to the retarded nature of the stretching/shrinking wall velocity. The results figured out for the shrinking disk flow are reported in Chapter 7 and are under consideration for possible publication. To present an overall conclusion of the whole dissertation. Chapter 8 is included at the end of this dissertation. The conclusions drawn are supposed to be extremely helpful for the exploration of the other hidden aspects of stretching/shrinking surface flows regarding the existence of duality of solution with regard to the other various physical ingredients.

# Contents

Chapter 1	Introduction and preliminaries	1	
1.1	Overview on history		
1.2	Preliminaries	14	
	1.2.1 Fluid Mechanics	14	
	1.2.2 Fluid	16	
	1.2.3 Flow	17	
	1.2.4 Boundary-layer theory	17	
	1.2.5 Self-similar flows	20	
	1.2.6 Reynolds number	20	
	1.2.7 Skin-friction coefficient	20	
	1.2.8 Multiplicity of solution	21	
1.3	Objectives	21	
1.4	Governing equations	23	
	1.4.1 Continuity equation	24	
	1.4.2 Momentum equation	24	
1.5	Solution methodology2		
Chapter 2	Duality of solution for a stretching sheet flow	27	
2.1	Steady boundary-layer flow due to a stretching sheet	27	
	2.1.1 Mathematical formulation	28	
	2.1.2 Numerical solution	29	
	2.1.3 Results and discussion	32	

2.2	Unsteady boundary-layer flow due to a stretching sheet	32		
	2.2.1 Mathematical formulation	33		
	2.2.2 Numerical solution	35		
	2.2.3 Results and discussion	40		
2.3	Conclusion			
Chapter 3	Duality of solution for a shrinking sheet flow42			
3.1	Steady boundary-layer flow due to a shrinking sheet	43		
	3.1.1 Mathematical formulation	43		
	3.1.2 Numerical solution	45		
	3.1.3 Results and discussion	47		
3.2	Unsteady boundary-layer flow due to a shrinking sheet	48		
	3.2.1 Mathematical formulation	49		
	3.2.2 Numerical solution	51		
	3.2.3 Results and discussion	56		
3.3	Conclusion	57		
Chapter 4	Axisymmetric flow due to a non-linearly	stretching		
	cylinder: non-uniqueness of solution	59		
4.1	Steady boundary-layer flow past a stretching cylinder	60		
	4.1.1 Mathematical formulation	61		
	4.1.2 Numerical solution	64		
	4.1.3 Results and discussion	74		
4.2	Unsteady boundary-layer flow past a stretching cylinder	77		

	4.2.1	Mathematical formulation	77
	4.2.2	Numerical solution	80
	4.2.3	Results and discussion	83
4.3	Concl	usion	85
Chapter 5	Exist	tence of multiple solutions for a shrinking cylinder	: flow
			87
5.1	Steady	y boundary-layer flow over a shrinking cylinder	87
	5.1.1	Mathematical formulation	88
	5.1.2	Results and discussion	98
5.2	Unste	ady boundary-layer flow over a shrinking cylinder	100
	5.2.1	Mathematical formulation	101
	5.2.2	Results and discussion	107
5.3	Conci	usion	110
Chapter 6	Duali	ity of solution for a stretching disk flow	112
6.1	Steady	y boundary-layer flow due to a stretching disk	112
	6.1.1	Statement of the problem	113
	6.1.2	Duality of solution	116
6.2	Unstea	ady boundary-layer flow due to a stretching disk	117
	6.2.1	Mathematical formulation	118
	6.2.2	Numerical solution	120
	6.2.3	Results and discussion	124
6.3	Conch	usion	125

Chapter 7	Dual	ity of solution for a shrinking disk flow	127
7.1	Steady	y boundary-layer flow due to a shrinking disk	128
	7.1.1	Statement of the problem	128
	7.1.2	Duality of solution	131
7.2	Unstea	ady boundary-layer flow due to a shrinking disk	132
	7.2.1	Mathematical formulation	132
	7.2.2	Results and discussion	140
7.3	Concl	usion	143
Chapter 8	Conc	lusions	144
References			150

## Chapter 1

## Introduction and preliminaries

This chapter contains an overview aimed to introduce the readers with the developments carried out in the field of boundary-layer flows for Newtonian fluids stimulated by stretching/shrinking continuous surfaces. The literature incorporated in this research is related to the viscous fluids flows and the existence of multiple solutions therein. This chapter consists of two parts: first part includes the introductory information of the topic along with the historical background and developments, and in the second part some fundamental knowledge closely related to the presented research is gathered for the convenience of the reader.

### 1.1 Overview on history

The practical applications of fluid mechanics are witnessed by the human history from the existence of human life on the planet. The fluid mechanics started its journey from fulfilling the sanitary/drinking requirements of the inhabitants of various communities and now it became an integral part of the science & technology which deals with engineering, industry, aviation, space exploration, metallurgy and lot of exciting applications yet to be explored. Initially, most of the applications of fluid mechanics were solely related to practical purposes, such as distribution system for the irrigation of crops. For example, the ancient civilizations used to settle near the natural water reservoirs to fulfill their essential domestic needs. Indeed, knowingly/unknowingly, they went through with practical applications of hydraulic engineering. The early civilizations also used water systems for the development of cities, for example, the Harappa people developed

city-wide drainage system to collect rainwater. Throughout its history, the fluid mechanics is known as a field that has been constantly advanced by every day. It is a field that has been reached the point of scientific maturity, now. It is reality that most of its fundamentals are clearly understood, which made it a vital component of many engineering curricula. In 250 BC, a first theoretical reasoning about the behavior of fluid flow was unveiled by Archimedes in the form of his famous buoyancy postulates. Before, the invention of the Newton s' law of viscosity, in 1687, all attempts were focused to investigate the inviscid/ideal character of fluid flows. In 1730, the Newton s' contribution was ornamented by Daniel Bernoulli who put forwarded the law of fluid motion which was further renovated by Leonhard Euler in 1755. The well-known "Navier-Stokes equations" were formulated by Navier and Stokes, independently in 1827 and 1845, respectively, by introducing the viscous term in the equation of motion. These equations have been proved most beneficial tool to investigate the characteristics of the viscous flows.

In 1904, Prandtl [1] not only classified the viscous flow into two categories, namely, the potential flow and the boundary-layer flow but also provided an opportunity to link the two diverse branches of fluid mechanics (i.e., theoretical hydrodynamics and hydraulics). The flows with zero vorticity (i.e., the fluid particles are non-rotating therein) are regarded as potential flows. These flows are comparatively simple than other flows due to uniform flow pattern of fluid particles. However, in the thin area near the solid surface, where the vorticity is not small, another type of flow is visualized which is termed as boundary-layer flow. Such kind of flow exist in the immediate vicinity of leading edge of the surface in contact, where the effects of viscosity are prominent and

the fluid tends to cling to the surface. Definitely, the idea of the boundary-layer can be regarded as a ready reference to scrutinize the behavior of wall friction more precisely. His [1] theoretical contributions motivated the scientists to examine the characteristics of viscous flows in context of boundary-layer phenomenon. Indeed, from micro to macro level developments are bestowed by the glorious information presented by Prandtl. The various flow situations, within a boundary-layer in case of a flat-plate, have been studied by a number of authors. The list of contributors is sufficiently long however the most valuable contributions have been made by Goldstein [2], Batchelor [3], and Schlichting [4]. Soon after the appearance of boundary-layer awareness, Blasius [5], for the first time. analyzed the boundary-layer flow phenomenon over a flat-plate. The author [5] studied the two-dimensional steady flow within a boundary-layer formed at a semi-infinite body and such type of flow was regarded as Blasius flow. Later on, theoretical investigations under certain situations were carried out by the various authors [6-9], while Burgers [10] rectified the Blasius flow experimentally. In 1931, Falkner and Scan [11] investigated steady two-dimensional boundary-layer flow over a wedge. Infact, the authors [11] generalized the Blasius [5] flow, by taking power-law form of potential velocity, for the situation when the plates are not parallel to the flow. The authors of [1] & [5] were concentrated on a flow past a stationary boundary.

In 1960, Sakiadis [12-13] recognized the character of boundary-layer flow over a moving continuous flat plate whose velocity was considered as uniform. Afterwards, the boundary-layer flow of viscous fluid over a continuous flat-surface moving with constant velocity is regarded as Sakiadis' flow. Later, Tsou et al. [14] provided experimental justification of the findings of Sakiadis. Because of tremendous applications in the span

of engineering and industrial processes, the study of two-dimensional boundary-layer flow stimulated by stretching surfaces has become blooming topic for the researchers since the contributions presented by the Blasius and Sakiadis. It is a matter of interest that Blasius [5] considered the circumstances when fluid is moving over a stationary plate while the Sakiadis [12-13] chose the vice-versa aspects as taken by the author [5].

With the passage of time, more and more developments have been observed in engineering and industrial disciplines which enhanced the need to investigate the Sakiadis' flow under some other valuable aspects. In 1970, Crane came forward and investigated the Sakiadis' flow under the influence of variable linear wall velocity. Crane [15] excogitated the two-dimensional steady viscous flow originated by continuous stretching sheet moving with a variable linear wall velocity and also succeeded to explore a closed-form solution. Due to this marvelous achievement, Crane is considered as the pioneer of stretching sheet flow. A large numbers of well-known investigators inspired by the fabulous contribution of Crane [15] devoted their efforts to analyze the stretching sheet flow under the influence of different types of velocities and boundary-conditions. For instance, considerable efforts were made by the renowned authors who sort out the fluid flow phenomenon stimulated by the stretching surface for non-linear and power-law wall velocities under the influences of various kinds of physical parameters like suction/injection, porosity, and heat transfer etc. The effects of heat and mass transfer, in the presence of suction/blowing, on the stretching sheet has been analyzed by Gupta and Gupta [16]. In 1979, Chakrabarti [17] studied the hydromagnetic flow under the influence of heat transfer, over a stretching sheet. Later, in 1983, the work of Crane was extended by Banks [18] for power-law velocity where he found similarity solution of the

boundary-layer flow over a stretching wall, while, in 1999, exponential wall velocity was interrogated by Magyari and Keller [19], where the effects of heat and mass transfer were investigated by them. Similarly, the stretching surface flows also attracted number of investigators [20–26] who analyzed the effects of suction/injection along with heat transfer over boundary-layer flows and found a similarity solution by using numerical/analytical techniques. Afterwards, Crane's work was extended for the situation of three-dimensional flow by Wang [27] wherein he succeeded to sort out the exact similarity solution of the problem.

The studies cited above are related to the steady state viscous flows over continuous stretching surfaces. However, in daily life everyone has to undergo the circumstances when the flow becomes unsteady. It is a reality that the unsteady behavior of variety of fluid flows has gained significant importance due to their blooming practical importance. Although, normally a steady behavior is important during the investigations of fluid flow phenomenon, however, it is well experienced fact that unsteady state situations might also be of practical importance. That is, unsteadiness may be caused by self-induction of the object, inconsistent nature of the flow under consideration, and sometime an unsteady aspect is a prerequisite for particular devices to execute their functions. A detailed conversation, in this regard, can be consulted in valuable manuscript presented by McCroseky [28]. Moreover, to investigate the effects of unsteadiness, ample efforts were made by a number of well-known authors [29-39] who analyzed the unsteady stretching sheet flow phenomenon under the influence of various physical parameters.

The topic of self-similar flows has been proved to be more generative for highly spirited researchers who utilized their best abilities to investigate the boundary-layer flows stimulated by stretching surfaces. At the same time, there exists another significant class of self-similar flows which is now termed as shrinking surface flows. This class deals with the circumstances where the wall velocity is taken with opposite sign as chosen in the case of stretching surface flows. In this context, Miklavcic and Wang are also regarded as the pioneers of shrinking surface flows, who initially introduced the flow phenomenon stimulated by a shrinking sheet. In 2006, Miklaycic and Wang [40] considered a two-dimensional shrinking sheet flow with an interesting con1clusion of non-existence of solution. They reported that the existence of solution requires sufficient wall suction and that the solution is non-unique whenever it exists. Consequently, their idea of shrinking surface flow was immediately adopted by a number of above researchers. The fantasy as presented by Miklavcic and Wang provided a golden opportunity to the analysts who enthusiastically dealt with this innovative class of selfsimilar flows. Like the stretching sheet, this new-fangled also possessed a broader span wherein a lot of researchers contributed a huge literature. By getting inspired from the work [40], a large number of publications, addressing the effects of various physical parameters under different circumstances, have been furnished by well-known researchers and the similar efforts are still going on. To illustrate all the existing literature under one cover is like a long row to hoe, however, some valuable but most relevant findings can be seen in the references [41-48]. The study of Miklavcic and Wang [40] was related to steady state of shrinking sheet flow which was extended to unsteady scenario by Fang et al. [49]. During the analysis, the authors of [49] computed the dual

solutions for certain range of the involved parameters under the impact of heat transfer and also claimed that the flow caused by unsteady shrinking sheet is quite different from that of unsteady stretching sheet flow. The work of Fang et al. [49] was further studied by various authors for different aspects, for example, power-law fluid (Yacob et al. [50]). nanofluid flow (Rohni et al. [51]), stagnation point flow (Sualia et el. [52]), nanofluid flow using Buongiorno's model (Rohni et al. [53]), effects of slip and heat generation/absorption on MHD stagnation point flow (Nandy and Mahapatra [54]). Besides these, there are number of researcher papers available in literature that studied a shrinking surface flow and presented the duality of solution as an ultimate outcome. Recently, Mehmood and Usman [55] presented a comparative study regarding the existence of multiple solutions for stretching/shrinking surface flows and mathematically justified that the similar situations of duality of solution do also exist for the stretching surfaces as noticed in the shrinking surface flows. Further, the authors [55] made it clear that the fantasy of the existence of non-uniqueness of solution as well as exhibition of the non-linear phenomenon linked with the shrinking surface flows is perhaps beyond the reality.

Although, the steady/unsteady features of shrinking sheet flows are still charming and which are constantly magnetizing the students of self-similar flows that's why it is difficult to address all such publications herein. Further, it is worth noting that the most of the authors, who focused on the shrinking sheet flow, have concluded the non-uniqueness of the solution is a phenomenon totally opposite to the stretching surface flows. Infact, they extracted their conclusions due to the utilization of incorrect similarity transformations. An inspection of the existing literature on shrinking surface flows

reveals that neither the shrinking surface flows have been investigated completely; nor correctly. Although, there is a bulk of publications available on the account of steady/unsteady shrinking sheet flow and it is constantly increasing but neither the claims made by Miklaycic and Wang [40] present true picture nor the similarity transformations used by [40] and Fang et al. [49] are constructed correctly. Since, the findings of [40] & [49] have been adopted as a ready reference for any kind of study related to the shrinking surface flows, therefore, nobody dare to put a barrier therein because of the existence of well accepted and published volume of literature. Keeping in the view a well saying "hope is being able to see that there is a light despite all of the darkness (Desmond Tutu)", Mehmood devoted himself to scrutinize and reconcile the existing literature related to shrinking surface flows. Initially, he received no positive response from the journals and his arguments were treated as an unheard drum. It is a universally proven fact that the "truth always prevails" and the same happened here when Mehmood [56] derived his monograph namely, "Viscous flows: stretching and shrinking surface", wherein he unbosomed the facts in a comprehensive way. The author [56] analyzed the existing literature published in the domain of stretching/shrinking surfaces and not only pointed out the discrepancies existed in the literature but also presented a detailed and practical way-forward to rectify the ambiguities pertained in the literature. Mehmood [56] presented the correct similarity transformations for the shrinking surface flows, in detail. Moreover, he also discussed the existence/non-existence of the stretching/shrinking surface flows. This was not only the Mehmood [56] but Paullet and Previte [57] also reported that the flow phenomenon caused by the stretching sheet admits an uncountable number of solutions for the case of nonlinear (power-law) wall velocity, whenever the

power-law exponent m takes the values  $-1/3 \le m \le 0$ ; no solution for m < -1/3; and unique solution for m > 0.

Similar to the planner case of the stretching/shrinking surface flows, their axisymmetric case has also shown great potential to attract the scientists in the field. The presence of immense literature, in the sphere of axially-symmetric flows is an obvious evidence of wider acceptance. In 1961, Sakiadis presented his marvelous theoretical work in the form of his precious elucidations [12] & [13]. The author [12-13] was concentrated to unveil the secrets of axially-symmetric scenario of viscous flow due to moving continuous surfaces. In the continuation of these studies Sakiadis [58] considered the steady state of boundary-layer flow over a continuous cylinder moving with uniform velocity for the first time. The work presented in [58], was extended for the case of nonuniform velocity by Crane [59] in 1975. The steady flow caused by a stretching cylinder, moving with uniform velocity, also proved itself a fertile area of research. In 1988, Wang [60] determined the effects of heat transfer on a flow over a stretching cylinder and adopted a shooting technique to obtain a numerical solution. He also reported an asymptotic solution and gave a comparison with the numerical results for a large Reynolds number. After that, Burde [61] figured out an exact solution for an incompressible fluid flow near an infinite circular cylinder stretching linearly in the axial direction. Ishak et al. [62] analyzed the effects of uniform suction/blowing on the stretching cylinder flow under the influence of heat transfer. Later, Ishak and Nazar [63], concentrated on a numerical solution of a laminar boundary-layer flow along a stretching cylinder and claimed that the similarity solution is only possible if the cylinder is stretched, in the axial direction, with linear velocity. Fang and Yao [64], investigated the

viscous flow caused by the stretching and torsional motion of steady cylinder and reported an analytical solution. Mukhopadhyay [65], investigated the effects of uniform magnetic field on an axisymmetric, steady boundary-layer viscous flow due to stretching cylinder, wherein he reported analytic solution and numerical solution. Although, a bulk of literature is available regarding stretching cylinder moving with linear velocity, however the non-linear case was still unaddressed. This deficiency was filled by Mehmood [56] in his recently published monograph, wherein he clarified that the crosssection of the cylinder should be taken of variable form for the non-linear nature of a stretching wall velocity (bearing the pattern of power-law or exponential form) in order to obtain a similarity solution. Moreover, it is worth noting fact that before the appearance of ceremonial work of the author [56], non-uniqueness of the solution had been considered for boundary-layer flows stimulated by shrinking surface flows only. After a deep analysis of the existing literature on viscous flows, Mehmood [56] also concluded that, like the shrinking surfaces, the stretching surfaces also bear the capacity for the occurrence of multiple solutions which was later proved by Mehmood and Usman in their recently published paper [55].

The study of boundary-layer flows invigorated by stretching surfaces has become a fascinating field because of its prodigious applications in industrial and engineering disciplines. For instance, spinning of filaments/stripes, manufacturing of glass, polymer/rubber extrusion, wire drawing, cable coating, fiber technology, hot rolling, paper production etc., are some worthwhile applications of the steady/unsteady flow phenomenon induced by stretching surfaces. That is why an abundant literature can be sighted regarding unsteady prospective of stretching cylinder flows. In this context a

marvelous work has been done by Fang et al. [67] during the analysis of unsteady viscous flows caused by stretching cylinder. The author [67] assumed a variable radius (varying with time) of the cylinder expanding in a stationary fluid and calculated an exact solution therein. With a quick glance over the existing literature, it is revealed that all efforts were made to analyze the unique/single solution for steady/unsteady stretching cylinders. The reason behind this fact is that it is unanimously accepted by the researchers that the uniqueness of solution is confined to the stretching surface flows, only. Further, it is also a reality that, capturing multiple solutions is a too much tedious task which demands extraordinary concentration. However, being motivated from the findings presented in [56] and [55], we have succeeded to break the hard nut and ultimately reported multiple solutions for unsteady stretching cylinder which will be discussed in the coming sections of this thesis.

The boundary-layer flow, stimulated by the shrinking axisymmetric surfaces, is a continuation of the most appealing theme ascertained by Miklavcic and Wang [40], wherein they enlightened the possibility of non-uniqueness of the solution. There can be seen an abundance of practical applications of shrinking surface flows in the processes of manufacturing/refining/extrusion of artificial film, metallurgy, petroleum, plasma studies, etc. It is also a worth noting aspect that manipulation of rate of cooling plays a vital rule in the quality of final products. Keeping in view the explorations contained in the existing literature regarding planner shrinking surfaces, multiple solutions for viscous, incompressible self-similar flows caused by the axisymmetric surfaces have been analyzed by a lot of researchers. In this context, Lok and Pop [68] figured out triple solutions during the study of incompressible, viscous, stagnation point flow caused by a

steady shrinking cylinder. The authors [68] adopted a numerical technique to capture the solution for certain range of involved parameters. Interesting, features of unsteady viscous flow, with mass transfer, over a shrinking cylinder were studied by Zaimi et al. [69] where they reported dual solutions by the manipulation of suction and unsteadiness parameters. The outcomes presented in [69] were further scrutinized numerically, for nanofluid flow by choosing the Buongiorno's model, by Zaimi et al. [70] where they again reported multiple solutions. Misra and Singh [71] also observed the multiplicity of solution while studying the effects of various kinds of slip conditions on a viscous flow over a permeable shrinking cylinder. Similarly, shrinking cylinder flow was also investigated with the help of an analytic technique known as OHAM (optimal homotopy asymptotic method) by Marinca and Ene [72] and the duality of solution was reported. The laminar flow caused by a porous, stretching/shrinking cylinder under the influences of heat transfer, suction and partial slip parameters was examined by Abbas et al. [73]. wherein they observed dual solutions for shrinking case only. The boundary-layer flow due to an exponentially shrinking cylinder was analyzed by Najib et al. [74], where they also carried out a stability analysis (using byp4c solver) to rectify their results. Recently, Ali et al. [75] considered a stretching/shrinking cylinder of a non-uniform radius: however, they did not claim the duality of solution. To sort out the hidden aspects of shrinking cylinder, under the effects of various parameters, efforts are still going on (for instances see the references [76-78]). It is a matter of great interest that the authors who reported dual behavior of the solution for a shrinking cylinder, claimed that an adequate suction is a prerequisite for the existence of multiple solutions, which is, however, not true as per results reported in this thesis.

Although, continuous circular cylinder and disk belong to a family of axisymmetric objects but both have been studied separately due to the involvement of surface curvature in the case of cylindrical surfaces. It is due to the reason that the flow characteristics, within the boundary-layer, are primarily affected by the leading role of surface transverse curvature. Further, the cylindrical surfaces admit similarity solutions for both power-law and exponential wall velocities, but in the case of circular disk, similarity solutions are possible only for power-law form of the wall velocity. Furthermore, cylinder and disk surfaces also have different geometrical aspects. Therefore, it is assumed necessarily important to investigate the flow phenomenon stimulated by a disk separately. To explore the flow due to stretching/shrinking disk. motivations have been provided by Crane [59] due to his investigation of the boundarylayer flow for axisymmetric case. Keeping in view the outcomes of Wang's [60] research regarding three-dimensional stretching sheet flow, Fang [79] originated the study in respect of flow caused by a stretchable disk and reported an exact solution for it. Later, the work of [79] was extended by Hussain et al. [80] where they figured out a numerical solution of it. Although, the literature is quite rich regarding the rotating: stretching/shrinking disk flow, discussing the various aspects of physical parameters but the boundary-layer flow due to a stretching/shrinking disk only have rarely been investigated. However, in this study our primary objective is to investigate nonuniqueness of solution in a boundary-layer flow stimulated by a non-rotating stretching/shrinking disk.

From the above cited literature and the rest of the relevant published literature it is evident that the non-uniqueness of solution is generally believed to be a unique feature of shrinking surface flows. Moreover, the necessity of sufficient amount of wall suction for the existence of solution (surely non-unique) is also a well admitted fact. But we claim that the above mentioned facts are neither generally true nor particular to the shrinking surface flows. We claim that the non-uniqueness of solution can equally be observed in the stretching surface flows, also. Moreover, there exist situations when the non-uniqueness of solution can also be observed in the absence of any wall suction; or even in the presence of affordable wall injection. To prove these facts various flow situations (ranging from planner to the axisymmetric geometries) have been considered in the subsequent chapters. Finally, the overall conclusions regarding the occurrence of multiple solutions for the flows due to stretching/shrinking surfaces have been drawn in Chapter 8 of this dissertation.

#### 1.2 Preliminaries

This section contains a necessary description and basic information about the terminologies used in the subsequent chapters. It also addresses the fundamental laws, governing equations and the solution technique for the use of subsequent chapters.

#### 1.2.1 Fluid mechanics

It is a branch of science which has specific concern with the properties and behavior of fluids under the influence of some stress/force. The fluids, under question, may be at rest or moving with some velocity. The basic principles of fluid mechanics are involved in almost all the engineering disciplines and the list of fluid engineering applications is lengthened with every morning. It is a unique field of mechanics which encompasses a vast array of problems that may vary from micro to macro level. For example, flow of blood in the capillaries to the flow of water through canals is all studied

in the domain of fluid mechanics. All branches of engineering are benefited from fluid mechanics. Its principles are helpful to understand why airplanes are manufactured streamlined with smooth surfaces. Moreover, renewable energy, production of electrical energy form wind power, wind-pumps for water pumping, sails to propel ships, functioning of turbines, automobiles, airplanes, missiles, appropriate designing of modes of transportation, and construction of dams and canals etc., are all based on fluid mechanics principles. This subject is equally beneficent in medical sciences. The design of artificial hearts, blood substitutes, hearts-lung machines, MRI, breathing aids, and other such type of devices depends on the fundamental principles of fluid mechanics. Fluid mechanics is extremely helpful in weather forecasting mechanism. Recently, "sports" is also considered as a science. Scientific rules are used to develop equipments as well as sports kits. Athletes and swimmers use special types of kits to reduce the drag forces. Improved design of swimsuits is based on tests in a water flume and on computational fluid dynamics (CFD) analysis. The fabric has been modified, based on wind tunnel tests, to reduce drag based on the airflow direction. The new outfits also eliminate most of the fabric vibration (a major source of drag). For summer and winter sports, the facility of performing experimental and theoretical fluid dynamics analysis enables one to propose changes in the sports kits which result in improved outcomes by several percent. There are numerous interesting questions which can be answered by using relatively simple fluid mechanics ideas. Indeed, the fluid mechanics is a very important and practical subject.

#### **1.2.2** Fluid

Fluid is a substance that tends to deform or modify its shape continuously under the influence of some kind of stress. It does not matter that how small the magnitude of the applied stress would be. Both liquids and gases are regarded as fluids. One can also see that fluid has no fixed shape as it has the ability to mold itself according to the shape of vessels. Fluids can be classified, on the basis of viscosity, as ideal fluids and real fluids. A fluid for which viscosity is considered as zero is termed as ideal fluid and in a flow situation such type of fluids have no tendency to provide any resistance or the shearing force. Although, ideal fluids are not found in nature at all, however, under specific engineering applications some fluids retain almost negligible viscosity effects and considered are as ideal fluids. While all other fluids that possess non-zero viscosity and offer resistance during the fluid motion are known as real fluids. For comprehensive analysis, these fluids are further subdivided as Newtonian fluids and non-Newtonian fluids. The fluids that obey the Newton's law of viscosity (shear stress is directly and linearly proportional to rate of deformation) such as air, water, mineral oil, and gasoline, etc., are called the Newtonian fluids. On the other hand, all fluids that do not preserve the Newtonian's law of viscosity (in such fluids the shear stress is directly but non-linearly proportional to the rate of deformation) are considered in the domain of non-Newtonian fluids. Examples of non-Newtonian fluids are gel, shampoo, paste, polymer solutions etc. Newtonian fluids generally have simple molecular structures and low molecular weight while non-Newtonian fluids are compressed of complex mixtures.

#### 1.2.3 Flow

A fluid tends to prevent deformation, whenever external/internal stress is applied on it, however, normally remains incapable to avoid deformation. If such deformation exceeds beyond a certain limit then this phenomenon is termed as a flow. A flow can be categorized in many ways on the basis of different features, however, in context to the "confining boundaries" flow phenomenon can be marked as external flows (fluids flow outside/over a surface) and internal flows (fluids flow through confined spaces). A flow may also be classified in terms of its properties (i.e., velocity, pressure, density) and pattern attained during the course of motion. For example, steady flow (flow properties are time-independent), unsteady flow (flow properties are time-dependent), uniform flow (flow with constant velocity), non-uniform flow (flow with variable velocity), compressible flow (variable fluid density), incompressible flow (constant fluid density), rotational flow (fluid particles have some angular velocity), non-rotational flow (fluid particles don't have any angular velocity), laminar/streamlined flow (fluid flows in parallel layers), and turbulent flow (fluid flows randomly).

#### 1.2.4 Boundary-layer theory

The beginning of twentieth century will always remain innovative and remarkable in the prospective of fluid mechanics history. In August, 1904, a scientific meeting with title "Third International Congress of Mathematician" was held at Heidelberg, Germany. Ludwig Prandtl, a German Physicist, presented his idea "On the motion of fluid with very small viscosity" in his eight minutes of demonstration and proposed the notion of boundary-layer. This concept marked as epoch in fluid mechanics history by opening the

new way of understanding the motion of real fluids. No one had suggested like this before and even scientific community of that time did not follow this idea except Prandtl's students for almost two decades.

Although, the equations of motion for viscous fluids had been modeled in the first half of ninetieth century by Navier (1823) and Stokes (1845) and had attained the form now called Navier-Stokes equations. The exact solution of these equations was impossible to determine. No one has succeeded to solve the complete Navier-Stokes equations to date because of nonlinear terms appeared in their viscous parts. Stokes obtained the exact solutions of these equations by confining himself to some special cases where the nonlinear terms could be either negligibly small or identically vanishing. However this had not been the case in most of the problems dealt in practice. Therefore, there was a need to establish some ideas or approximations for solution. The simplest way was no doubt to ignore the fluid viscosity and this way led about nothing but the d'Alembert paradox which states "a solid body of any shape placed in a uniform stream experiences no resistance".

The mathematical difficulties to solve full Navier-Stokes equations made it compelling to disappear the non-linear terms. It was justified only for slow motion flows but this approximation was also adopted for faster flows. It was almost universally accepted about the concept of no-slip at the solid surface in the case of slow motion flows. However the opinion divided in the case of faster flows. Meanwhile, huge number times, efforts were devoted to constitute an empirical formula for the law of friction which could be acceptable for both slow as well as faster flows.

Prandl pointed out the behavior of the fluid of small viscosity at the surface of the solid boundary. He explained that variation in the fluid velocity takes place only from the corresponding value of irrotational flow to zero velocity due to no-slip when fluid flows almost near to the wall and all this happens within a thin layer adjacent to the wall of the solid boundary. Although the layer is thinner for small viscosity but the velocity gradients yield significant effects. This shows that viscous effects are prominent only inside the thin layer which is called the boundary layer. Outside of the boundary layer, the flow remains inviscid and irrotational, and its behavior can be described from Euler's equations of motion. Further, there is a most attractive class of laminar boundary-layer flows that is termed as self-similar flows. These flows have admissible solutions of the most valuable Navier-Stokes equations in unbounded domains. The small thickness of the boundary layer allows some assumptions for the Navier-Stokes equations within the boundary layer: the variation in the velocity along the solid wall is much smaller in comparison with its variation normal to the wall, and the variation in the pressure normal to the solid wall is much smaller in comparison with its variation along the wall.

Further, at the edge of the domain, the boundary conditions effects are supposed practically limited/local, while self-similar solution will be effective/authentic in most of the fluid domain. This class has the ability to convert partial differential equations to ordinary differential equations, smoothly and easily, by using suitable similarity transformations. It facilitates the investigators to greatly/completely simplify the governing equations in the form of a single nonlinear one-dimensional pdes (or odes for steady flow phenomena) and, without some kind of approximation, exact solutions of the Navier-Stokes equations can be obtained. Moreover, these flows are extremely helpful

for complete understanding of flow mechanism in a prescribed boundary-layer. In fluid mechanics, exact or similarity solutions of the "Navier-Stokes equations" have significant practical as well as theoretical importance which bears great attractiveness for the researchers.

### 1.2.5 Self-similar flows

There is a most attractive class of laminar boundary-layer flows that is termed as self-similar flows. These flows have admissible solutions of the most valuable Navier-Stokes equations in unbounded domains.

### 1.2.6 Reynolds number

The Reynolds number (Re) is frequently used in fluid mechanics as it mainly characterizes the flow as laminar or turbulent. It is named after a British scientist Osborne Reynolds. This is a dimensionless number and determines the ratio of inertial forces to viscous forces, which can be written as:

$$Re = \frac{Inertial forces}{Viscous forces}.$$

$$= \frac{Ud}{v},$$
(1.1)

where, U is the reference velocity, d is the characteristics length, and  $\nu$  is viscosity.

### 1.2.7 Skin-friction coefficient

It provides a measure of friction and drag between a fluid and the surface of solid object moved through it. The skin-friction coefficient  $(C_f)$  increases with the square of wall velocity and is directly proportional to surface area contacted to the fluid. Mathematically, it can be interpret as:

$$C_f = \frac{\tau_w}{\frac{1}{2}\rho U^2},\tag{1.2}$$

where  $\tau_w$  is a shear stress,  $\rho$  denotes fluid density, and U denotes characteristic velocity.

# 1.2.8 Multiplicity of solutions

Since the last couple of decades, in the exploration of various aspects of selfsimilar flows, a significant prospective of solutions termed as "multiple solutions" inspired a huge number of enthusiastic scholars who have been continuously engaged to sort out it under different circumstances. This new-fangled of solutions received a noticeable prestige due to its mathematical aspects. Although in the existing literature it is frequently claimed that this branch of solution has no physical significance, however, to present a complete profile of the flow phenomenon, it really demands a due care to be investigated thoroughly. Particularly, for the situation of retarded flows, the flow velocity exhibits complex characteristics due to which uneven scenario may be observed, and consequently it boosts up the probability for the existence of multiple solutions. At the same time, it is also a matter of great concern that this new type of solution is normally seen to exist for specific range of the involved parameter(s), and after that a unique solution may be pertained. Further, there appear some circumstances where the flow phenomenon becomes more and more sensitive. To explore such situations it demands extra-ordinary attention and devotion. Therefore, to present a comprehensive picture of the flow phenomenon, definitely it is mandatory to touch all axes of the problem under consideration.

### 1.3 Objectives

The current study is devoted to investigate the reasons behind the non-uniqueness of solution of the self-similar boundary-layer flow phenomenon caused by

stretching/shrinking continuous surfaces. A bulk of literature is available which has explored the various aspects of boundary-layer flows regarding the existence of multiple solutions. Besides the available reasoning about the multiplicity of solution, there are some other facts which determine the true nature of non-unique solution. In this regard the efforts have been put into this matter and the outcomes of this research have been presented in this dissertation. Chapter 2 contains the study of steady/unsteady aspects of vicious flow stimulated by a flat stretching sheet, wherein interesting information is obtained in respect of existence of dual solutions. The flow phenomenon initiated by shrinking surfaces has become more popular due to the duality/multiplicity of solution supposed to be confined therein, only. Keeping in view this common perception, Chapter 3 is devoted to analyze the shrinking sheet (steady/unsteady) flow for the existence of dual solution in the presence of involved physical parameters. The outcomes of Chapter 3 have been published in International Journal of Nonlinear Sciences and Numerical Simulation, in 2020, [81]. It is extremely desirable that the findings of planner surfaces should be extended towards axisymmetric surfaces case. For this purpose, the true facts for the possible occurrence of dual solutions for steady/unsteady stretching cylinder have been captured and compiled in Chapter 4. The steady aspects are studied for power-law velocity while linear nature of wall velocity is taken to investigate the unsteady stretching cylinder. The multiple solutions that are figured out for unsteady flow due to a stretching cylinder have been published in Journal of Applied Mechanics and Technical Physics, in 2020, [82], while the results computed for steady stretching cylinder are under review for possible publication. The outcomes presented in Chapter 4 are further extended by taking shrinking wall velocity. Obviously, dual

solutions are captured therein for both steady and unsteady situations. The outcomes figured out regarding unsteady shrinking cylinder have been published in the European Journal of Mechanics / B Fluids, in 2020, [83], whereas the findings in respect of steady shrinking cylinder are in review process.

The axisymmetric surfaces also bear another important shape named as the disk shape. The disk surface, different from the cylindrical surface, involves no surface curvature effects due to which it possesses different flow phenomenon. In Chapter 6, we have focused to figure out the steady/unsteady character of stretching disk flow. The information gathered during the study is under consideration for possible publication. Further, Chapter 7 contains the investigations of steady/unsteady cases of shrinking disk flow for the investigation of the existence of duality of solution. During the investigation, dual solutions are sorted out and have been presented in this chapter. The contents of this chapter are also in review process for possible publication.

### 1.4 Governing equations

The fundamental laws (i.e., the law of conservation of mass and law of conservation of momentum) that define the mechanism of fluid flow are as usually termed as the governing equations. On the basis of these basic laws, governing equations are also known as the equation of continuity, and the equation of motion. Detailed derivation of these laws can be found in any good book concerning the dynamics of fluids, such as, Schlitching [4]. In this section their final and convenient forms have been given for the use of next chapters.

# 1.4.1 Continuity equation

The partial differential equation which is based upon the law of conservation of mass is termed as equation of continuity. Mathematically, in Cartesian coordinates, it has the following form:

$$\frac{\partial \rho}{\partial t} + \nabla \cdot \rho V = 0. \tag{1.3}$$

In case of incompressible fluid,  $\frac{\partial \rho}{\partial t} = 0$  and Eq. (1.3) takes a form:

$$\frac{\partial u}{\partial x} + \frac{\partial v}{\partial y} + \frac{\partial w}{\partial z} = 0. \tag{1.4}$$

Further, in cylindrical coordinates, the equation of continuity for incompressible flows resembles as:

$$\frac{1}{r}\frac{\partial(rv_r)}{\partial r} + \frac{1}{r}\frac{\partial v_{\theta}}{\partial \theta} + \frac{\partial v_z}{\partial z} = 0. \tag{1.5}$$

# 1.4.2 Momentum equation

The partial differential equation pertains the law of conservation of momentum (a direct consequence of Newton's third law of motion) is known as momentum equation.

Mathematically, it has three components which in Cartesian coordinates (without body forces) have the following form:

x – component:

$$\rho(\frac{\partial u}{\partial t} + u \frac{\partial u}{\partial x} + v \frac{\partial u}{\partial y} + v \frac{\partial u}{\partial z}) = -\frac{\partial p}{\partial x} + \mu(\frac{\partial^2 u}{\partial x^2} + \frac{\partial^2 u}{\partial y^2} + \frac{\partial^2 u}{\partial z^2}), \tag{1.6}$$

y - component:

$$\rho(\frac{\partial v}{\partial t} + u\frac{\partial v}{\partial x} + v\frac{\partial v}{\partial y} + v\frac{\partial v}{\partial x}) = -\frac{\partial p}{\partial y} + \mu(\frac{\partial^2 v}{\partial x^2} + \frac{\partial^2 v}{\partial y^2} + \frac{\partial^2 v}{\partial x^2}),\tag{1.7}$$

z - component:

$$\rho(\frac{\partial w}{\partial t} + u\frac{\partial w}{\partial x} + v\frac{\partial w}{\partial y} + v\frac{\partial w}{\partial z}) = -\frac{\partial p}{\partial z} + \mu(\frac{\partial^2 w}{\partial x^2} + \frac{\partial^2 w}{\partial y^2} + \frac{\partial^2 w}{\partial z^2}),\tag{1.8}$$

where (u, v, w) are the velocity components in Cartesian coordinates, and p denotes the pressure function.

Similarly in cylindrical coordinates, its three components are written as:

radial component:

$$\rho\left(\frac{\partial v_r}{\partial t} + v_r \frac{\partial v_r}{\partial r} + \frac{v_\theta}{r} \frac{\partial v_r}{\partial \theta} - \frac{v_{\theta}^2}{r} + v_z \frac{\partial v_r}{\partial z}\right) = -\frac{\partial p}{\partial r} + \mu\left(\frac{\partial^2 v_r}{\partial r^2} + \frac{1}{r} \frac{\partial v_r}{\partial r} - \frac{v_r}{r^2} + \frac{1}{r^2} \frac{\partial^2 v_r}{\partial \theta^2} - \frac{2}{r^2} \frac{\partial v_{\theta}}{\partial \theta} + \frac{\partial^2 v_r}{\partial z^2}\right),\tag{1.9}$$

circumferential component:

$$\rho\left(\frac{\partial v_{\theta}}{\partial t} + v_{r}\frac{\partial v_{\theta}}{\partial r} + \frac{v_{\theta}}{r}\frac{\partial v_{\theta}}{\partial \theta} + \frac{v_{r}v_{\theta}}{r} + v_{z}\frac{\partial v_{\theta}}{\partial z}\right) = -\frac{1}{r}\frac{\partial p}{\partial \theta} + \mu\left(\frac{\partial^{2}v_{\theta}}{\partial r^{2}} + \frac{1}{r}\frac{\partial v_{\theta}}{\partial r} - \frac{v_{\theta}}{r^{2}} + \frac{1}{r^{2}}\frac{\partial^{2}v_{\theta}}{\partial \theta^{2}} + \frac{2}{r^{2}}\frac{\partial v_{r}}{\partial \theta} + \frac{\partial^{2}v_{\theta}}{\partial z^{2}}\right),\tag{1.10}$$

axial component:

$$\rho\left(\frac{\partial v_z}{\partial t} + v_r \frac{\partial v_z}{\partial r} + \frac{v_\theta}{r} \frac{\partial v_z}{\partial \theta} + v_z \frac{\partial v_z}{\partial z}\right) = -\frac{\partial p}{\partial z} + \mu\left(\frac{\partial^2 v_z}{\partial r^2} + \frac{1}{r} \frac{\partial v_z}{\partial r} + \frac{1}{r^2} \frac{\partial^2 v_z}{\partial \theta^2} + \frac{\partial^2 v_z}{\partial z^2}\right)$$
(1.11)

where  $(v_r, v_\theta, v_z)$  denote the velocity components in cylindrical coordinates.

# 1.5 Solution methodology

During the current study, we have to deal with the self-similar boundary-layer viscous flows stimulated by stretching/shrinking continuous surfaces. Since, the resulting governing equations involve strong non-linearity and their exact solutions are usually impossible. The problems considered in this dissertation are of self-similar nature for which the governing partial differential equations are transformed to ordinary differential equations. Due to the development of high performance computing machines it has now became possible to integrate the complicated non-linear equations numerically with high degree of accuracy. The techniques are so compatible that the captured solutions are

usually considered as exact solutions and are known as "numerical exact solutions". To sort out the solutions of the derived self-similar equations of this thesis, numerical method, namely, the shooting method is utilized. The availability of high speed computing machines as well as the flavor of authentic softwares like MATLAB and MATHEMATICA are equally facilitating the researchers to solve the various problems involved in their research.

To obtain a numerical solution, the 4<sup>th</sup>-order RK shooting technique has been coded in most efficient computing software MATHEMATICA. As the pre-requisite of the said numerical method, we convert the governing higher order ordinary differential equation to a system of first order ordinary differential equations. For instance, we reduce the Eqs. (5.6)—(5.7) (which are obtained for self-similar boundary-layer flow induced by the steady shrinking cylinder) into the following form:

$$y_3 = \frac{yy_2 - my_1^2 - 2\kappa y_2}{1 + 2\kappa \eta}, \quad y_1(0) = 1, \quad y(0) = \frac{2 \cdot S}{m+1}, \quad y_1(\infty) = 0.$$
 (1.12)

Here, we take 
$$f(\eta) = y$$
,  $f'(\eta) = y_1$ ,  $f''(\eta) = y_2$  and  $f'''(\eta) = y_3$ .

Now, the shooting method is used to obtain the numerical solution of the systems similar to Eq. (1.12). With the help of this numerical technique, we were enabled to capture not only the first solution but also the second one, in very precise way with desired level of accuracy and authenticity. During the procedure of computing the solutions, it is obvious that the first solution can be sighted quite quickly, while to capture the second solution, time taking efforts with utmost devotions have to be made. It is a fact that the second solution is assured after several runs and experimentations.

# Chapter 2

# Duality of solution for a stretching sheet flow

In this chapter we consider the steady as well as unsteady character of the boundary-layer flow stimulated by a continuous stretching sheet. It is assumed that the sheet is stretching continuously in x — direction, with a variable velocity. The governing equations obtained for steady/unsteady cases are solved numerically by using the shooting method. During the current analysis, dual solutions are also captured for both cases. The current chapter has been divided into two major parts to consider steady and unsteady cases separately.

### 2.1 Steady boundary-layer flow due to a stretching sheet

In this section we consider a steady two-dimensional viscous flow due to a stretching sheet. This problem has already been considered by Mehmood and Usman [55] but it is included in this chapter for the sake of completion of the picture presented in this dissertation. Therefore, the work presented in this section should be considered as a review of the work published in [55].

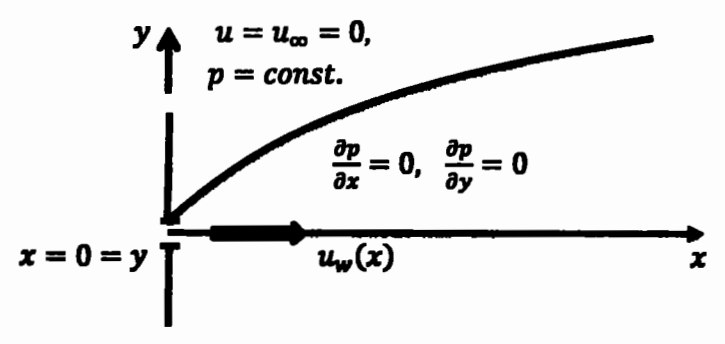


Fig. 2.1: Schematic of two-dimensional stretching surface flow and the associated coordinate system.

### 2.1.1 Mathematical formulation

Consider an incompressible, two-dimensional, steady, boundary-layer flow induced by a permeable stretching sheet in a viscous fluid. The fluid under consideration is supposed to be stationary. The sheet is issuing outward from the slit with a velocity  $u_w(x)$  in the x – direction. Further, beyond the vicinity of boundary-layer the velocity of fluid is zero, whereas pressure is regarded as constant. In view of above mentioned assumptions, the continuity equation (1.3) and the equation of motion (1.6) for the considered steady flow take the following forms:

$$\frac{\partial u}{\partial x} + \frac{\partial v}{\partial y} = 0, \tag{2.1}$$

$$u\frac{\partial u}{\partial x} + v\frac{\partial u}{\partial y} = v\frac{\partial^2 u}{\partial y^2},\tag{2.2}$$

$$u = u_w(x), v = v_w(x), at y = 0 u = 0, at y = \infty$$
 (2.3)

where, u and v are the velocity components which are taken along x – and y – axes, respectively, while v is termed as kinematic viscosity. Mehmood [56] reported that a similarity solution of the above system is possible if one chooses  $u_w(x) = ax^m$  (of power-law form) as reported by Banks [18], initially. Corresponding to this particular form of wall velocity let us introduce the similarity transformations

$$\eta = \sqrt{\frac{a}{v}} x^{\frac{m-1}{2}} y, \qquad u = a x^m f'(\eta), \qquad v = -\sqrt{av} x^{\frac{m-1}{2}} \left( \frac{m+1}{2} f + \frac{m-1}{2} \eta f' \right), \quad (2.4)$$

due to which Eq. (2.1) is satisfied identically and the Eqs. (2.2) and (2.3) are transformed to a form given by

$$f''' = mf'^2 - \frac{m+1}{2}ff'', \tag{2.5}$$

$$f'(0) = 1,$$
  $f(0) = -\frac{2S}{m+1},$   $f'(\infty) = 0,$  (2.6)

where, a > 0 is a constant stretching rate, m is a real number and is called the power-law index, and  $S = \frac{d}{\sqrt{av}}$  designates the wall suction/injection velocity. Positive values of S > 0 correspond to wall injection and the negative values of S < 0 represent the wall suction velocity. To ensure the self-similarity of the solution  $v_w(x)$  is chosen of the form  $v_w(x) = dx^{\frac{m-1}{2}}$ ; d being a constant.

### 2.1.2 Numerical solution

The numerical solution of the considered problem is obtained by using a reliable method termed as shooting method. During the current study well-known and frequently used mathematical computational software "MATHEMATICA" is adopted. The availability of such types of softwares made the numerical solutions as authentic as the exact solutions are. The method is testified for a number of problems, particularly results reported in the Table 6.1 of [56], for steady stretching sheet (both for power-law and exponential form of wall velocities), are recomputed and found in excellent agreement therein. The results figured out for the present investigation are referred in Table 2.1.

**Table 2.1:** A comparison with the results reported in Table 6.1 of [56], for f''(0) in the case of steady stretching sheet flow.

•	Mehmo	ood [56]	Present results		
m	Power-law	Exponential	Power-law	Exponential	
-1/3	0.0000		0.0000		
-1/5	-0.23426		-0.23426		
-1/10	-0.35026		-0.35026		
0.0	-0.44375		-0.44375		
1/10	-0.52353	-0.2870	-0.52353	-0.2870	
1/2	-0.77037	-0.6409	-0.77037	-0.6409	
1	-1.00000	-0.9064	-1.00000	-0.9064	
2	-1.34846	-1.2818	-1.34846	-1.2818	
5	-2.06894	-2.0267	-2.06894	-2.0267	
10	-2.89607	-2.8662	-2.89607	-2.8662	

**Table 2.2:** Some numerical values of the skin-friction coefficient at S=-3.

	Mehmood an	d Usman [55]	Present results		
m	1ª SoL	2 <sup>nd</sup> SoL	1ª Sol.	2 <sup>nd</sup> SoL	
-2	-2.5233	4.3224	-2.5233	4.3224	
-1.5	-2.6830	9.7166	-2.6830	9.7166	
-0.7	-2.9069	215.5061	2.9069	215.5061	
0.0	-3.0805		-3.0805		
1.5	-3.4052		-3.4052		
2	-3.5029		-3.5029		
2.5	-3.5964		-3.5964		

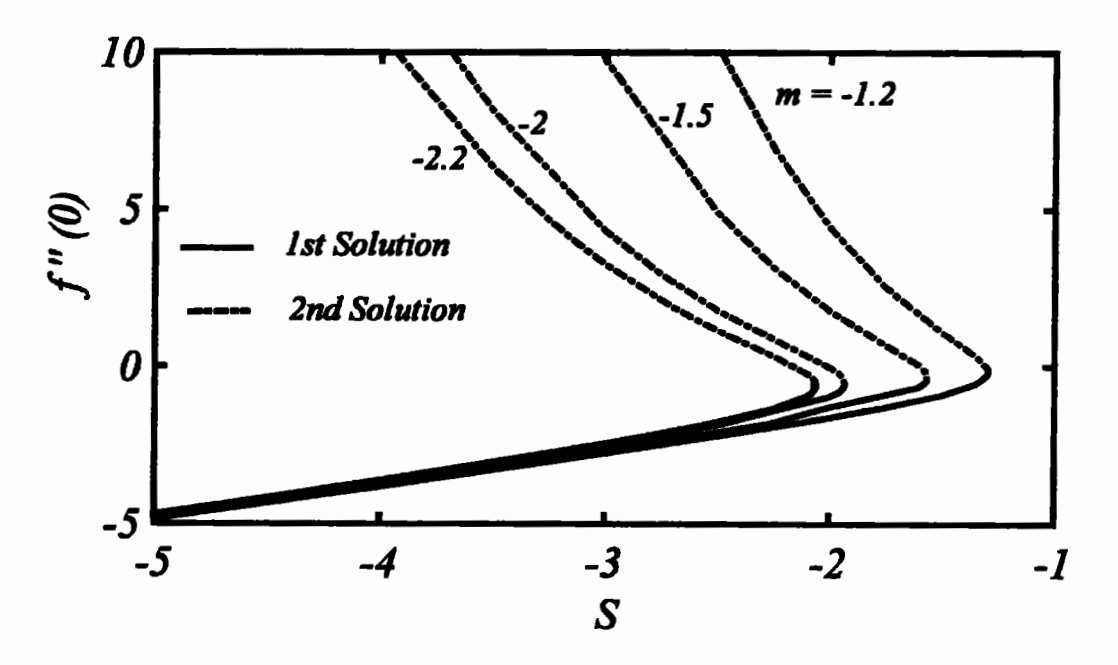


Fig. 2.2: Skin-friction coefficient of the stretching sheet flow plotted against S at different values of m.

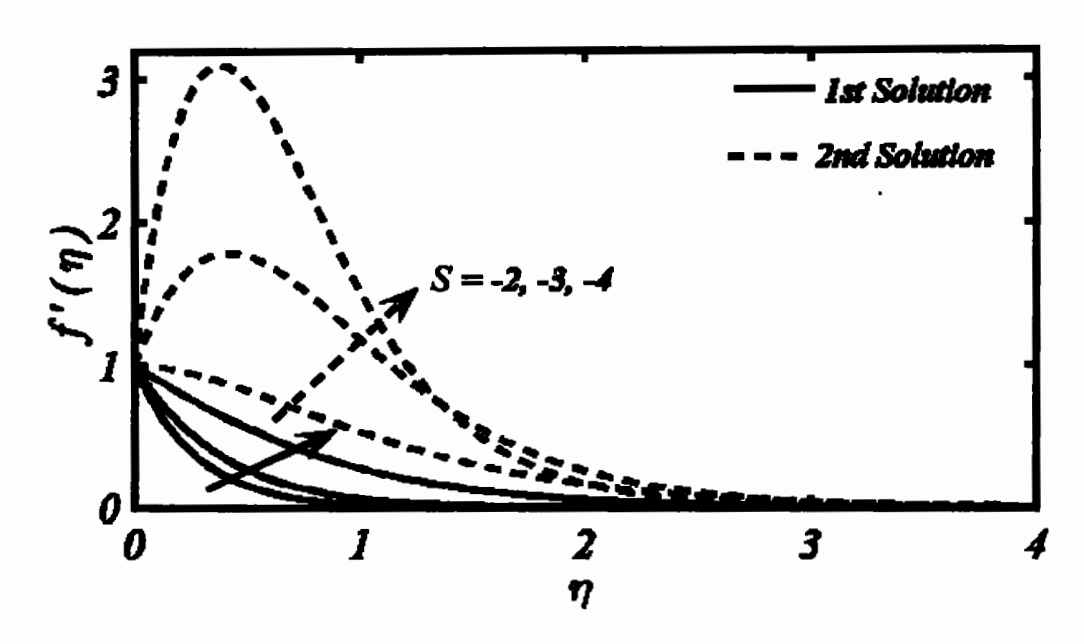


Fig. 2.3: Velocity profile of stretching sheet flow for different values of S, at m = -2.

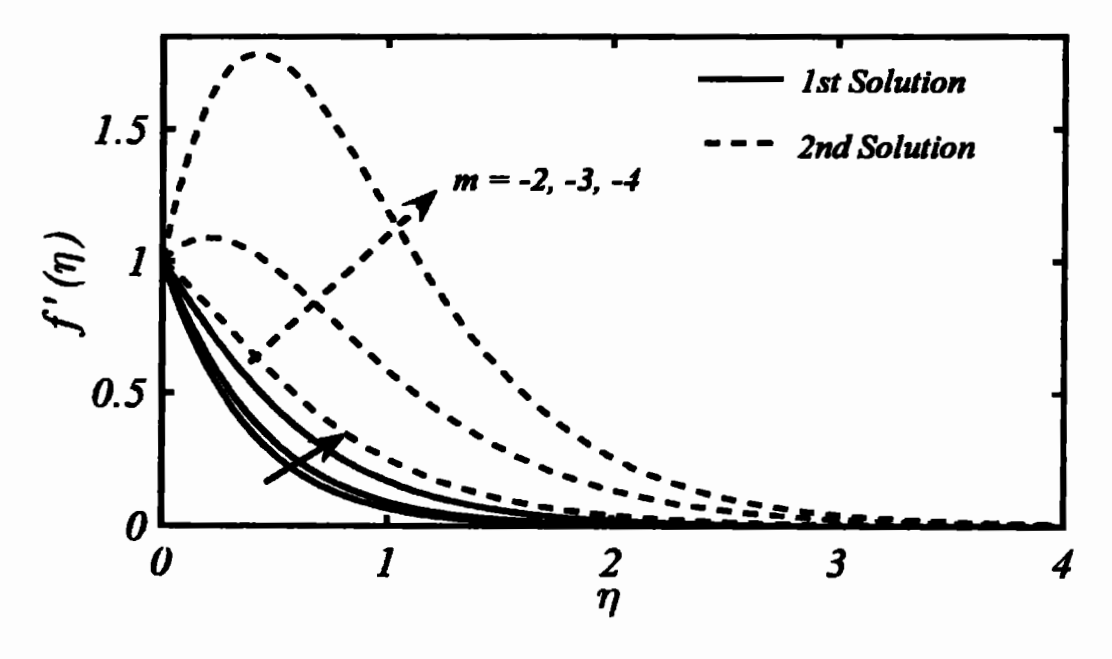


Fig. 2.4: Velocity profile of the stretching sheet flow at different values of the power-law index, m, at S = -3.0.

#### 2.1.3 Results and discussion

The self-similar system of equations (2.5)-(2.6) acquired for boundary-layer flow induced by a steady non-linearly stretching sheet is solved numerically. Since, during the present study our keen desire was to investigate the possibility of dual solution. Mehmood and Usman [55] also considered this problem for the same purpose. They reported the duality of solution in the stretching sheet flows, following a non-linear form of the wall velocity. They clearly explained the reasons for the existence of dual solution in this case. The duality of solution was captured for m < 0 which corresponds to the situation of retarded wall velocity. The duality of solution has been reported in Table 2.2 and Fig. 2.2, accordingly, while dual velocity profiles are portrayed in Figs. 2.3-2.4. For further information about this flow the reader is referred to follow [55].

# 2.2 Unsteady boundary-layer flow due to a stretching sheet

Similar to the steady case, the unsteady flow is also an important characteristic of the self-similar boundary-layer flow stimulated by a continuous moving surface. The unsteady nature of the flow depends upon various aspects. For, example, sometimes it may be originated by the object itself and sometimes it is developed because of inconsistent features of fluid under investigation. In this regard, an ample analysis is given by McCroseky [28] wherein the author made a critical survey of the unsteady fluid flows particularly involved in engineering and technology domain. A valuable material is available on the deak of unsteady boundary-layer flows. In this context, Surma et al. [29] extended the Wang's [27] work and examined the role of unsteadiness in the wall velocities during the study of stagnation point flow. The author [29] found a self-similar numerical solution for the involved problem. Later, Wang [30] investigated liquid film

flow phenomenon passed over an unsteady stretching surface and found an asymptotic as well as numerical solution therein. A pulse-like motion of the unsteady stretching surface was discussed by Smith [31] by considering the same geometry as taken by Wang [27], and reported an exact solution. Pop and Na [32] calculated perturbation solution for unsteady flow past a stretching sheet by taking the Shanks transformation. The effects of heat transfer were analyzed in an unsteady stretching surface flow by the authors [33-35]. Mehmood and Ali [36] investigated the unsteady boundary-layer flow caused by a flat plate which is set into motion impulsively with a constant velocity. The authors [36] figured out an analytic solution. The effects of porosity were also analyzed by Mehmood and Ali [37] during the study of unsteady boundary-layer flow caused by impulsively started moving plate. Heat transfer aspects on an unsteady stretching surface were studied by Tsai et al. [38]. Later, Mukhopadhyay [39] carried out a detailed investigation of unsteady flow mechanism on a porous stretching surface embedded in a porous medium. The current analysis is conducted to search out the existence of multiple solutions for fluid flow prospective induced by unsteady stretching sheet.

#### 2.2.1 Mathematical formulation

In this section we extended the steady case of continuous stretching sheet to unsteady scenario by assuming a flat sheet started impulsively at t=0. The difference between the current study and that presented in Sec. 2.2, is the spontaneous start of the sheet upon which the fluid flows. All other assumptions of the case of stretching sheet are supposed to be the same herein. The wall unsteady velocity, in the x – direction, is taken of the form  $u_w(x,t) = \frac{ax}{1-yt}$  to ensure the self-similarity of solution. The impulsive start of the stretching sheet has no effect on the continuity equation (2.1), however, requires an

extra term  $\frac{\partial u}{\partial t}$  on the left hand side of Eq. (2.2) and also modifies the auxiliary data (Eq. (2.3)) as presented below:

$$\frac{\partial u}{\partial t} + u \frac{\partial u}{\partial x} + v \frac{\partial u}{\partial y} = v \frac{\partial^2 u}{\partial y^2}, \qquad (2.7)$$

$$u(x, y, t = 0) = 0, \forall (x, y) u(x, y, t > 0) = u_w(x, t), v(x, y, t > 0) = v_w(x, t), at y = 0 u(x, y, t > 0) = 0, at y = \infty$$
 (2.8)

By consulting the self-similarity criterion, presented by Mehmood [54], the following similarity transformations, unanimously satisfying the continuity equation, are adopted to obtain the self-similar equations:

$$\eta = \sqrt{\frac{a}{\nu(1-\gamma t)}} y, \qquad u = \frac{ax}{1-\gamma t} f'(\eta), \qquad v = -\sqrt{\frac{av}{1-\gamma t}} f(\eta). \tag{2.9}$$

The utilization of Eq. (2.9) in Eqs. (2.7) and (2.8) enables one to reach the following set of equations:

$$f''' + ff'' - f'^2 - \beta \left( f' + \frac{\eta}{2} f'' \right) = 0, \tag{2.10}$$

$$f'(0) = 1, \quad f(0) = -S, \quad f'(\infty) = 0.$$
 (2.11)

Here,  $\beta = \frac{\gamma}{a}$  is a unsteadiness parameter corresponding to accelerated and decelerated cases according to  $\beta > 0$  and  $\beta < 0$ , respectively. By considering  $\beta = 0$ , the Eq. (2.10) reduces to Eq. (2.5), for m = 1, that is, the steady case of linearly stretching wall velocity is recovered. In order to ensure the self-similar solution the wall suction/injection velocity is chosen of the form  $v_w = \frac{d}{\sqrt{1-\gamma t}}$ , where d being a constant. Dimensionless form of d is given by  $S = \frac{d}{\sqrt{av}}$ : S > 0 correspond to wall injection while S < 0 correspond to wall suction velocity.

### 2.2.2 Numerical solution

The solution of the non-linear self-similar ordinary differential equations has become too easy due to the availability of built-in numerical packages frequently used in different softwares. In this study the resulting equations (2.10) & (2.11) are solved numerically to figure out the possibility of multiple solutions. As per requirement of the shooting technique, the obtained non-linear third order differential equations (2.10) & (2.11) are converted into a system of first order ordinary differential equations. In context to our problem (Eqs. (2.10) & (2.11)), the initial value problem takes the following form:

$$y_3 = y_1^2 - 2yy_2 + \beta \left(y_1 + \frac{\eta}{2}y_2\right), \quad y_1(0) = 1, \quad y(0) = -S, \quad y_1(\infty) = 0.$$
 (2.12)

Here, we use 
$$f(\eta) = y$$
,  $f'(\eta) = y_1$ ,  $f''(\eta) = y_2$  and  $f'''(\eta) = y_3$ .

To sort out the dual solution, the system (2.12) is solved numerically by using the shooting method. The dual solutions are captured and are reported in the succeeding Tables, and graphs.

**Table 2.3:** The values of skin friction coefficient, f''(0), for unsteadiness parameter  $\beta$ .

١ ـ	$\beta = -3$		β =	<del>-2</del>	β =	-1	β =	0	β =	1
S	1" Sol.	2 <sup>nd</sup> Sol.	1 <sup>st</sup> Sol.	2 <sup>nd</sup> Sol.	1ª Sol.	Z <sup>ad</sup> SoL	1ª Sol.	2 <sup>nd</sup> Sol.	1" Sol.	2 <sup>nd</sup> Sol.
7.4	0.2914	0.2914								
6.1	0.3698	0.3688	0.1744	0.1744						
5.0	0.4793	0.4703	0.2199	0.2189						
4.8	0.5050	0.4923	0.2307	0.2292	0.0000	0.0000				
4.0	0.6254	0.5804	0.2828	0.2747	-0.0005	-0.0008				
3.0	0.7859	0.6217	0.3571	0.3122	-0.0071	-0.0111		-		
2.0	0.8526	0.3980	0.3773	0.2058	-0.0510	-0.0801	-0.4142	-		
1.4	0.7762	0.0376	0.3072	-0.0212	-0.1307	-0.2071	-0.5206			
1.0	0.6538	-0.3196	0.2044	-0.2739	-0.2238	-0.3583	-0.6180			
0.0	0.0669	-1.6963	-0.2950	-1.3565	0.6516	-1.0962	-1.0000	-		
-1.0	0.8289	<del>-4.0545</del>	<b>-1.0928</b>	-3.3197	-1.3559	-2.5835	-1.6180	-		
-2.0	-1.8403	-7.92 <del>69</del>	-2.0317	-6.6178	-2.2230	-5.1983	-2.4142			
-3.0	-2.8681	-13.8175	-3.0130	-11.7299	-3.1579	-9.3745	-3.3027		-3.4476	
-4.0	-3.8914	-22.1756	-4.0063	-19.1024	-4.1212	-15.5437	-4.2360		-4.3509	
<b>5.0</b>	-4.9089	-33.4369	-5.0034	-29.1697	-5.0980	-24.1299	-5.1925		-5.2871	
8.0	-7.9398	<b>-88.9549</b>	-8.0009	-79.8099	-8.0620	-68.5494	-8.1231		-8.1841	
-10.0	-9.9512	-148.3378	-10.0004	-134.7987	-10.0497	-117.7787	-10.0990		-10.1482	

**Table 2.4:** The values of skin friction coefficient, f''(0), for suction/injection parameter S.

β	S=2		S=1		S = 0		S = -1		S = -2	
P	1 Sol	2ª Sol	1ª Sol	2 Sol	1" SoL	2ª Sol	1ª Sol.	2ª Sol.	1ª Sol.	2" Sol.
0.50				-					-2.5097	
0.40							-1.7224		-2.4906	
0.10			-0.6544	1	-1.0341		-1.6441		-2.4333	
0.05	-0.4302		-0.6363	1	-1.0170		-1.6310		-2.4237	
0.003	-0.4151	-	-0.6191	-0.6191	-1.0010	-	-1.6188		-2.4147	
0	-0.4142		-0.6180	-0.6182	-1.0000	-	-1.6180		-2.4142	
$-1/10^{16}$	-0.4142	-	-0.6180	-0.6182	-0.9999	-1.0056	-1.6180		-2.4142	
-1/10 <sup>9</sup>	-0.4142		-0.6180	-0.6182	-0.99 <del>99</del>	1.0060	-1.6180	-1.6855	-2.4142	
1/10 <sup>a</sup>	-0.4142		-0.6180	-0.6182	-0.9999	~1.0065	-1.6180	-1.6914	-2.4142	-2.7656
0.05	-0.3979	-0.3979	-0.5995	-0.6012	-0.9828	-1.0141	-1.604 <del>9</del>	-1.8487	-2.4046	-3.4027
-1.0	-0.0510	-0.0801	-0.2238	-0.3583	-0.6516	-1.0 <del>9</del> 62	-1.3559	-2.5835	-2.2230	-5.1983
-2.0	0.3773	0.2058	0.2044	-0.2739	-0.2950	-1.3565	-1.0928	-3.3197	-2.0317	-6.6178
-3.0	0.8526	0.3980	0.6538	-0.3196	0.0669	-1.6963	-0.8289	-4.0545	-1.8403	-7.9269
-4.0	1.3629	0.4946	1.1179	-0.4481	0.4327	-2.0742	-0.5643	-4.7848	-1.6488	-9.1762
-5.0	1.9003	0.5116	1.5933	-0.6270	0.8014	-2.4723	-0.2993	-5.5100	-1.4572	-10.3859
-6.0	2.4595	0.4689	2.0775	-0.8369	1.1725	-2.8819	-0.0338	-6.2300	-1.2656	-11.5665
<b>-7.0</b>	3.0366	0.3839	2.5690	-1.0664	1.5455	-3.2984	0.2319	-6.9453	-1.0739	-12.7245
-8.0	3.6289	0.2696	3.0666	-1.3087	1.9203	-3.7192	0.4981	-7.6561	-0.8821	-13.8643
-9.0	4.2342	0.1350	3.5694	-1.5598	2.2964	-4.1428	0.7645	-8.3630	-0.6903	-14.9889
-10.0	4.8508	-0.0136	4.0767	-1.8170	2.6739	-4.5681	1.0312	-9.0663	-0.4985	-16.1006

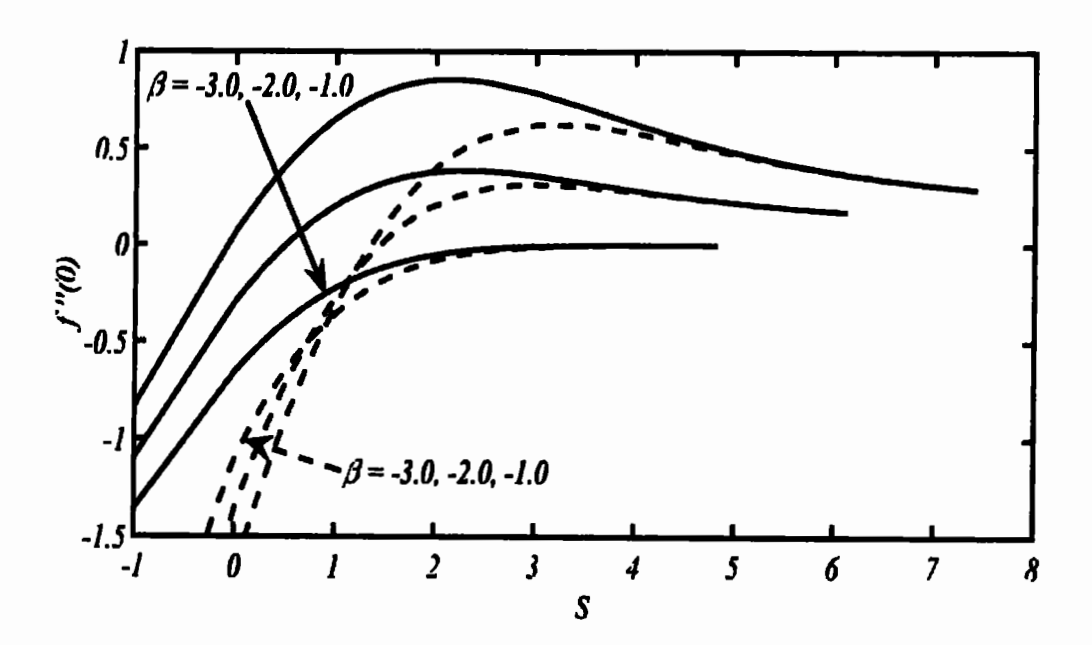


Fig. 2.5: Dual solutions shown by f''(0) for some selected values of unsteadiness parameter,  $\beta$ , against suction / injection parameter S.

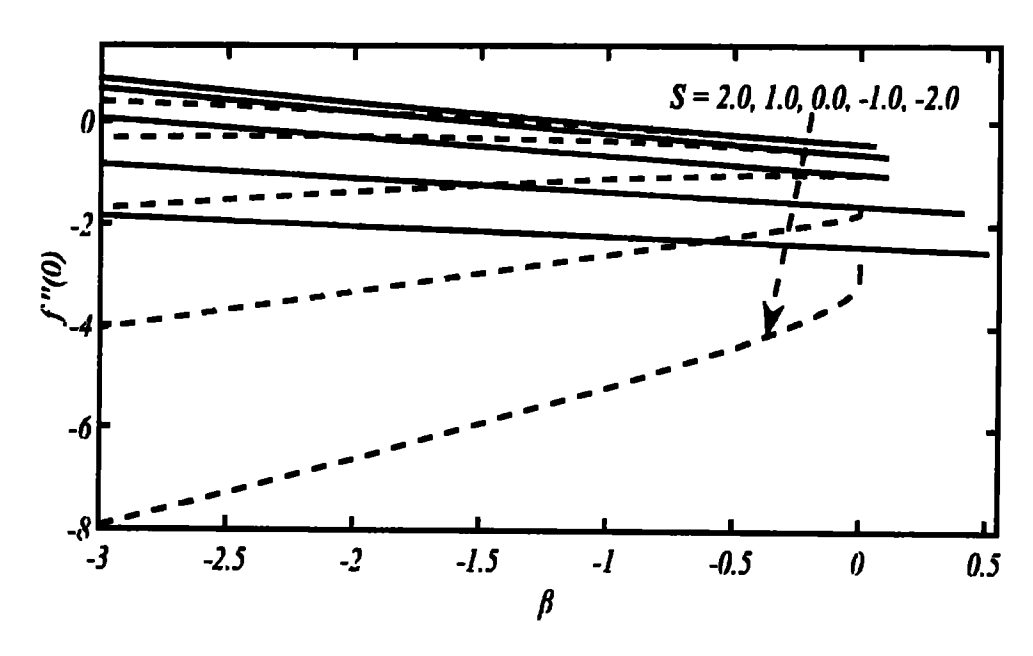


Fig. 2.6: Dual solutions shown by f''(0) for some selected values of suction/injection parameter S against unsteadiness parameter,  $\beta$ .

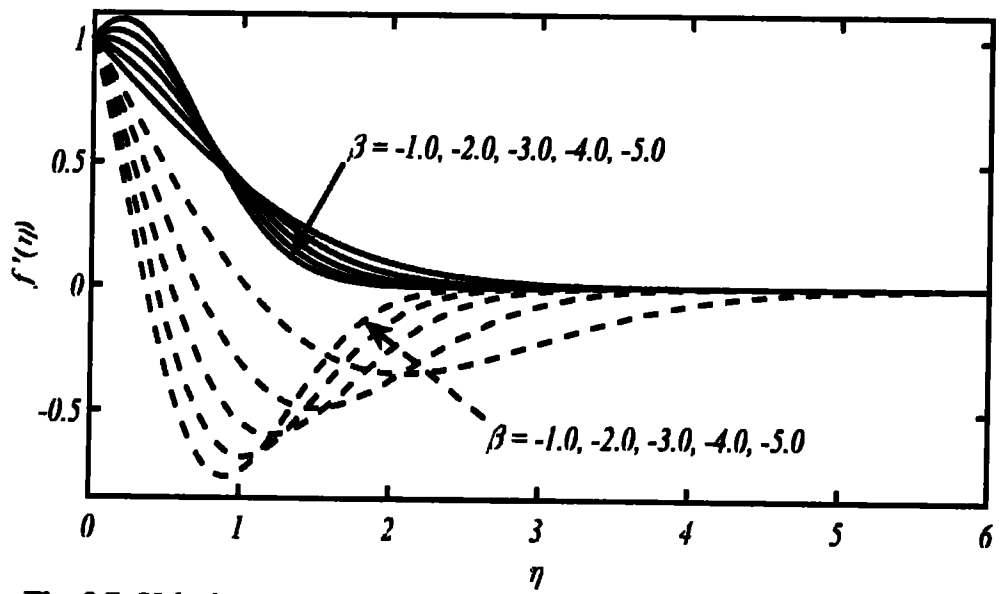


Fig. 2.7: Velocity profiles for some chosen values of unsteadiness parameter,  $\beta$ , in the absence of suction/injection parameter, S.

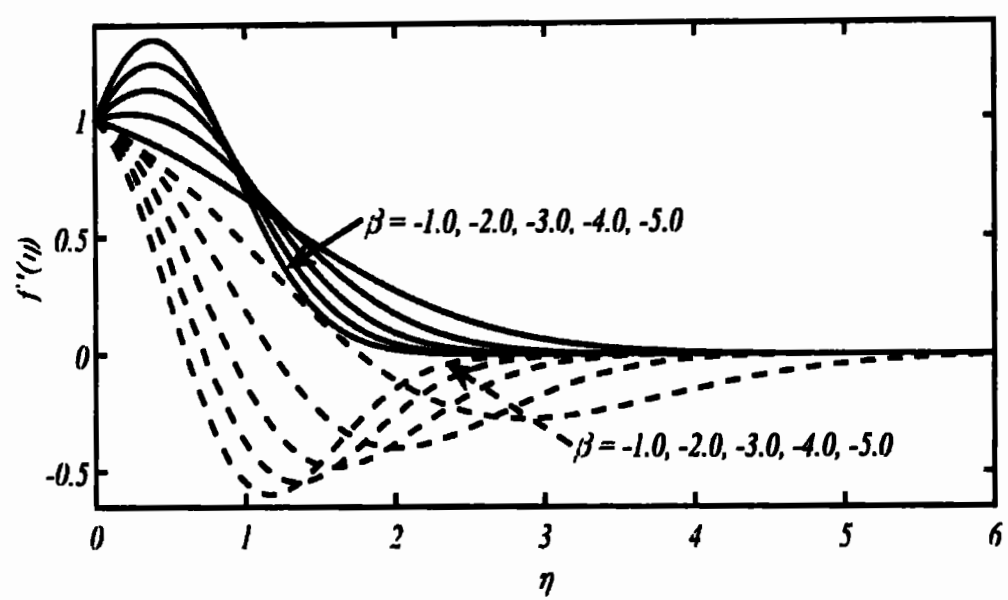


Fig. 2.8: Velocity profiles for some chosen values of unsteadiness parameter,  $\beta$ , in the presence of injection parameter (S=1).

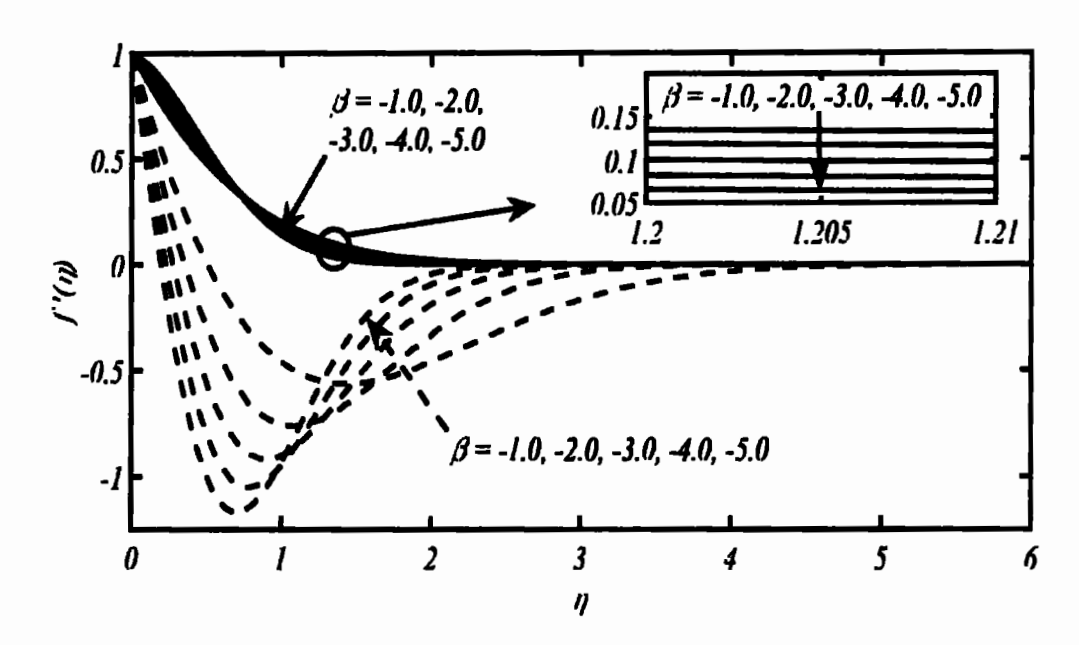


Fig. 2.9: Velocity profiles for some chosen values of unsteadiness parameter,  $\beta$ , in the presence of suction parameter (S = -1).

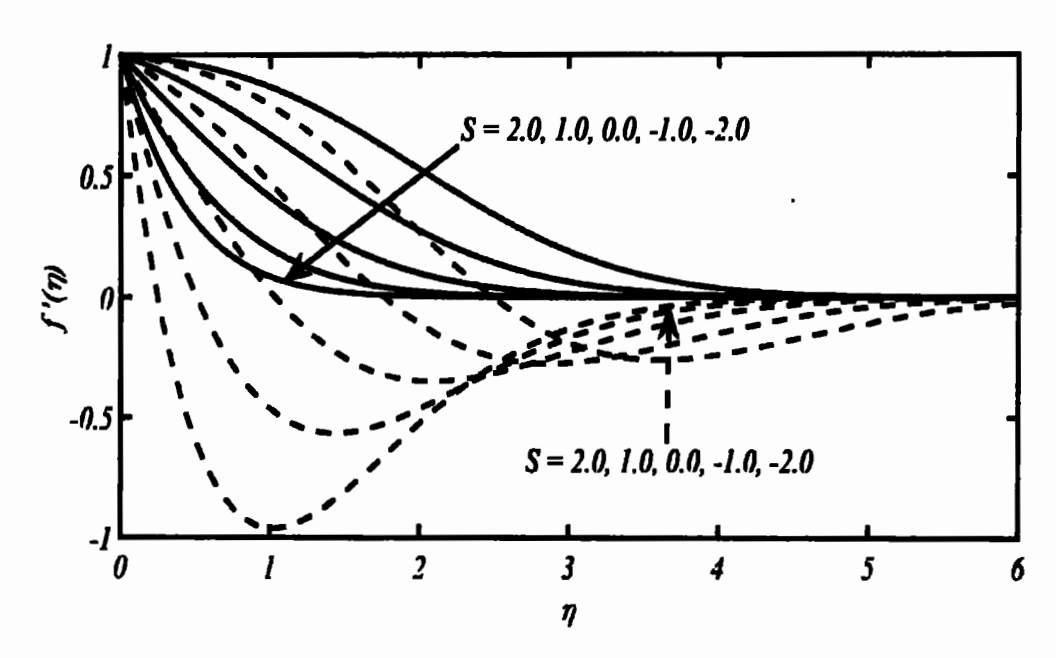


Fig. 2.10: Velocity profiles for some chosen values of suction/injection parameter S at  $\beta = -1$ .

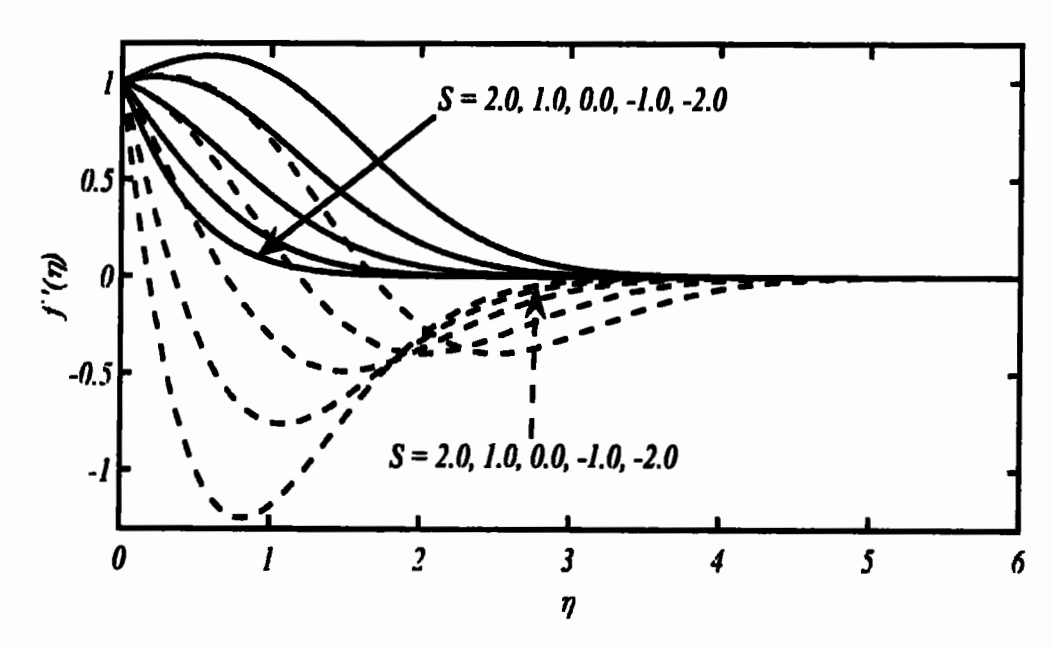


Fig. 2.11: Velocity profiles for some chosen values of suction/injection parameter S at  $\beta=-2$ .

#### 2.2.3 Results and discussion

An inspection of the system (2.10) – (2.11) reveals the presence of two parameters, namely,  $\beta$  the unsteadiness parameter and S the suction/injection parameter. Clearly, the accelerated/decelerated nature of boundary-layer is attributed to the parameter  $\beta$ . Dual solutions for unsteadiness parameter,  $\beta$ , at some selected values of suction/injection parameter, S, are figured out during the present analysis. It is well observed that the dual solutions can easily be captured for decelerated flow not only for both suction and injection parameters but also in the absence of these. However, in the case of accelerated flow only a unique solution is possible. From the numerical solution reported in Table 2.3, it is noted that there exists large variation in the second solution, for increasing magnitudes of suction parameter, as compared to the first solution. However, by reducing the suction parameter both solutions tend to come closer and closer. The dual solutions have been presented not only for suction velocity but also for injection velocity. Interestingly, the duality is also captured for the case of a non-porous stretching sheet. From the computed data it is depicted that as the effects of injection are intensified, both the solutions converge more rapidly and ultimately overlap at some critical point. Such convergence is displayed in Table 2.3, for some chosen values of unsteadiness parameter  $\beta$ . As the flow is more decelerated, more suction is required to obtain the solution. Moreover, the solution exists in a further restricted injection-domain; the corresponding results are portrayed in the Fig. 2.5. Further, from the results displayed in Fig. 2.6, it is observed that both solutions exhibit more variance for suction parameter and no convergence is reported therein.

To see the effects of unsteadiness parameter on the velocity profiles in the absence of suction/injection as well as in the presence of these, the Figs. 2.7–2.9 are drawn. From these figures, it is revealed that the second solution has almost similar behavior while the first solution presents relatively different attitude, particularly; the first solutions are very close to each other (Fig. 2.9). To examine the velocity profiles completely, the effects of suction/injection parameter at  $\beta = -1$  and  $\beta = -2$ , are presented in Fig. 2.10 & Fig. 2.11, wherein a smooth variation is noted in both cases.

#### 2.3 Conclusion

The existence of dual solution is supposed to be a unique feature of the shrinking surface flows and for stretching surfaces only a single/unique solution is assumed to exist. Further, the provision of sufficient wall suction is regarded as an integral part for the existence of dual/multiple solutions. However, in the current investigation quite different facts are found for the existence of dual solutions. During the current study, we have figured out dual solutions for both suction/injection velocities as well as without any of these velocities. Moreover, it is observed that dual solutions exist for decelerated flow while only a unique solution prevails for the cases of accelerated situations. It is also noted that the dual solution is not possible for  $m \ge 0$ , whether potency of the external agents (suction/injection etc.) may be intensified. In the decelerated case (m < 0 or  $\beta < 0$ ) duality of solution is a sure which has been reported with the aid of tabulated data and graphical results. Finally, it is concluded that the duality of solution is not a unique feature of the shrinking surface flows rather it can also be observed for stretching surface flows, equally. The fundamental reason behind the occurrence of dual solution is the retarded nature of the boundary-layer flow.

# Chapter 3

# Duality of solution for a shrinking sheet flow

The viscous fluid flows due to moving continuous surfaces bear another important class of self-similar flows which is known as "shrinking surface flows". Unlike the flows caused by stretching surfaces, the shrinking surface flows have attained sufficient attention from the scientists. There exists an abundant literature in the domain of shrinking surface flows and the relevant contributions are being made from known researchers to sort out its various aspects. The reason behind the inclinations of the researchers towards the fantasy of shrinking surface flows was just due to the claim made by Miklavcic and Wang [40]. On the basis of their analysis the involved authors made the following remarks:

- a) Sufficient amount of suction is mandatory for the existence of solution(s)
- b) The shrinking surface flows pertained strong non-linear phenomenon

Following the above mentioned claims, a bulk of literature has been contributed by the reputable researchers which made these claims as well-established facts. Consequently every new comer used such findings as ready reference. However, the authors [55] made it crystal clear that all such claims about shrinking surface flows are totally baseless and are far beyond the reality. On a deep and detailed analysis, Mehmood and Usman [55] put forwarded a correct self-similar formulation for the flows stimulated by continuous shrinking surfaces. The current study is carried out in the light of findings presented by the authors [55] and [56] in their recently published researches. The flow caused by the continuous moving surface beers a lot of significant aspects in the

extrusion process. The shrinking sheet has a unique prospective being to open a new type of solution i.e., dual/multiple solutions. To investigate this new class of solutions, for both steady/unsteady mechanisms, the shrinking surfaces have always been proved attractive field for researchers. During the current study, we will sort out the possibility of the existence of dual solutions by utilizing the correct self-similar formulation suggested by Mehmood [56]. It is worth noting that before the author's [56] marvelous work it was unanimously believed that the dual solutions are only existent for permeable shrinking surfaces. However, the author [56] devoted himself to counter the prevailing assumptions frequently circulated in the literature and succeeded in his attempt. The current investigation is the continuation of author's [56] contributions.

# 3.1 Steady boundary-layer flow due to a shrinking sheet

In this section we intend to investigate a steady two-dimensional viscous flow due to a shrinking sheet. As said in the previous chapter (i.e., Chapter 2), this problem has already been analyzed by Mehmood and Usman [55] but it is referred hare in order to exhibit a comprehensive picture presented in this thesis. Therefore, the current analysis is just a review of the work reported in [55] regarding the flow phenomenon caused by a steady shrinking sheet.

#### 3.1.1 Mathematical formulation

Consider an incompressible, two-dimensional, steady, boundary-layer flow caused by a permeable shrinking sheet in a stationary viscous fluid. The sheet is shrinking inward from some kind of slit with a velocity  $u_w(x)$  in the x — direction. Also, velocity of the fluid is regarded as zero beyond the vicinity of boundary-layer, while

pressure is taken as constant. In the light of assumptions stated above, the continuity equation (Eq. (2.1)), as well as the equation of motion (Eq. (2.2)) will remain the same, moreover, the similarity criterion used herein is also the same as narrated for the stretching wall velocity. However, it is obvious that the only difference between the two case (i.e., steady stretching sheet flow and steady shrinking flow), is the opposite sign of the wall velocities used therein. In view of above, we are taking following similarity transformations:

$$\eta = \sqrt{\frac{-a}{v}} x^{\frac{m-1}{2}} y, \qquad u = -a x^m f'(\eta), \qquad v = \sqrt{-av} x^{\frac{m-1}{2}} \left( \frac{m+1}{2} f + \frac{m-1}{2} \eta f' \right), \quad (3.1)$$

due to which Eq. (2.1) is satisfied identically and the Eqs. (2.2) and (2.3) are transformed to a form

$$f''' = \frac{m+1}{2}ff'' - mf'^2, \tag{3.2}$$

$$f'(0) = 1, f(0) = \frac{2S}{m+1}, f'(\infty) = 0,$$
 (3.3)

where, a < 0 is a constant shrinking rate, m is referred as the power-law index, which is a real number, and  $S = \frac{d}{\sqrt{-av}}$  is the dimensionless wall suction/injection velocity. Positive values of S (> 0) correspond to wall injection and the negative sign of S (< 0) represents the wall suction velocity. To ensure the self-similarity of the solution  $v_w(x)$  is taken of the form  $v_w(x) = dx^{\frac{m-1}{2}}$ ; d being a constant.

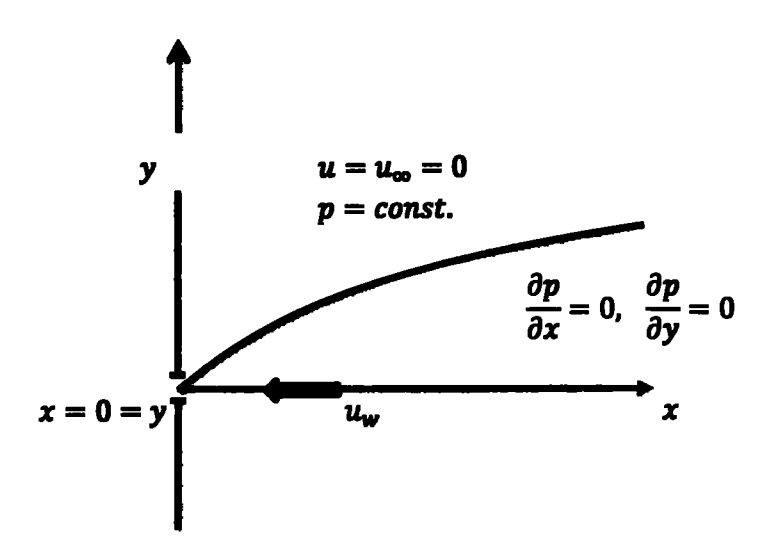


Fig. 3.1: Schematic of two-dimensional shrinking sheet flow and the related coordinate system.

### 3.1.2 Numerical solution

To solve the system (3.2)—(3.3), similar numerical method is adopted as utilized in the case of stretching sheet flow, to obtain the numerical solution of the problem. To avoid the repetition we go ahead to scrutinize the problem under consideration. A comparison of the current solution with that of [55] is given in Table 3.1. Obviously, an excellent agreement is evident which authenticates the solution presented in this chapter.

**Table 3.1:** Some numerical values of the skin-friction coefficient at S=-3.

	Mehmood an	d Usman [55]	Present results		
m	1st Sol.	2 <sup>nd</sup> Sol.	1 <sup>st</sup> Sol.	2 <sup>nd</sup> Sol.	
-2	-3.3783		-3.3783		
-1.5	-3.2727		-3.2727		
-0.7	-3.0903		-3.0903		
0.0	-2.9133		-2.9133		
1.5	-2.4408	-0.1335	-2.4408	-0.1335	
2	-2.2285	-0.3445	-2.2285	-0.3 <del>44</del> 5	
2.5	<b>-1.9460</b>	-0.6587	-1.9460	-0.6587	

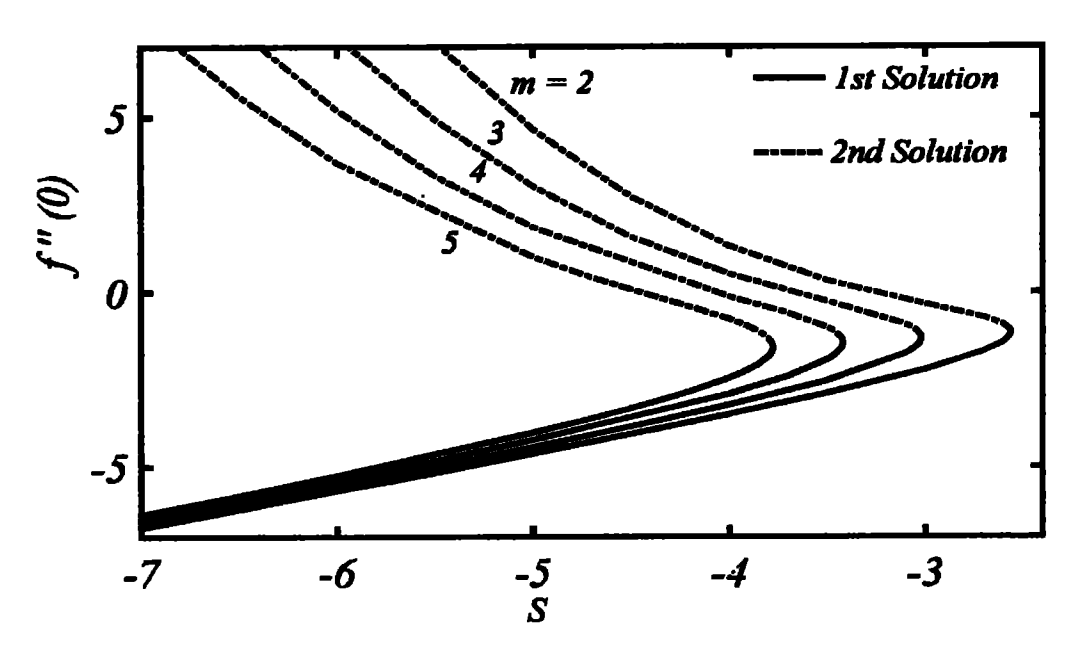


Fig. 3.2: Skin-friction coefficient (shrinking sheet) plotted at different m as a function of suction parameter S.

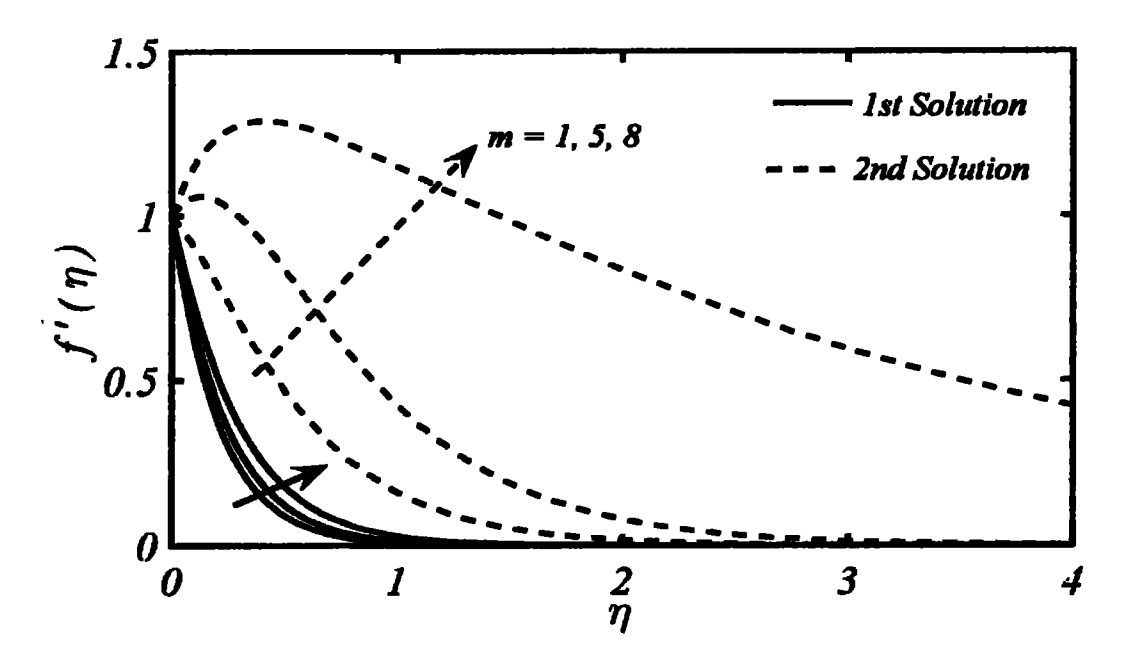


Fig. 3.3: Velocity profile of the shrinking surface flow for different values of the power-law index m, at S=-5.

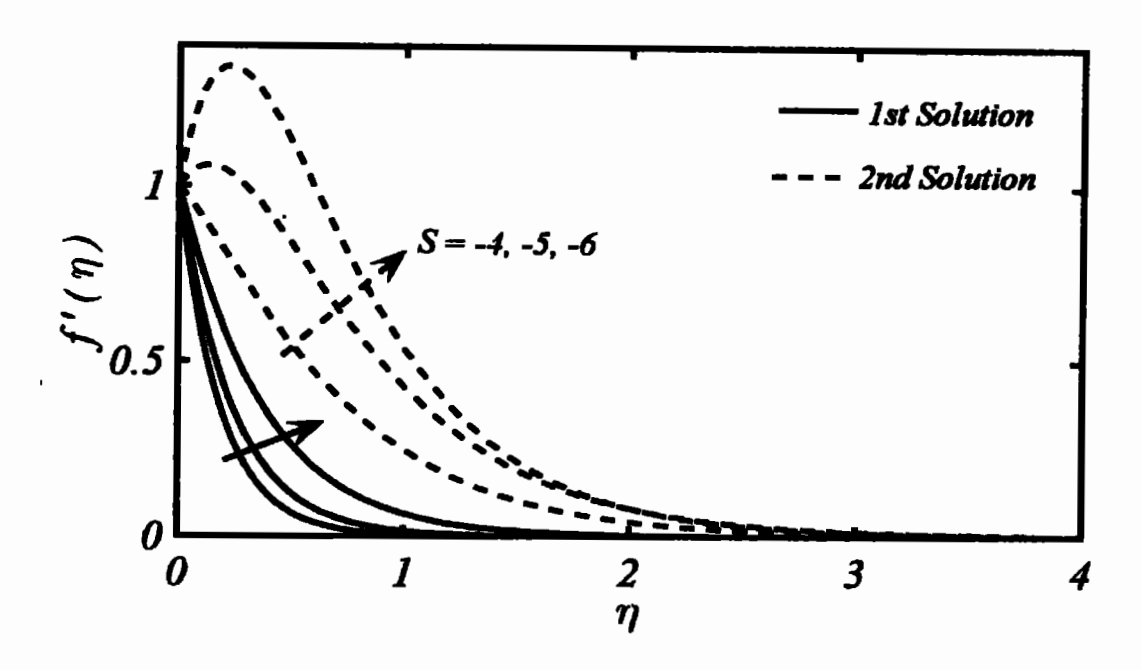


Fig. 3.4: Velocity profile of the shrinking surface flow for different values of the suction parameter S, at m = 5.

### 3.1.3 Results and discussion

The self-similar system of equations (3.2)—(3.3), obtained for the boundary-layer flow due to a steady non-linearly shrinking sheet is solved numerically, for the possibility of existence of non-unique solution. Mehmood and Usman [55] already scrutinized the same problem for the same goal and succeeded to sort out the duality of solution in the shrinking sheet flow by taking a non-linear form of the wall velocity. The authors [55], briefly explained the details for the occurrence of non-unique solution, therein. The duality of solution was captured for m > 0 which refers to the case of retarded wall velocity. The duality of solution has been reported in Table 3.1 and also in Fig. 3.2, accordingly, whereas the velocity profiles are presented in Figs. 3.3—3.4. To explore the other hidden aspects as well as more information on the duality of solution for steady shrinking sheet, one can consult ref. [55].

### 3.2 Unsteady boundary-layer flow due to a shrinking sheet

In this section our aim is to analyze the unsteady self-similar flow stimulated by a permeable shrinking sheet. The motivation of current investigation has received motivation from the already available literature on this topic where the contributing authors have neither formulated the flow correctly nor investigated rightly. It is worth noting aspect that most of the authors utilized an unsteady (accelerated/decelerated) shrinking wall velocity of the form  $u_w(x,t) = \frac{-ax}{1-\gamma t}$  (a > 0) due to which nonuniqueness of solution is reported. However, it is also a fact that the similarity transformations adopted therein are incorrect. The reason behind the utilization of incorrect similarity transformation is due to the mistake conducted by the pioneer authors [40], during the process of non-dimensionalization. It is worth mentioning aspect that the followers of [40] made the literature, related to steady/unsteady shrinking surfaces, too much voluminous which created sufficient problems for the researchers who desired to reconcile the mistake made therein. Therefore, no successful attempt could be materialized. Recently, Mehmood and Usman [55], and Mehmood [56] have ultimately succeeded in his struggle and presented the details about the mishaps existed in the realm of stretching/shrinking surface flows. The author [56] has not only figured out the ambiguity pertained in the existing literature but also sorted out the mater by presenting correct formulation of the problem. The contributions of [56], provide an apple opportunity for the scientists to investigate the flow mechanism in a correct manner. It is noted that the nature of the wall velocity  $(u_w(x,t) = \frac{ax}{\tau} \text{ or } \frac{ax}{1-\gamma t} (a < 0))$  is assumed to be retarded (in x) and the utilization of this kind of wall velocity assured the existence of dual solutions. It is also a fact that the retarded wall velocity requires some kind of

assistance in the shape of wall suction/injection velocity so that a meaningful solution could be captured.

### 3.2.1 Mathematical formulation

In the current study we assume an unsteady, incompressible, two-dimensional boundary-layer flow stimulated by a permeable shrinking sheet, which is flexible in nature. The sheet is supposed to be started into motion, in negative x -direction, at time t=0 in a stationary fluid with a velocity  $u_w(x,\tau)$ . Further, the ambient conditions are prevailed outside the boundary-layer region, which implies that fluid has zero velocity and uniform pressure there. The x-axis is considered to coincide with the shrinking sheet in positive x-direction whereas the y-axis is assumed to be normal to the x-direction. In view of above assumptions, flow schematic is shown in Fig. 3.1, whereas the continuity equation has the same form as presented in Eq. (2.1), while the equation of motion is similar to Eq. (2.7), given by

$$\frac{\partial u}{\partial t} + u \frac{\partial u}{\partial x} + v \frac{\partial u}{\partial y} = v \frac{\partial^2 u}{\partial y^2}, \tag{3.4}$$

while the corresponding initial and boundary conditions read as

$$u(x, y, t) = 0,$$
 at  $t = 0$ , for all  $(x, y)$ , (3.5)

and

$$u(x, y, t > 0) = u_w(x, t), \quad v(x, y, t > 0) = v_w(x, y), \quad \text{at } y = 0,$$
 (3.6)

$$u(x, y, t > 0) = 0, at y = \infty. (3.7)$$

Recently, Mehmood [56] pointed out that the self-similar flow, in the case of an unsteady shrinking surface, prevails if the wall velocity pertains the following form:

$$u = u_{\mathbf{w}}(x,\tau) = \frac{ax}{\tau}; \quad \tau = at , \qquad (3.8)$$

where a is a constant referred to the shrinking rate when one choses its negative behavior. It is also a worth mentioning aspect that wall velocity of the form  $u_w(x,\tau) = \frac{-ax}{1-\gamma t}$ , is also adopted by most of the authors and same form of wall velocity was utilized by Fang et al. [49] during the analysis of unsteady shrinking surface flow. Corresponding to the said forms of wall velocity, the following similarity transformations are introduced:

$$\eta = \sqrt{\frac{-u_w(x,\tau)}{vx}}y, \quad u = u_w(x,\tau)f'(\eta), \text{ and } v = \sqrt{\frac{-u_w(x,\tau)v}{x}}f(\eta). \quad (3.9)$$

The unique feature of above similarity transformations is the appearance of negative sign therein, which distinguishes it from the similarity transformations existed in the literature. This fact has also been mentioned by Batchelor [3] in his book. In the current study, the transformation Eq. (3.9) is a key for further exploration. The use of Eq. (3.9) merges the initial condition Eq. (3.5) and the boundary condition Eq. (3.7) into a single one as given by

$$f'=0, \qquad \text{at } \eta=\infty. \tag{3.10}$$

The self-similar nature of the flow under question as well as the wall velocity presented in Eq. (3.8) demands that the normal wall velocity  $v_w(x,\tau)$  must be of the form (for detailed study one may consult [56])

$$v_{w}(x,\tau) = d\tau^{-1/2}. (3.11)$$

Here d is a constant and its positive/negative values designate to unsteady injection/suction velocities, respectively.

In view of Eqs. (3.8), (3.9) and (3.11) the boundary conditions defined in Eq. (3.6) at y = 0 take the form

$$f' = 1,$$
  $f = S,$  at  $\eta = 0,$  (3.12)

where  $S = \frac{d}{\sqrt{-\alpha v}}$  represents the suction/injection parameter, whereas, its positive/negative values determine the wall injection/suction, accordingly. Further, the adoption of stream function in the similarity transformations (3.9) identically satisfies the continuity equation (Eq. (2.1)) while Eq. (3.1) (i.e. momentum conservation equation) develops in a self-similar form as:

$$f''' = ff'' - f'^{2} - (f' + \frac{\eta}{2}f''). \tag{3.13}$$

Notice that Eq. (3.13) recovers the Eq. (6) of [49] (for  $\beta = 1$ ) if one replaces the term f''' by -f''' in it. Utilization of the correct similarity transformations (i.e., Eq. (3.9)), modified the problem considered in [49] as given by

$$f''' = ff'' - f'^{2} + \beta(f' + \frac{\eta}{2}f''), \tag{3.14}$$

while the corresponding boundary conditions are given by

$$f(0) = S, f'(0) = 1, f'(\infty) = 0.$$
 (3.15)

Here  $S = \frac{d}{\sqrt{-av}}$  and  $\beta = \frac{\gamma}{a}$  whereas the corresponding wall suction/injection velocity is taken as  $v_w(x,t) = \frac{d}{\sqrt{1-\gamma t}}$ . Positive values of  $\beta$  represent an accelerated case while its negative values refer to the decelerated nature of flow.

### 3.2.2 Numerical solution

In order to solve the resulting equations (3.13), along with boundary conditions Eqs. (3.11) & (3.12) and Eq. (3.14), subject to boundary conditions Eq. 3.15, we transform them into a system of first order ordinary differential equations, given by

$$y_3 = 2yy_2 - y_1^2 - (y_1 + \frac{\eta}{2}y_2), \quad y_1(0) = 1, \quad y(0) = S, \quad y_1(\infty) = 0,$$
 (3.16)

$$y_3 = 2yy_2 - y_1^2 - \beta \left(y_1 + \frac{\eta}{2}y_2\right), \quad y_1(0) = 1, \quad y(0) = S, \quad y_1(\infty) = 0.$$
 (3.17)

Here, we take 
$$f(\eta) = y$$
,  $f'(\eta) = y_1$ ,  $f''(\eta) = y_2$  and  $f'''(\eta) = y_3$ .

To sort out the dual solution, Eqs. (3.13) are solved numerically by using the shooting technique. The dual solutions are figured out which are presented in Table 3.2.

An excellent agreement ensures the correctness of solution scheme.

**Table 3.2:** Comparison of the values of f''(0) with those of Mehmood [56] and the listing of second solution for different values of S.

C	Mehmood [56]	Present Results			
<b>.</b>	1st Sol.	1ª Sol.	2ª Sol.		
-2.074799052		-0.5043	-0.5043		
-3.0	-2.4115	-2.4115	2.5881		
-4.0	-3.5930	-3.5930	6.9590		
-5.0	-4.6846	-4.6846	13.6528		
-6.0	-5.7414	-5.7414	23.1453		
-7.0	-6.7804	-6.7804	35.8671		
-8.0	-7.8090	-7.8090	52.2334		
<b>-90</b>	-8.8309	-8.8309	72.6507		
-10.0	-9.8482	-9.8482	97.5194		

**Table 3.3:** Numerical values of f''(0) against  $\beta$  for different values of S.

β	S =	S = -2.1		S = -2.1 $S = -2.15$		S =	S = -2.2		S = -2.5		S = -3.0	
<u> </u>	I" SoL	2nd SoL	1ª Sol.	2 <sup>nd</sup> Sol.	1 <sup>st</sup> Sol.	2 <sup>nd</sup> Sol.	1ª Sol.	2nd Sol.	I Sol.	2 <sup>nd</sup> Sol.		
0.0	-1.3701	-0.7298	-1.4 <del>69</del> 4	-0.6805	-1.5582	-0.6417	-2.0000	-0.4999	-2.6180	-0.3819		
-0.5	-1.0933	-0.4262	-1.2342	0.2859	-1.3479	-0.16 <del>9</del> 6	-1.8558	0.4277	-2.5147	1.5506		
-1.0	-0.7 <del>849</del>	-0.2103	-0.9893	0.0232	-1.1329	-0.2000	-1.7112	1.0618	-2.4115	2.5881		
-1.5	-0.4029	-0.0942	-0.7336	0.2901	-0.8692	0.5901	-1.5662	1.6209	-2.3081	3.4777		
-2.0	-	!	-0.4650	0.5250	-0.6897	0.8295	-1.4209	2.1391	-2.2047	4.2912		
-2.5			-0.1796	0.7298	-0.4612	1.1114	-1.2753	2.6304	-2.1013	5.0559		
-3.0					-0.2278	1.3769	- 1.1295	3.1022	-1.9978	5.7860		
-3.5							-0.9834	3.5589	-1.8943	6.4897		
-5.0							-0.5437	4.8641	-1.5837	8.4903		
-6.5							-0.1021	6.1016	-1.2728	10.3777		
-7.0									-1.1692	10.9688		
-8.0									- 0.9618	12.1895		
-10									-0.5468	14.5217		

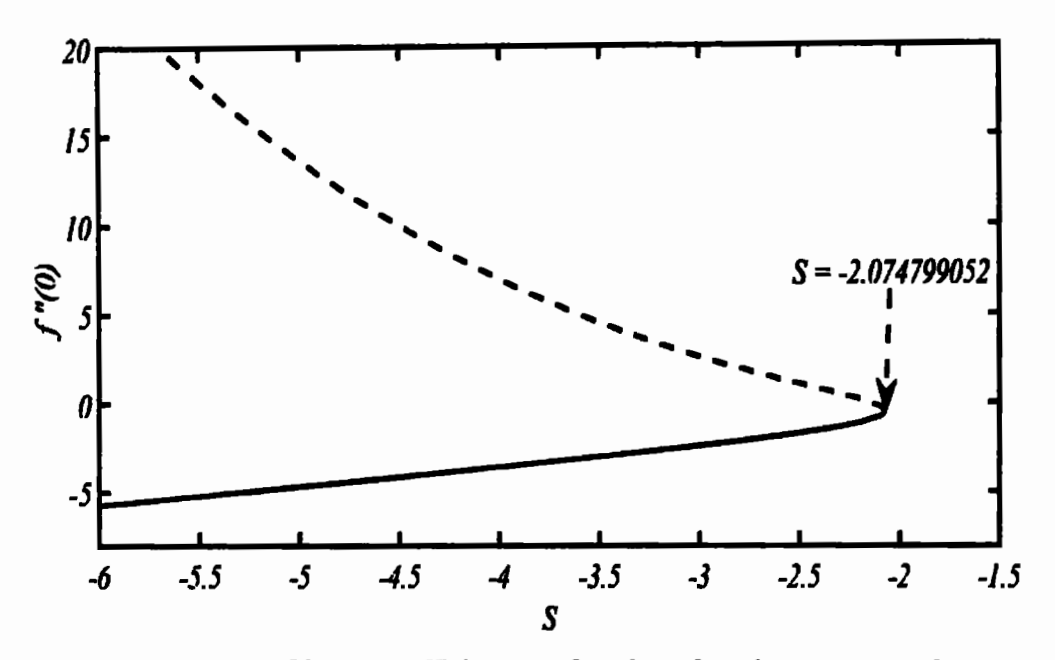


Fig. 3.5: Skin-friction coefficient as a function of suction parameter S.

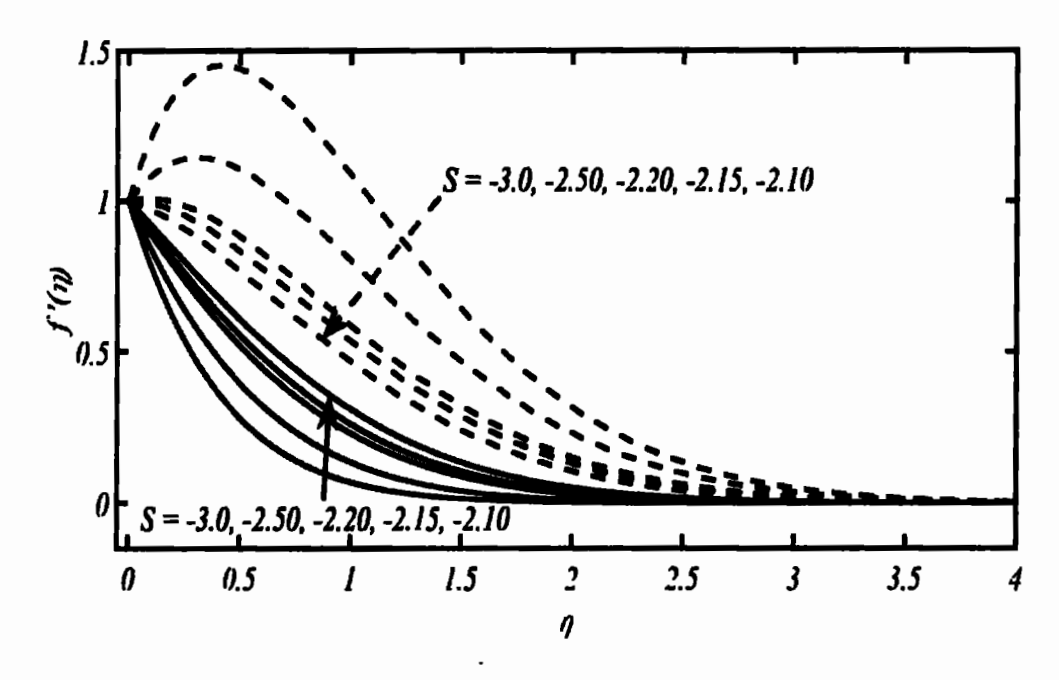


Fig. 3.6: Velocity profile of dual solutions for some values of S.

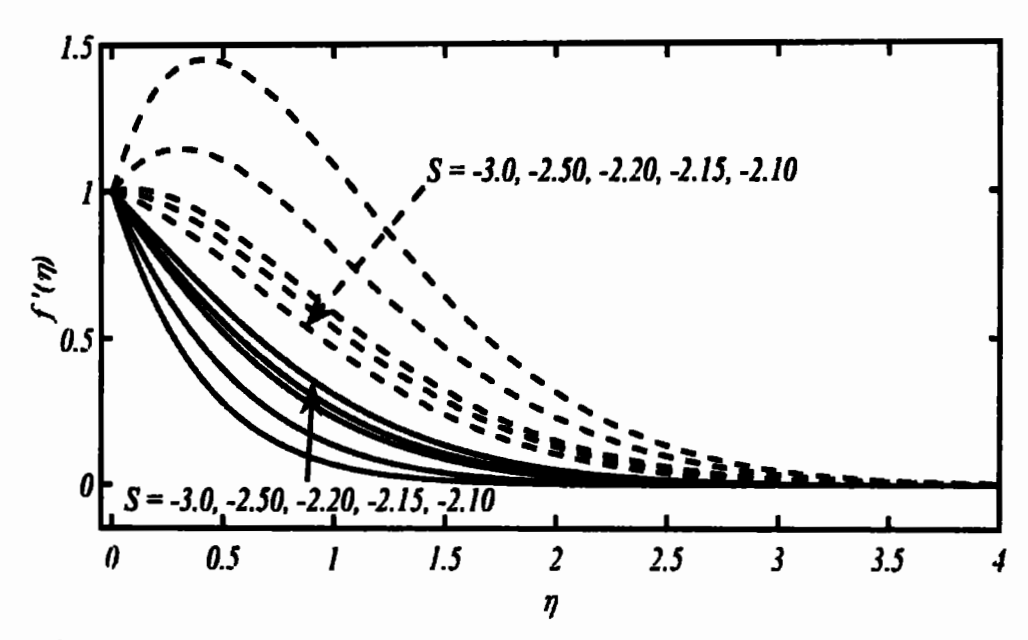


Fig. 3.7: Velocity profile of dual solution at  $\beta = -1.0$  for some values of S (obtained due to Eqs. (3.14)-(3.15)).

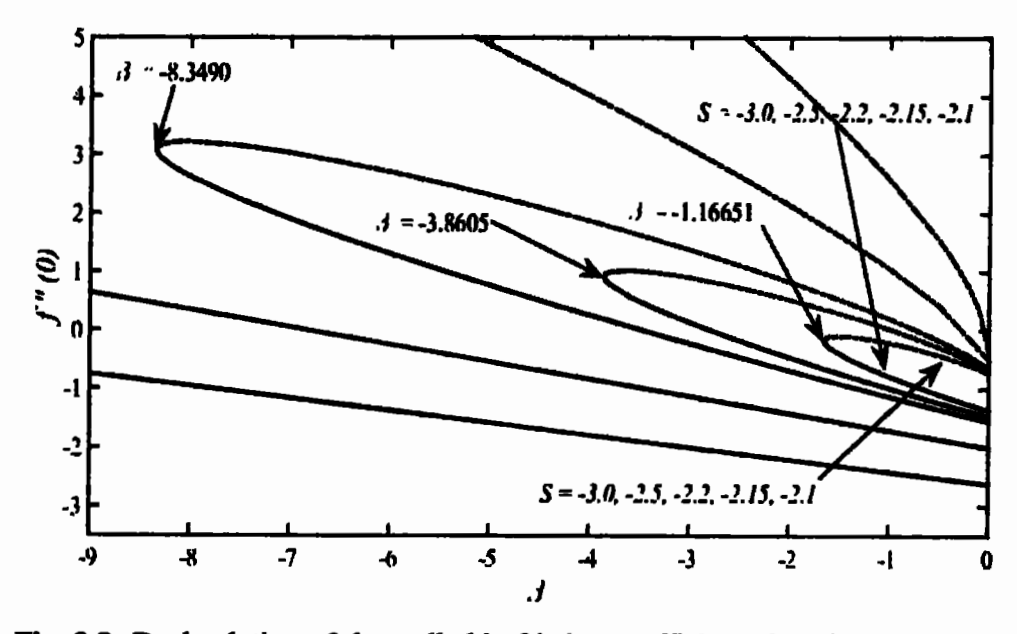


Fig. 3.8: Dual solution of the wall skin-friction coefficient plotted against  $\beta$  for some values of S (obtained due to correct formation Eqs. (3.14)—(3.15)).

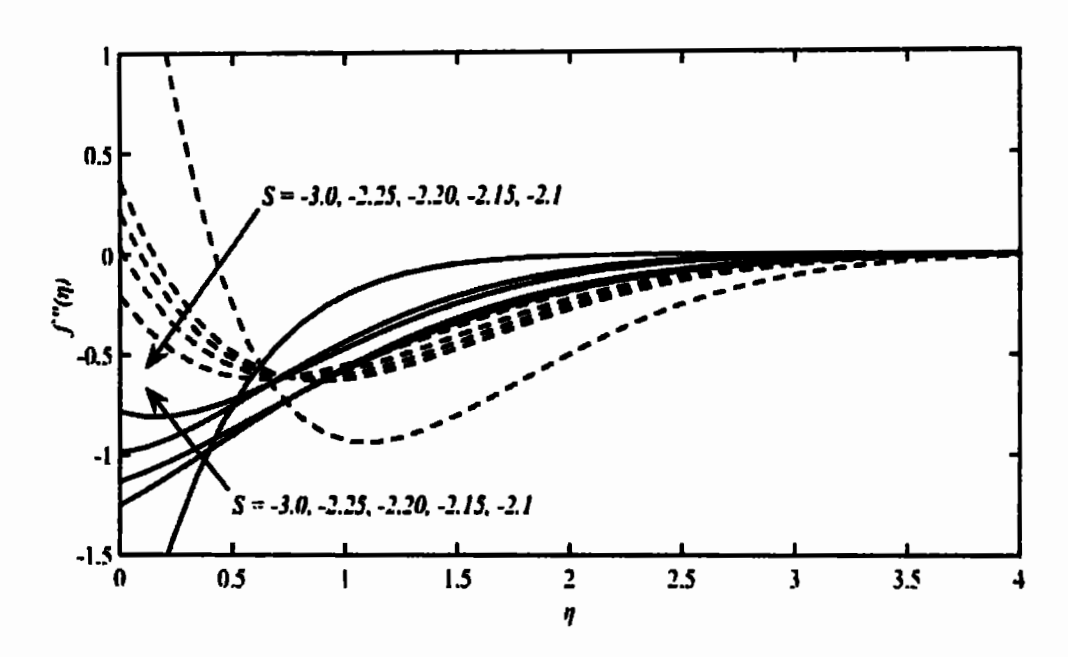


Fig. 3.9: Dual solution of wall shear stress at  $\beta = -1.0$  for some values of S (obtained due to Eqs. (3.14)-(3.15)).

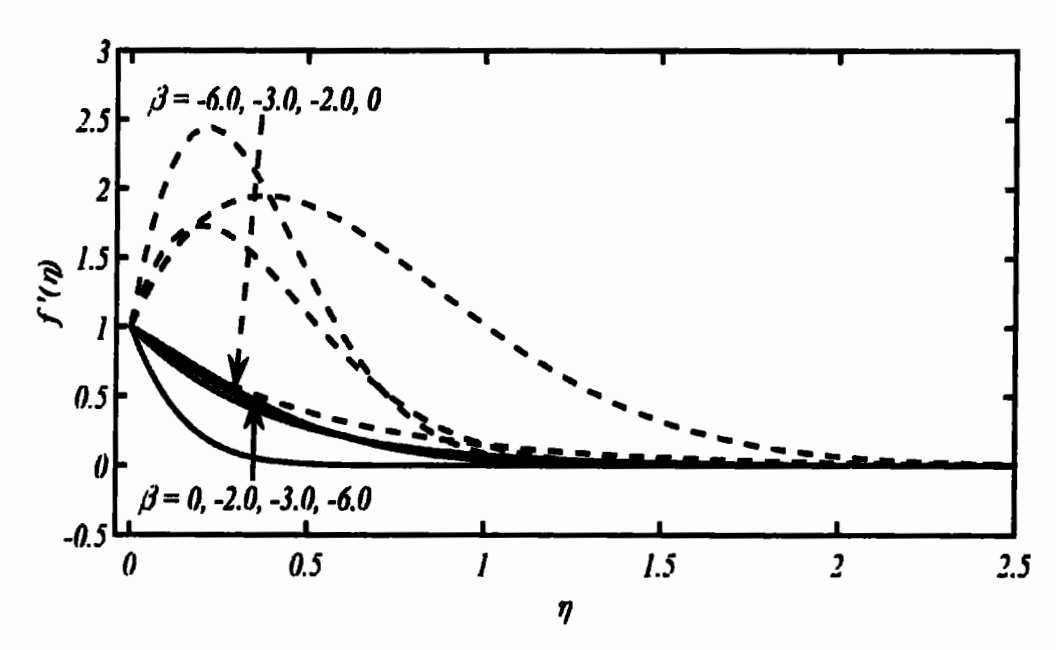


Fig. 3.10: Dual velocity profile at S=-3.0 for some values of  $\beta$  (obtained due to Eqs. (3.14)-(3.15)).

#### 3.2.3 Results and discussion

Investigation of the existence of dual solutions for unsteady shrinking sheet flow is the keen desire of the present study which has become efficiently fructified with the aid of present numerical method. The dual solutions captured during the present investigation, for some chosen values of suction parameter, are portrayed in Fig. 3.5, wherein it is observed that there is a smooth variation in the first solution; however, the second solution has broader span. Further, the solution is not possible beyond a certain value of suction parameter. This critical value  $S_c$  is sorted out after a great deal of attempts and it is reported as  $S_c = -2.074799052$ . Earlier to this critical value no solution is possible which implies that the provision of sufficient wall suction is necessary for the existence of solution, in this case. It is also observed that as the solution approaches the critical value,  $S \to S_c$ , the existence of dual solutions demands more and more attention. The reported value, i.e.,  $S = S_c$ , is the least amount of suction at which the retarded boundary-layer survived, however, the skin-friction coefficient does not become zero which means that there is no presence of reverse flow as well as the separation point therein. Fig. 3.5 presents the regions wherein the dual/unique/nosolutions prevail. The complete analysis of the study also demanded that the velocity profile be interpreted with clear visibility, and this has been done in the Fig. 3.6, where the velocity profile is displayed for some chosen values of suction parameter and dual solutions are figured out during the analysis. It is also observed that as the magnitude of suction is enhanced the span of velocity profile amplifies accordingly. Almost same pattern is noted for both branches of solution.

To report the correct analysis of [49] the formulation used in the current study is also applied to the problem considered by [49] and resultantly Eqs. (3.14)-(3.15) are obtained. On comparison, it is noted that the Eq. (3.13) can be retrieved by just taking  $\beta = -1$  in the Eq. (3.14). For further analysis, the system of Eqs. (3.14)–(3.15) has been solved and some graphs (for various  $\beta$ ) of [49] are re-plotted for some chosen values of S. The dual solutions are captured for certain values of S against  $\beta$  and  $\eta$  which are presented in Fig. 3.8 and Fig. 3.9, respectively. From Figs. 3.8-3.9, it can be seen that both graphs are the reverse images of the graphs reported by Fang et al. [49] in their Figs. 1a, 4 & 5 during his study. From these findings it is clearly observed that the magnitude of skin-friction enhances with the increasing values of suction velocity. This implies that boundary-layer strengthens as the availability of suction is amplified. Consequently, flow behavior exhibits more stability. By choosing  $\beta = -1$ , the velocity profile portrayed in the Fig. 3.7, which is as same as drawn in the Fig. 3.6. Further, the velocity profiles for Eqs. (3.14)-(3.15) (obtained by utilizing the correct formulation) are already presented in Figs. 2 & 3 of [49], are also re-presented here in Fig. 3.10 (of present study), wherein it is depicted that the second solution becomes more strengthened with  $\beta$ . Although, it is a fact that only first solution is a meaningful solution and second solution has no such ability. However, the existence of second solution cannot be ignored and it has to be studied for complete analysis of the flow phenomenon.

#### 3.3 Conclusion

In a study shrinking sheet flow, when the shrinking wall velocity follows a powerlaw form, both scenarios, namely, the existence of unique and non-unique solution have been observed. The boundary-layer flow is of accelerated nature for m < 0 and of

decelerated nature for m > 0. Therefore, the duality of solution has been captured for the case of m > 0. The current analysis is an attempt to study the various aspects of the unsteady, two-dimensional self-similar flow stimulated by a shrinking sheet and to sort out the possibility of the existence of dual solution in the presence/absence of suction parameter. The correct reference velocity as suggested by Mehmood [56] is chosen for self-similar formulation of the problem. The resulting equations have been solved using an efficient numerical scheme. Critical values of the suction velocity are also captured with due care which enabled us to rectify the results already reported in literature. During the current analysis it is noted that the shrinking sheet must be permeable in nature as well as the provision of adequate amount of suction is mandatory for the existence of meaningful solution. Further, the dual solution is only possible if sufficient wall suction is provided, whereas the solution prevails for a certain limit (critical value  $|S_c|$ ) of suction wall velocity, and it disappears to exist after the critical point i.e.,  $|S| < |S_c|$ . The presence of wall suction velocity definitely affects the skin-friction coefficient and the velocity profile in a noticeable way. Here, it is observed that the span of skin-friction coefficient expands with the increasing values of suction parameter and the duality of velocity profile is also affected by the suction parameter in the same pattern as noted in the case for skin-friction coefficient. The effect of suction parameter on velocity function is seemed more prominent for second solution as compared to the first solution.

As a final remark, it is obvious that in both the (steady and unsteady) cases of shrinking sheet flow, duality of solution has been captured in only those scenarios when the boundary-layer flow is of retarded nature. In the accelerated case of shrinking sheet no such duality of solution has been noticed.

# Chapter 4

# Axisymmetric flow due to a non-linearly stretching cylinder: non-uniqueness of solution

In the previous two chapters, steady and unsteady characteristics of the twodimensional planner cases of stretching and shrinking sheet flows have been analyzed in details wherein presence of dual solutions is not only reported for shrinking sheet flow but also observed for stretching sheet flow. It had been a well mentioned fact that the availability of dual solutions is considered a special feature of shrinking surface flows whereas the stretching surface flows were supposed to be infertile regarding the existence of dual solutions. Ample efforts are made, in chapter 2 to analyze the steady/unsteady stretching sheet flow and the existence of dual solutions in this case has broken out the established facts about the non-uniqueness of shrinking surface flows, only. The results reported in chapter 2, stimulated us to search out the possibility of duality/multiplicity of solution for the axisymmetric cases. In the current chapter, our entire consideration will be limited to investigate the steady/unsteady characteristics of stretching cylinder in context of the presence of dual solutions.

The dual solutions are reported, not only, in the presence of wall suction/injection effects but also observed without these effects. Further, the continuous cylinder chosen during the current analysis is of variable radius, which also involves effects of surface curvature on the flow phenomenon. The surface transverse curvature has appeared as an interesting and influential ingredient on the boundary-layer flow due to moving

continuous surfaces. Interesting effects of the surface transverse curvature with regard to the capturing of non-unique solution have been reported in this chapter.

### 4.1 Steady boundary-layer flow past a stretching cylinder

The boundary-layer flow phenomenon caused by the moving continuous surfaces is regarded as an important class of self-similar flows. Like the two-dimensional, selfsimilar planner boundary-layer flows, the axisymmetric flows also attracted a wider community of researchers. In the continuation of theoretical investigations of the boundary-layer flows due to continuous moving surfaces, Sakiadis [12-13] also extended his work for axisymmetric scenario, wherein Sakiadis [58] analyzed the self-similar boundary-layer flow over a continuous cylinder moving with constant velocity. The flow due to variable velocity was investigated by Crane [59] during the analysis of boundarylayer flow induced by stretching cylinder. A number of attempts can be seen [60-65]. where the authors are remained focused upon linear nature of stretching velocity. However, there is utmost need to investigate the non-linear prospectus of the flow related to stretching cylinders. This gap has been recently been filled by Mehmood [56] during the study of viscous flows caused by stretching/shrinking surfaces. After a deep analysis, the author [56] concluded that the cross-section of the cylinder should be of variable nature for supporting the different forms (power-law or exponential) of non-linear stretching wall velocity in order to ensure a similarity solution. This new vision regarding non-linear behavior of the wall velocity motivated us to explore the different hidden features of stretching surface flows, particularly to search out the possibility of dual solutions for the self-similar flows stimulated by the moving continuous surfaces. Although, there is a bulk of literature available for shrinking surface flows regarding the

existence of dual/multiple solutions due to which duality of solution is assumed to be confined to the shrinking surfaces only, while the stretching surfaces are usually known for pertaining the unique solution. These accepted facts in respect of presence of dual solutions were countered by Mehmood and Usman [66], wherein the authors made a claim that the duality of solution is not the characteristics of shrinking surfaces only but the stretching surfaces do also bear a capacity of exhibiting dual nature of solution. The claim made by the authors [66] came into reality in the form of Tabassum et al. [82] wherein the authors reported dual solutions not only in the presence of suction/injection situations but also in the absence of these. During the present analysis, the duality of solution has been explored for the self-similar boundary-layer flow caused by steady stretching cylinder. The presence of dual solution has been observed with and without providing the wall suction/injection velocity. These findings made the current study a valuable reference for forthcoming researches.

#### 4.1.1 Mathematical formulation

We consider a steady, self-similar boundary-layer flow caused by a continuous permeable stretching cylinder of variable radius of the form R(z). It is supposed that the flow is two-dimensional, non-rotational, and having symmetry about z—axis. The schematic diagram exhibits the flow geometry and the corresponding coordinate system is referred in Fig. 4.1. The body forces as well as the pressure-gradient are assumed to be absent. In the light of above assumption the boundary-layer equations in cylindrical coordinates are given as

$$\frac{\partial(ru)}{\partial x} + \frac{\partial(rv)}{\partial r} = 0,\tag{4.1}$$

$$u\frac{\partial u}{\partial x} + v\frac{\partial u}{\partial r} = v\frac{1}{r}\frac{\partial}{\partial r}(r\frac{\partial u}{\partial r}),\tag{4.2}$$

subject to the following boundary conditions:

$$u = u_w(z), v = v_w(z), at r = R(z) u = 0, at r = \infty$$
(4.3)

where u and v are the velocity components taken along z – and r –directions, respectively, and v is termed as kinematic viscosity. For the nature of the cylinder considered herein demands that the similarity variables should be of the forms

$$\eta = rz^{\frac{m-1}{2}}, \qquad \psi = zf(\eta). \tag{4.4}$$

The above similarity transformations have been derived for the case when

$$u_w = az^m, \qquad R = R_0 z^{\frac{1-m}{2}}, \tag{4.5}$$

where  $R_0$  is the reference radius of the cylinder having constant radius referred to linear (m=1) wall velocity, whereas, for non-linear wall velocity  $(m \neq 1)$  the cylinder radius obeys the power-law form given in Eq. (4.5). The stream function  $(\psi)$  is related to the velocity components u and v in the form  $u = \frac{1}{r} \frac{\partial \psi}{\partial r}$ , and  $v = \frac{-1}{r} \frac{\partial \psi}{\partial z}$ . Using Eqs. (4.4)-(4.5) in Eqs. (4.1)-(4.2), we get the following form of equations:

$$m\left(\frac{f'}{\eta}\right)^2 - \frac{f}{\eta}\left(\frac{f''}{\eta} - \frac{f'}{\eta^2}\right) = \nu \frac{1}{\eta} \frac{d}{d\eta} \left(\eta \frac{d}{d\eta}\left(\frac{f'}{\eta}\right)\right),\tag{4.6}$$

$$f' = aR_0, f = -\frac{2d}{m+1}R_0, at \eta = R_0$$
  
 $f' = 0, at \eta = \infty$  (4.7)

thereby, satisfying the equation of continuity, identically. Here, it is also a noteworthy aspect that, in the case of steady stretching cylinder, for the existence of self-similarity solution the radius of cylinder must vary in the same manner as does the boundary-layer thickness  $(i.e, z^{\frac{1-m}{2}})$ . Moreover, the suction/injection wall velocity also follows the

power-law form given by  $v_w(z) = dz^{\frac{m-1}{2}}$  where the constant d is a dimensional constant and designates the normal wall velocity as suction/injection corresponding to its -ve/+ve values, respectively.

The system (4.6)—(4.7) can be put in dimensionless form by modifying the transformations (4.4) as

$$\eta = \sqrt{\frac{a}{v}} z^{\frac{m-1}{2}} r, \quad u = \frac{az^m}{\eta} f'(\eta), \quad v = -\sqrt{av} z^{\frac{m-1}{2}} (\frac{f}{\eta} + \frac{m-1}{2} f').$$
(4.8)

Consequently, the system (4.6)-(4.7) in dimensionless form reads as

$$m\left(\frac{f'}{\eta}\right)^2 - \frac{f}{\eta}\left(\frac{f''}{\eta} - \frac{f'}{\eta^2}\right) = \frac{1}{\eta}\frac{d}{d\eta}\left(\eta\frac{d}{d\eta}\left(\frac{f'}{\eta}\right)\right),\tag{4.9}$$

$$f' = Re_{R_0}, f = -\frac{2S}{m+1}Re_{R_0}, at \eta = Re_{R_0}$$
  
 $f' = 0, at \eta = \infty$ 

$$(4.10)$$

where,  $Re_{R_0} = \sqrt{\frac{aR_0^2}{\nu}}$  is the Reynolds number based on the reference radius  $R_0$ . Eqs. (4.9) and (4.10) can be simplified by removing the variable coefficients from most of the terms and the constant  $Re_{R_0}$  from the boundary conditions by using the following new variables:

$$\bar{\eta} = \frac{\eta^2 - Re^2_{R_0}}{2Re_{R_0}}, \qquad f = \bar{f}Re_{R_0},$$
 (4.11)

due to which the resulting system after dropping the bars reads as

$$mf'^2 - ff'' = ((1 + 2\kappa\eta)f'')',$$
 (4.12)

$$f'(0) = 1,$$
  $f(0) = -\frac{2S}{m+1},$   $f'(\infty) = 0,$  (4.13)

where  $\kappa = \frac{1}{Re_{R_0}}$  is the curvature parameter, and  $S = \frac{d}{\sqrt{\alpha v}}$  denotes the dimensionless suction/injection parameter. Note that the large values of  $Re_{R_0}$  correspond to the

cylinders of large radius whose surface transverse curvature is relatively small which corresponds to small value of  $\kappa$ . Similarly, large values of  $\kappa$  correspond to large transverse curvature. The definition of suction/injection parameter S reflects that negative values of S correspond to the wall suction situation while the positive values of S correspond to wall injection situation.

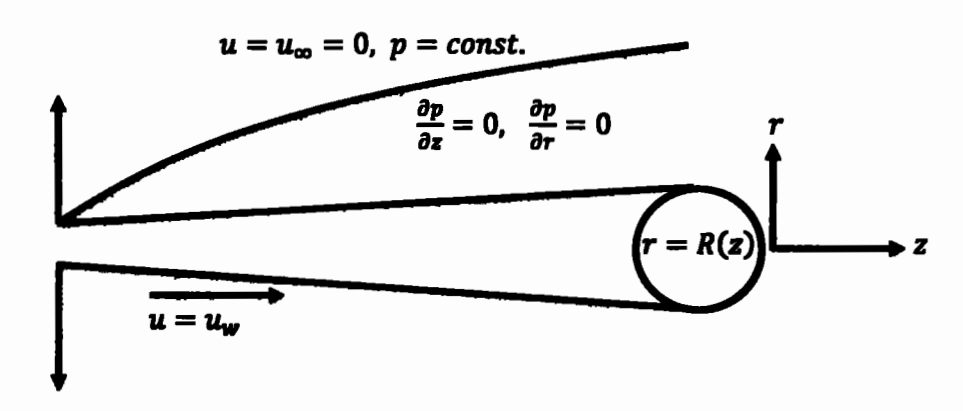


Fig. 4.1: Schematic of the axisymmetric flow and the associated coordinate system.

#### 4.1.2 Numerical solution

The system of self-similar Eqs. (4.12)—(4.13), obtained during the current investigation become more compatible to be solved numerically. As previous, shooting method is utilized to sort out the solution. During the present analysis, dual solutions are reported which are presented in the tabular form as well as portrayed graphically. A comparison of the current results with the already existing data in literature has been carried out in Table 4.1. An excellent agreement is obvious which ensures the accuracy and validity of the current solution.

Table 4.1: A comparison of present analysis with the results reported in [56].

	κ =	0.25	κ=	= 0.5	κ =	2.0
m	Data of [56]	Present study	Data of [56]	Present study	Data of [56]	Present study
10	-2.7336	-2.7335	-2.8290	-2.8289	-3.3596	-3.3594
7	-2.3224	-2.3223	-2.4172	-2.4170	-2.9393	-2.9393
5	-2.0001	-2.0000	-2.0940	-2.0938	-2.6077	-2.6078
3	-1.6120	-1.6119	-1.7042	-1.7042	-2.2047	-2.2048
1	-1.0905	-1.0905	-1.1778	-1.1777	-1.6486	-1.6485
0_	-0.7056	-0.7056	-0.7826	-0.7825	-1.2078	-1.2064
-0.2	-0.6057	-0.6057	-0.6779	-0.6778	-1.0832	-1.0809
-0.4	-0.4925	-0.4925	-0.5576	0.5575	<b>~0.5576*</b>	-0.9294
-0.8	-0.2021	-0.2020	-0.2373	-0.2373	-0.4698	-0.4593
-1.0	0.0000		0.0000		-0.0172	

<sup>\*</sup> Might be a typo mistake.

**Table 4.2:** Numerical values of f''(0) against S for various values of  $\kappa$  at m=1.

	κ =	0.25	κ =	0.5	κ =	1.0	κ =	2.0
S	1st Sol.	2 <sup>nd</sup> Sol.	1st Sol.	2 <sup>nd</sup> Sol.	1st Sol.	2 <sup>md</sup> Sol.	1ª Sol.	2 <sup>nd</sup> Sol.
10.0							-0.1575	
9.0					-0.1390		-0.1835	
7.0		~~-	-0.1614		-0.1889		-0.2639	-0.2639
4.0	-0.2630		-0.2938	-	-0.3653		-0.5342	-0.5349
3.5	-0.2985		-0.3359		-0.4202	-0.4202	-0.6110	-0.6121
2.5	-0.4014		-0.4557	-0.4557	-0.5701	-0.5704	-0.8071	-0.8096
1.4	-0. 5985	-0.5985	-0.67 <del>49</del>	-0.6751	-0.8234	-0.8242	-1.1057	-1.1113
1.0	-0.7049	-0.7050	-0.7880	-0.7883	-0.9462	-0.9474	-1.2405	-1.2479
0.0	-1.0905	-1.0914	-1.1778	-1.1792	-1.3433	-1.3472	-1.6486	-1.6638
-1.0	-1.6815	-1.6864	1.7488	-1.7555	-1.8889	-1.8997	-2.1693	-2.1990
-4.0	-4.2496	-4.3206	-4.2647	-4.3411	-4.3001	-4.3926	-4.3982	-4.533
-6.0	-6.1688	-6.360	-6.1760	-6.369	-6.1921	-6.407	-6.2344	-6.510
-8.0	-8.1269	-8.531	-8.1309	-8.522	-8.1399	-8.551	-8.1619	-8.651
-10	-10.1014	-10.84	-10.1041	-10.8	-10.1097	-10.8	-10.1229	-10.913

**Table 4.3:** Numerical values of f''(0) against S for various values of  $\kappa$  at m=3.

S	κ =	0.25	κ =	0.5	κ =	1.0	κ =	2.0
	1# Sol.	2 <sup>nd</sup> Sol.	1# SoL	2 <sup>nd</sup> Sol.	1st Sol.	2 <sup>nd</sup> Sol.	1ª Sol.	2 <sup>nd</sup> Sol.
14.0							-0.6247	
13.0							-0.6736	-0.6736
7.0			1				-1.1176	-1.1179
6.0			1		-0.9727	~	-1.2261	-1.2267
5.0			-0.9411		-1.0770	-1.0770	-1.3478	-1.3486
3.0	-1.0954		-1.1764	1	-1.3344	-1.3347	-1.6363	-1.6382
2.0	-1.2384	<u>-1.2384</u>	-1.3254	-1.3254	-1.4924	-1.4928	-1.8062	-1.8089
1.0	-1.4088	<del>-1.40</del> 90	-1.5000	-1.5002	-1.6732	-1.6740	-1.9952	-1.9992
0.0	-1.6119	-1.6123	-1.7042	-1.7048	-1.8795	-1.8810	-2.2048	-2.2107
-1.0	-1.8526	-1.8542	<b>-1.9418</b>	-1.9432	-2.1138	-2.1166	-2.4363	<b>-2.4451</b>
-5.0	-3.2001	-3.3167	-3.2486	-3.2842	-3.3565	-3.3818	-3.6011	-3.6372
-6.0	-3.6105	-4.6200	-3.6500	-3.7134	-3.7393	-3.7798	-3.9526	-4.0017
8.0	<u>-4.4806</u>	-8.4150	<b>-4.5071</b>	-4.6806	-4.5675	-4.6596	-4.7211	-4.8083
-10.0	<u>-5.3933</u>	-14.9872	-5.4118	-5.8570	<b>-5.4535</b>	-5.6341	-5.5608	-5.7070

**Table 4.4:** Numerical values of f''(0) against of m for various values of  $\kappa$  at S=-1.

	κ =	0.25	κ =	0.5	κ =	1.0	κ =	2.0
<i>m</i>	1ª Sol.	2 <sup>nd</sup> Sol.	1ª Sol	2 <sup>nd</sup> Sol	1ª Sol	2nd Sol.	1 <sup>st</sup> Sol.	2 <sup>nd</sup> Sol.
10	-2.8105	-2.8106	-2.9061	-2.9063	-3.0902	-3.0908	-3.4375	-3.4396
9	-2.6892	-2.6893	-2.7846	-2.7848	-2.9680	-2.9687	-3.3135	-3.3159
8	-2.5628	-2.5630	-2.6579	-2.6582	-2.8406	-2.8413	-3.1840	-3.1867
7	-2.4310	-2.4312	-2.5256	-2.5260	-2.7073	-2.7082	-3.0484	-3.0514
6	-2.2933	-2.2936	-2.3874	-2.3879	-2.5678	-2.5690	-2.9060	-2.9097
5	-2.1497	-2.1502	-2.2429	-2.2435	-2.4217	-2.4230	-2.7562	-2.7610
4	-2.0012	-2.0021	-2.0931	2.0940	<b>-2.2694</b>	-2.2712	-2.5990	-2.6052
3	-1.8526	-1.8542	-1.9418	-1.9432	-2.1138	-2.1166	-2.4363	-2.4451
2	-1.7208	-1.7238	-1.8040	-1.8068	-1.9674	-1.9725	-2.2776	-2.2917
1	-1.6815	-1.6864	-1.7488	-1.7550	-1.8889	-1.8997	-2.1693	-2.1990
0.5	-1.7965		-1.8469		-1.9591	*	-2.2030	
0.2	-1.9943		-2.0304	-	-2.1154		-2.3190	
0.1	-2.1016		-2.1324		-2.2062		-2.3915	
0	-2.2403		-2.2658		-2.3278		-2.4917	
-0.2	-2.6601		-2.6754		-2.7131		-2.8254	
-0.4	-3.4255		-3.4326					
-0.6	-5.0412		-5.0434		_			

**Table 4.5:** Numerical values of f''(0) against m for various values of  $\kappa$  at S=1.

	κ =	0.25	κ =	0.5	κ =	1.0	κ =	2.0
m	1st Sol.	2 <sup>nd</sup> Sol.	1ª Sol.	2nd Sol	1ª Sol.	2 <sup>nd</sup> Sol.	1st Sol.	2nd Sol.
10	-2.6592		-2.7543	-2.7544	-2.9377	-2.9379	-3.2834	-3.2849
9	<b>-2.5222</b>	-2. 5222	-2.6170	-2.6171	-2.7995	-2.7999	-3.1434	-3.1452
8	-2.3764	-2.3765	-2.4710	-2.4711	-2.6527	-2.6531	-2.9945	-2.9964
7	-2.2201	-2.2202	-2.3143	-2.3144	-2.4950	-2.4955	-2.8343	-2.8365
6	-2.0505	-2.0506	-2.1443	-2.1444	-2.3238	-2.3243	-2.6602	-2.6626
5	-1.8637	-1.8638	-1.9569	-1.9571	-2.1350	-2.1356	-2.4677	-2.4706
4	-1.6534	-1.6535	-1.7458	-1.7460	-1.9219	-1.9226	-2.2501	-2.2534
3	-1.4088	-1.4090	-1.5000	-1.5002	-1.6732	-1.6740	-1.9952	-1.9992
2	-1.1088	-1.1089	-1.1976	-1.1979	-1.3662	-1.3672	-1.6787	-1.6840
1	-0.7049	-0.7050	-0.7880	-0.7883	-0.9462	-0.9474	-1.2405	-1.2479
0.50	-0.4302		-0.5053		-0.6505		-0.9250	-0.9346
0.20	-0.2292		-0.2939		-0.4230		-0.6748	
0.10	-0.1559		-0.2150		-0.3357		-0.5762	
0	-0.0802		-0.1321		-0.2419		-0.4678	
-0.2	0.0699		0.0405		-0.0354		-0.2159	
-0.4			0.1913		0.1784			
-0.6	0.1699		0.2127		0.2918			

**Table 4.6:** Numerical values of f''(0) against m for various values of  $\kappa$  at S=0.

	κ =	0.25	κ =	0.5	κ =	1.0	κ =	2.0
m	1" Sol.	2 <sup>nd</sup> Sol.	1 <sup>st</sup> Sol.	2 <sup>nd</sup> Sol.	1st Sol.	2 <sup>nd</sup> Sol.	1" Sol.	2nd Sol.
10	-2.7335		-2.8289		-3.0127	-3.0131	-3.3596	-3.3613
9	-2.6038		-2.6991		-2.8823	-2.8828	-3.2274	-3.2293
8	-2.4673		-2.5622		-2.7447	-2.7452	-3.0877	-3.0899
7	-2.3224	-2.3224	-2.4172	-2.4172	-2.5986	-2.5992	2.9393	-2.9417
6	-2.1673	-2.1675	-2.2617	-2.2620	-2.4422	-2.4430	-2.7802	-2.7832
5	-2.0001	-2.0002	-2.0940	-2.0942	-2.2731	-2.2740	-2.6078	-2.6114
4	-1.8167	-1.8169	-1.9099	-1.9104	-2.0875	-2.0886	-2.4181	-2.4226
3	-1.6119	-1.6123	-1.7042	-1.7048	-1.8795	-1.8810	-2.2048	-2.2107
2	-1.3762	-1.3768	-1.4668	-1.4677	-1.6387	-1.6410	-1.9564	-1.9651
1	-1.0905	-1.0914	-1.1778	-1.1792	-1.3433	-1.3472	-1.6485	-1.6638
0.50	-0.9162	-	-1.0000		-1.1595	-1.1652	-1.4540	-1.4777
0.25	-0.8167		-0.8977		-1.0525	-1.0597	-1.3392	-1.3726
0.20	-0.7955	-	-0.8758		-1.0295	-1.0371	-1.3143	-1.3518
0.15	-0.7738		-0.8534		-1.0058		-1.2887	-1.3379
0	-0.7056		-0.7825		-0.9306		-1.2064	
-0.2	-0.6057		-0.6778		-0.8179		-1.0809	
-0.4	-0.4925		-0.5575		-0.6855		-0.9294	
-0.6	-0.3608		-0.4148		-0.5232		-0.7347	
-0.8	-0.2020		-0.2373		-0.3104		-0.4593	

**Table 4.7:** Numerical values of f''(0) against S for various values of m at  $\kappa = 0.25$ .

S	m=	-2.0	m = -3.0		m =	-4.0	m =	<b>-5.0</b>	m=	-6.0
	1ª Sol	2ªd Sol.	1" Sol.	2ª Sol	1ª Sol	2ªd Sol	1ª Sol	2ª Sol.	1ª Sol.	2ª Sol
1	-1.7142									
2	-3.8666		-1.3490	33.3063						
3	-5.9130		-2.6186	144.038	-0.7931	5.7072				
4	-7.9354		-3.7266	379.21	-1.9529	20.9230				
5	-9.9487		-4.7862	785.8	-2.8067	48.0201	-1.3043	6.1202		
6	-11.9574	+	-5.8242	1410.6	-3.5788	90.781	-2.1393	14.1883	0.1297	0.8472
7	-13.9636		-6.8507	2300	-4.3144	152.80	-2.8118	25.9917	-1.4537	5.2142
<b>®</b>	-15.9682		-7.8702	3502	-5.0301	237.67	-3.4219	42.3797	-2.1598	10.1649
10	-19.9746		-9.8970	7029	-6.4289	490.1	-4.5582	92.008	-3.2543	25.1124

**Table 4.8:** Numerical values of f''(0) against S for various values of m at  $\kappa = 0.50$ .

S		-2.0	m=	-3.0	m =	<b>-4</b> . 0	m =	-5.0	m =	-6.0
L	1ª Sol.	2ª Sol	1 Sol.	2 Sol	1ª Sol.	2 Sol	1ª Sol.	2ª Sol.	1ª Sol.	2 Sol.
1	-1.6666									
2	-3.8571		-1.1816	15.6450				-		
3	-5.9090		-2.57 <del>49</del>	94.86				-		
4	-7.9333	1	-3.7057	282.57	-1.8255	11.0237				
_ 5	-9.9473		-4.7738	625.8	-2.7485	30.7343	-0.8020	1.6107		
6	-11.9565	1	-5.8160	1171.5	-3.5442	64.028	-1.9936	7.3874		
_ 7	-13.9629	1	-6.8448	1966.6	<del>-4.2911</del>	114.546	-2.7325	15.9955	-0.9213	1.2673
8	-15.9677		-7.8658	3057	-5.0133	185.86	-3.3703	28.5387	-1.9741	5.0021
10	-19.9743		-9.8943	6315	-6.4189	405.1	-4.5304	68.618	-3.1812	16.152

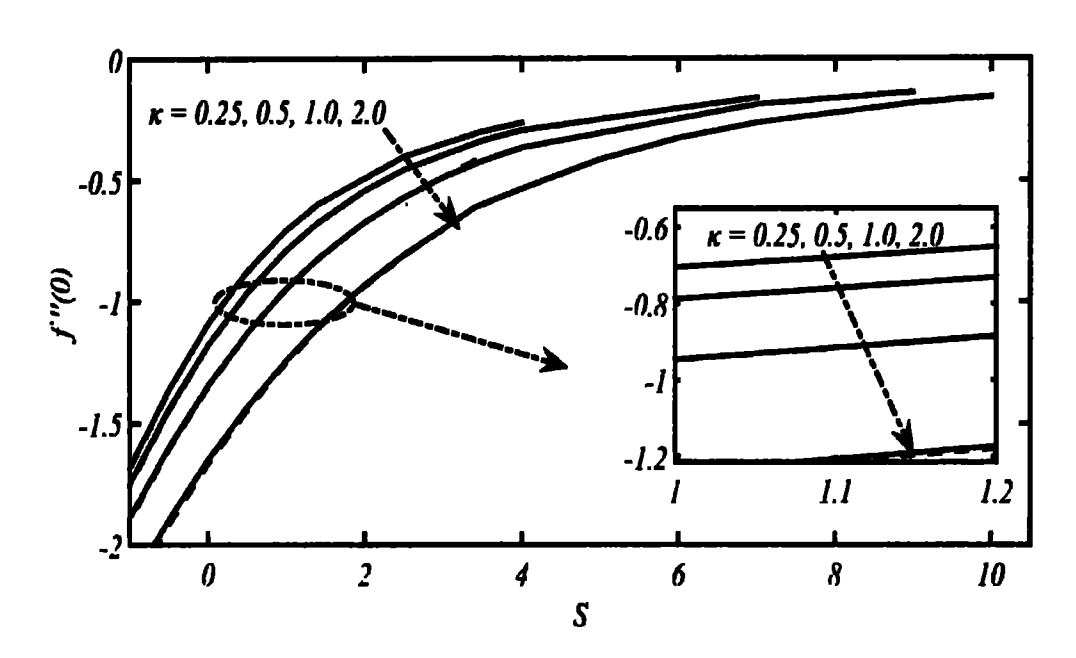


Fig. 4.2: Dual solutions shown by f''(0) for some selected values of curvature parameter  $\kappa$  against suction/injection parameter S at m=1.

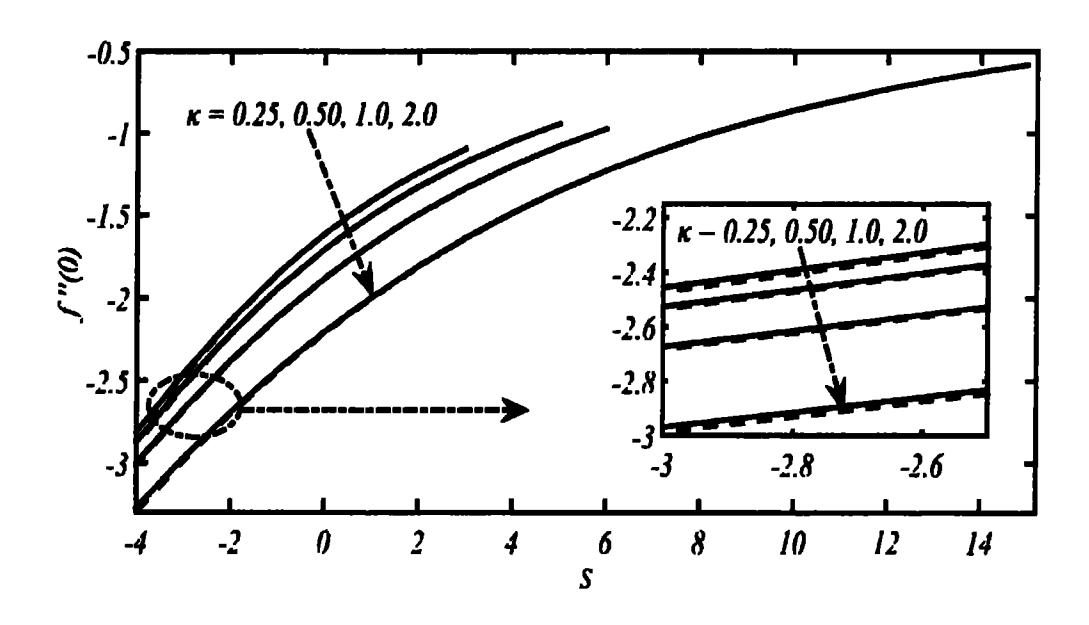


Fig. 4.3: Dual solutions shown by f''(0) for some selected values of  $\kappa$  as a function of suction/injection parameter S at m=3 (non-linear case).

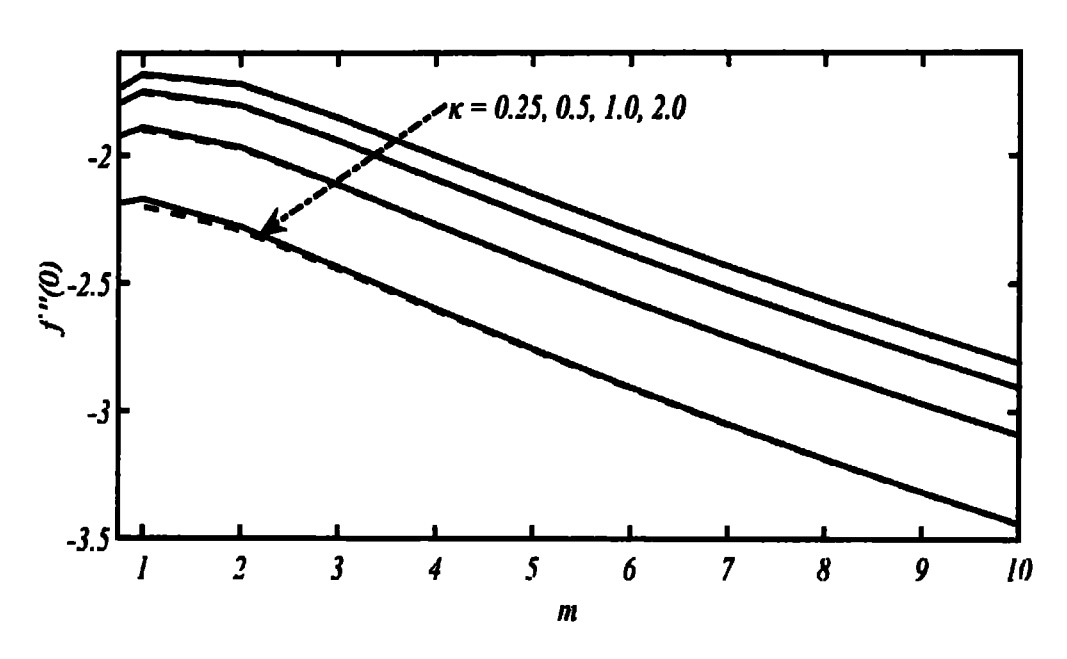


Fig. 4.4: Dual solutions shown for f''(0) as a function of m for various values of  $\kappa$  at S=-1.

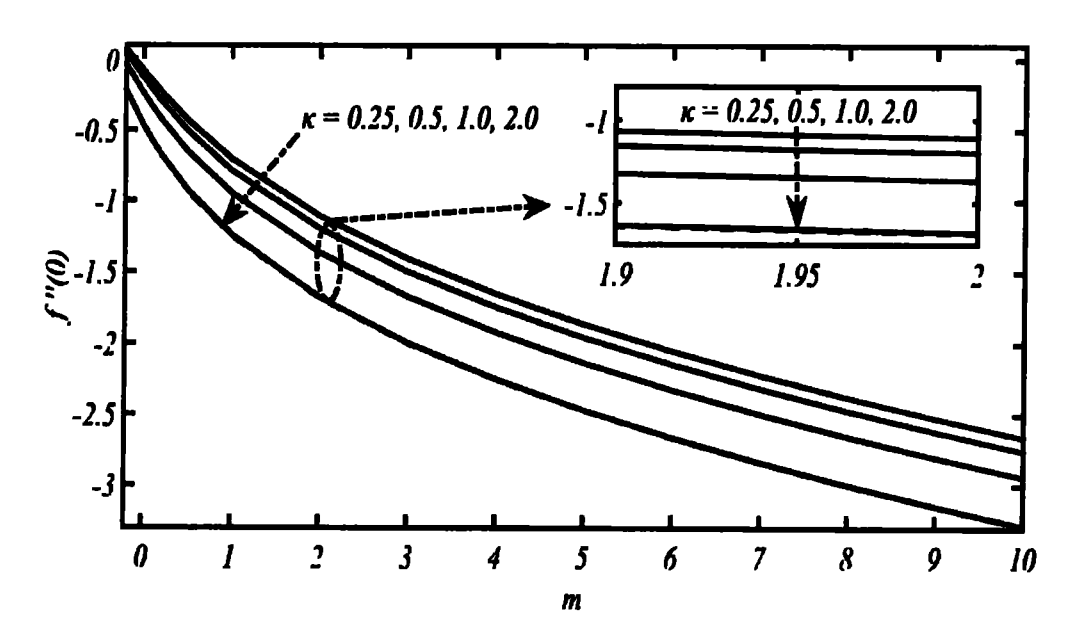


Fig. 4.5: Dual solutions shown for f''(0) as a function of m for various values of  $\kappa$  at S=1.

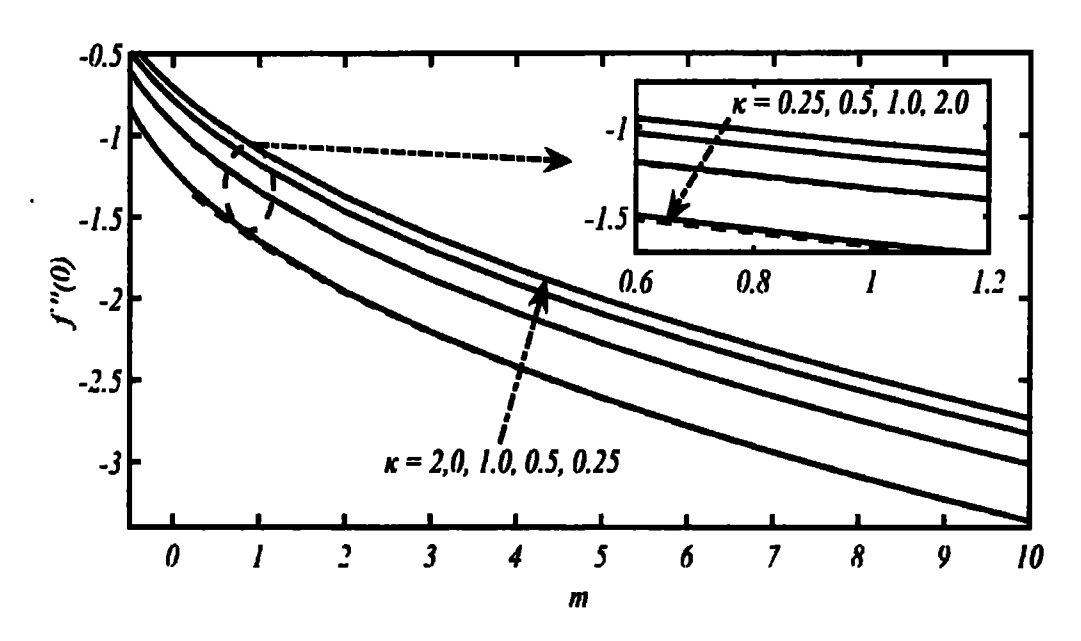


Fig. 4.6: Dual solutions shown for f''(0) as a function of m for various values of  $\kappa$  at S=0.

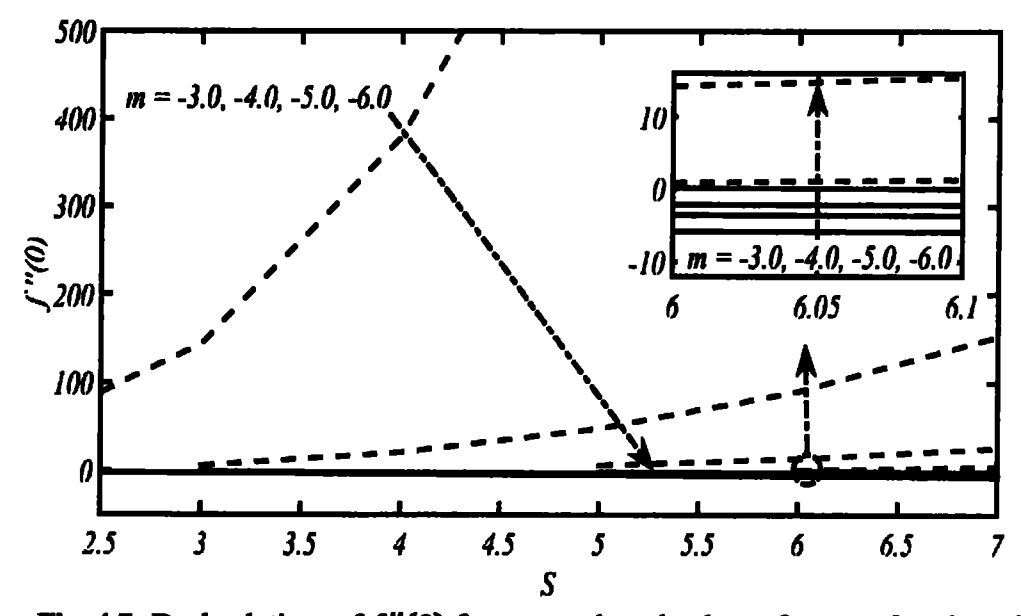


Fig. 4.7: Dual solutions of f''(0) for some selected values of m as a function of suction parameter S at  $\kappa = 0.25$ .

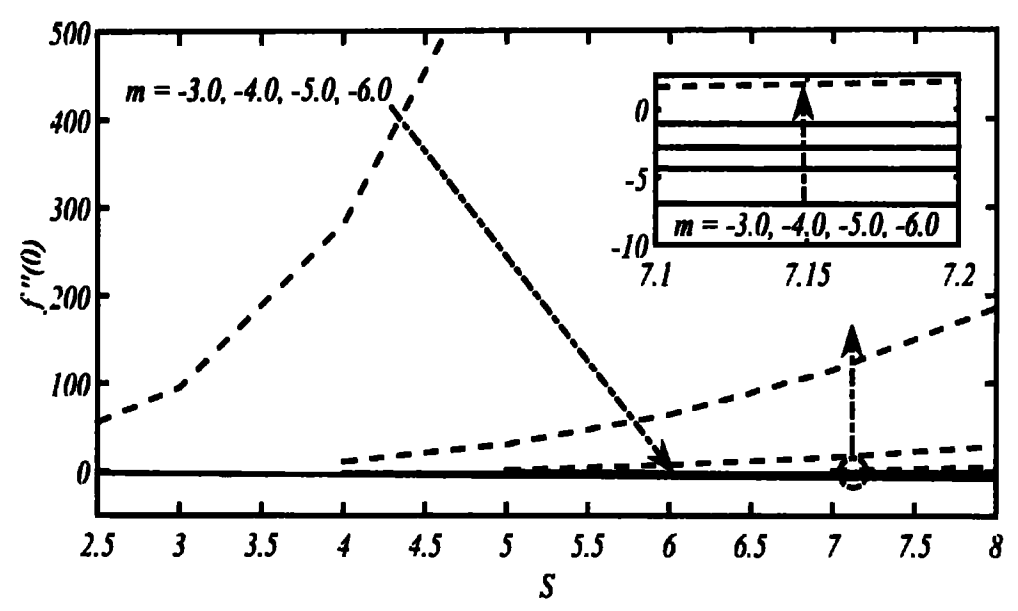


Fig. 4.8: Dual solutions of f''(0) for some selected values of m as a function of suction parameter S at  $\kappa = 0.50$ .

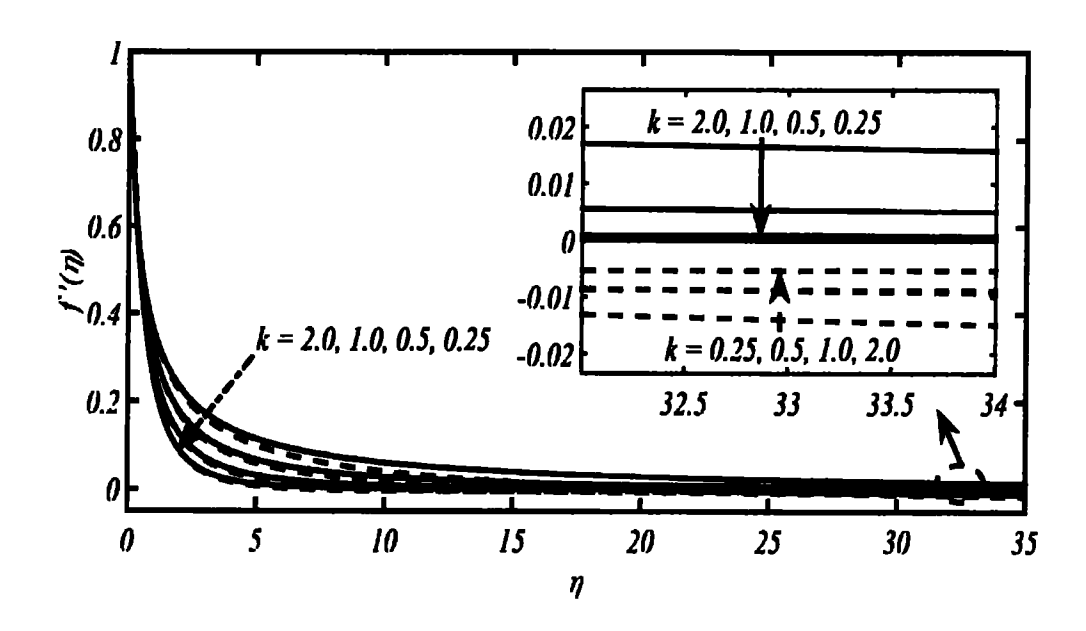


Fig. 4.7: Velocity profile for different values of curvature parameter at S = -1, for linear wall velocity.

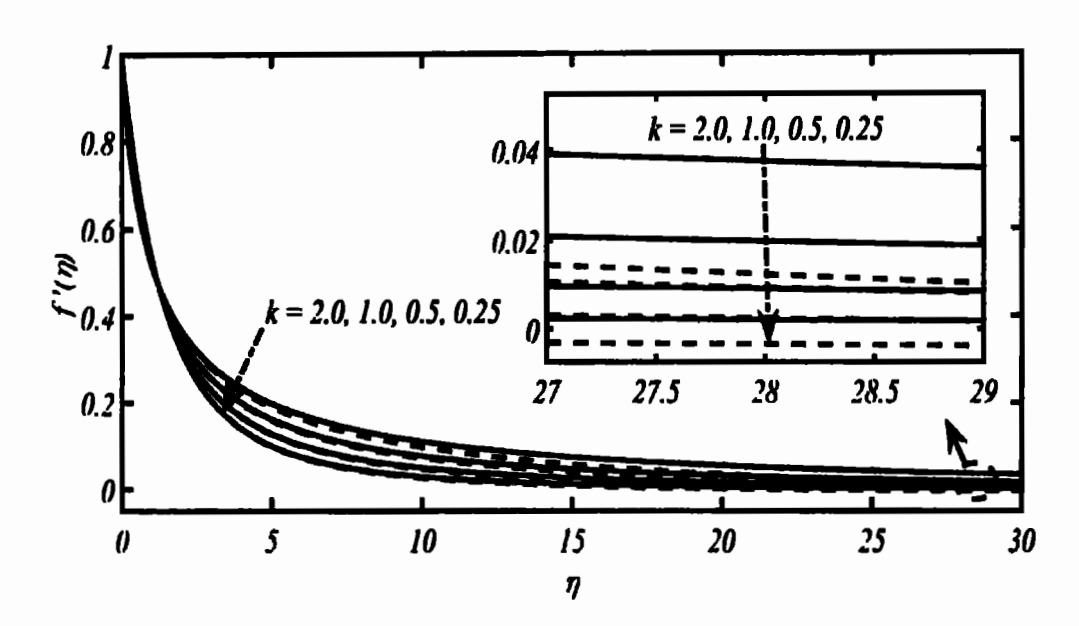


Fig. 4.8: Velocity profile for different values of curvature parameter at S=1, for linear wall velocity.

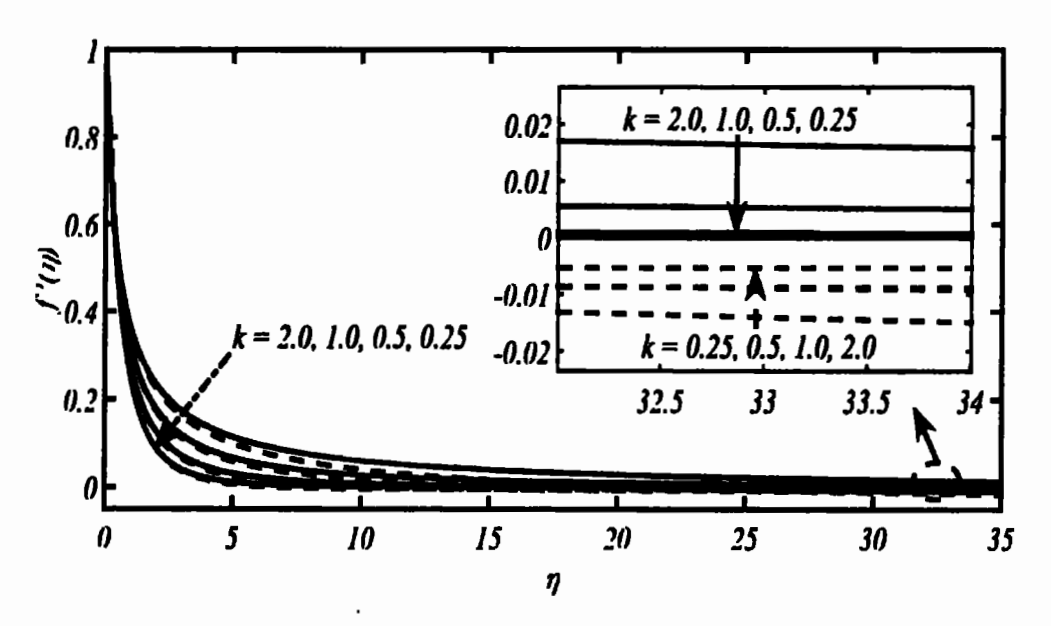


Fig. 4.9: Velocity profile for different values of curvature parameter in the absence of suction/injection for linear wall velocity.

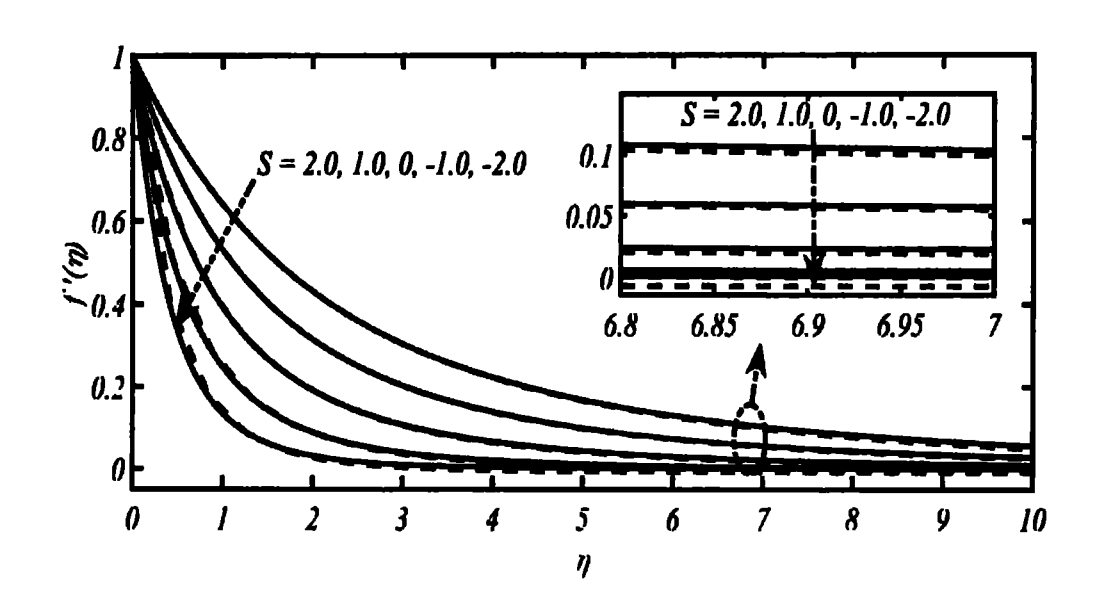


Fig. 4.10: Velocity profile for different values of suction/injection parameter at  $\kappa = 0.25$ , for linear wall velocity.

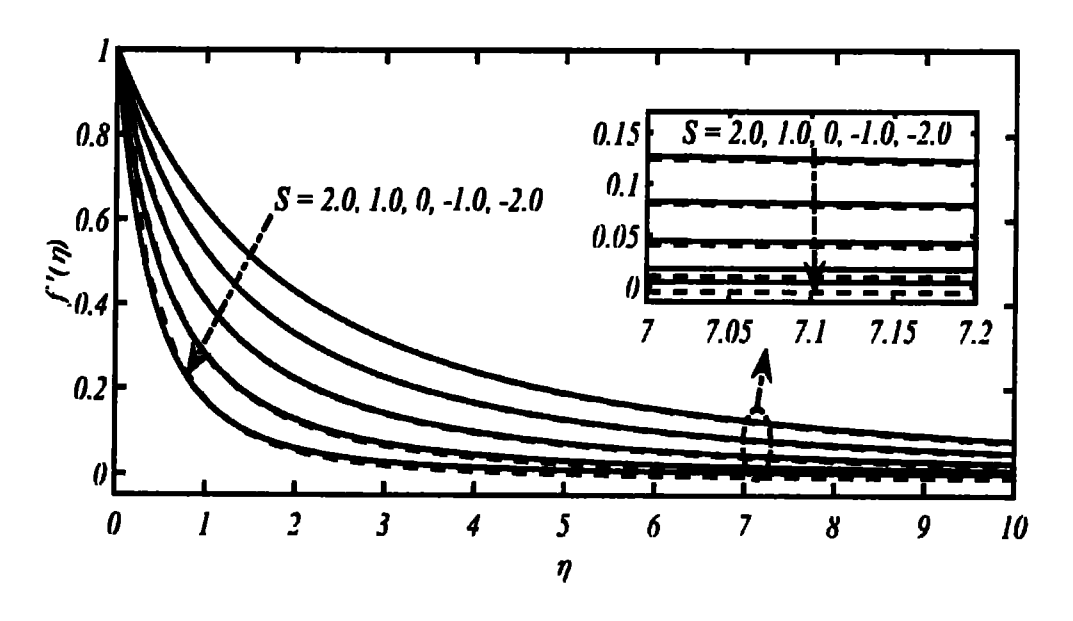


Fig. 4.11: Velocity profile for different values of suction/injection parameter at  $\kappa = 0.50$ , for linear wall velocity.

#### 4.1.3 Results and discussion

During the current analysis the dual solutions have been figured out in context to the involved physical parameters, where ever possible. In the while after figures, solid lines indicate first solution whereas second solution is represented by broken lines. Fig. 4.2 depicts the duality of solution for the case of linear stretching wall velocity (m = 1). It is depicted that the dual solutions occur for both suction and injection cases. It is clearly noted that for chosen values of  $\kappa$ , the magnitude of f''(0) starts decreasing by changing the domain from suction to injection regime where both the solutions become closer and closer to each other and ultimately become identical at some critical value of  $S = S_c$ . Such critical values have been computed very carefully beyond which the dual solutions seize to exist. After that a unique solution prevails to some extent by enhancing the injection effects as well as by magnifying the curvature parameter, which definitely reflect the supportive role of the surface transverse curvature (sees Tables 4.2 & 4.3). Obviously, for increasing values of the injection parameter, magnitude of coefficient of skin-friction also decreases, which is of course a well-known fact. It is also observed that there are slight variances in both branches of the solution and one has to put lot of efforts to capture the second solution. This might be the reason due to which very rear attempts were made in the past to figure out these solutions. The most interesting aspect, noted during the current investigation, is that the dual solutions are not only available for wall suction/injection cases but can also be seen in the case of no wall suction/injection velocity (i.e., S = 0). This is a big achievement because it was a well-established fact that the duality of solution is possible only when a sufficient amount of wall suction is provided.

The duality of solution is also observed for power-law wall velocity, for example, by taking m=3 (as displayed in Fig. 4.3). A similar behavior of two solutions can be observed as it was in the case of linear wall velocity, however, both solution branches converge more rapidly in this case as compared to linear wall velocity case. Interestingly, the domain of solution has been extended in this case (see Fig. 4.3) because of more accelerated nature of the flow. Now, the two solutions have become possible for some stronger wall injection velocities, as depicted in Fig. 4.3 and Table 4.3.

The information depicted in Figs. 4.2 & 4.3 and the data reported in Tables 4.2 & 4.3 provide an opportunity to make important findings towards the understanding of the facts behind the presence of non-unique solutions even for the wall injection case and no wall suction/injection. From Fig. 4.2 it is obvious that for increasing values of surface curvature parameter k the critical values of the injection parameter are also increased. That is, for the cases of large surface curvature the solution survives for some further larger values of the wall injection parameter. The same fact can also be seen and confirmed from Fig. 4.3. This means that the curvature parameter,  $\kappa$ , serves as a favorable pressure gradient which assists the boundary-layer to sustain against some further increased values of the injection velocity. Such an assistive role of  $\kappa$  has already been reported by Probstein and Elliott [57]. Another important observation noted from Figs. 4.2 & 4.3 and Tables 4.2 & 4.3, is that when the value of power-law exponent 'm' for stretching wall velocity is increased then solution becomes possible to exist for some increased values of the injection parameter. Obviously, reason behind this fact is that for higher values of m the stretching wall velocity becomes higher accordingly which consequently strengthens the flow within the boundary-layer. Because of this strength the

flow becomes able to sustain against further higher values of the injection velocity. In this regard the effects of linear and non-linear (accelerated) wall velocities, for some chosen values of S, over skin-friction coefficient are calculated for various values of  $\kappa$ . In Figs. 4.4–4.6 the solutions have been plotted against m for varied values of  $\kappa$  by choosing some selected values of S (i.e., -1, 0, 1). From these Figures it is obvious that the dual solutions are sighted in the presence of suction/injection effects, however, only unique solution becomes possible for sufficiently small values of m. The numerical data corresponding to these situations is reported in Tables 4.4-4.6. From this data one can again see that the difference between the two solutions is quite small which poses a serious challenge towards the capturing of second solution. For wall suction/injection cases the second solution disappears for m < 1, whereas in the absence of wall suction/injection situations (i.e., S = 0), it is possible to capture dual solutions, to some extent, against sufficiently small values of m by enhancing the values of curvature parameter,  $\kappa$ . This is again because of the assistive role of the curvature parameter in weakly accelerated flow. The current study also included an analysis regarding decelerated nature of wall velocity. In this regard, quite interesting information has been captured about the flow caused by steady stretching cylinder with retarded nature of wall velocity. In this context, dual solutions are reported in Figs. 4.7-4.8 and the corresponding numerical results are pre presented in Tables 4.7-4.8.

Velocity curves, especially for the second solution have been plotted for selected values of  $\kappa$  in the absence as well as in the presence of suction/injection in Figs. 4.9-4.11, while the behavior of velocity profiles for some chosen values of S, is displayed in Figs. 4.12-4.13. All the Figures ensure the existence of dual solutions;

moreover smooth patterns are noted for both branches of solution therein. From Figs. 4.9-4.11, one can easily observe that the boundary-layer thickness amplifies for higher values of curvature parameter. In Figs. 4.12-4.13, it is noticed that as the role of S is shifted from suction to injection velocity; the boundary-layer thickness amplifies significantly.

## 4.2 Unsteady boundary-layer flow past a stretching cylinder

Since the presentation of the duality of solution for axisymmetric flow due to a stretching cylinder is the primary focus of this chapter, therefore, in the continuation of above section, this section investigates the existence of dual/multiple solutions for the unsteady self-similar flow due to a stretching cylinder. It is found that corresponding to different values of the curvature parameter dual solutions exist with and without the suction/injection effects. This shows that the surface curvature is served as a supporting agent for the existence of dual solutions. The dual solutions are captured numerically and portrayed in the form of graphs and Tables. It is worth noting aspect that the present investigation is unique because of significant outcomes about the stretching cylinder that have never been visualized. Important findings of this study are believed to be helpful in further understanding about the nature of flow and as well as the associated non-linear flow phenomenon, therein.

#### 4.2.1 Mathematical formulation

Consider a long continuous circular cylinder, placed horizontally in an incompressible, viscous fluid. It is supposed that the system is at rest, initially, i.e., for  $t \le 0$ , both the fluid and cylinder are stationary. For admissibility of normal wall velocity the cylinder surface is taken as porous. During the entire flow phenomenon, there is no

influence of body force and pressure-gradient, at all. Under the role of above assumptions, the equation of continuity will remain the same as given in steady case (Eq. (4.1)), while the equation of motion, in cylindrical coordinates, is described by the following form:

$$\frac{\partial u}{\partial t} + u \frac{\partial u}{\partial z} + v \frac{\partial u}{\partial r} = v \frac{1}{r} \frac{\partial}{\partial r} (r \frac{\partial u}{\partial r}). \tag{4.14}$$

Due to a sudden motion (linear stretching) of the cylinder, the unsteady stretching wall velocity is assumed of the form

$$u_{\mathbf{w}}(z,t) = \frac{az}{\tau}; \quad a > 0; \quad \tau = at.$$
 (4.15)

For such kind of wall velocity, similarity solution exists if the cylinder's radius expands continuously following a form given by

$$R(z,t) = R_0 \tau^{1/2}. (4.16)$$

The flow stimulated by stretching cylinder of time dependent radius (expanding with time), was also investigated by Fang et al. [67]. The corresponding initial conditions, which are also the ambient conditions, for the flow under consideration are given by

at 
$$t \le 0$$
:  $u = 0$ ,  $v = 0$ ,  $\forall (r, z)$  (4.17)

The impulsive start of the cylinder results in a sudden motion of the fluid and consequently boundary-layer develops in time according to the relation " $\sim \sqrt{\nu}$ " which is also similar to the classical Rayleigh's problem. Since the surface of the cylinder is taken as permeable that enables the normal flow through itself. For the time t > 0, the resultant boundary conditions can be taken as

$$u = u_w(z, t), \quad v = v_w(z, t), \quad \text{at } z = R(z, t),$$
 (4.18)

$$u \to 0$$
, as  $z \to \infty$ . (4.19)

Here, it is a worth mentioning fact that for the existence of self-similar solution, the normal wall velocity should be of the form  $v_w(z,t) = d\tau^{-1/2}$  (where d is a constant and its positive/negative values designate the time dependent injection/suction velocity, respectively). A meticulous description regarding this fact can be seen in [56], wherein the author also presented a detailed criterion of self-similar formation of the problem. The similarity variables for an unsteady shrinking cylinder, considered during the current investigation, are of the form:

$$\eta = \frac{1}{\sqrt{vt}}r, \quad u = \frac{z}{t\eta}f'(\eta), \quad v = -\sqrt{\frac{v}{t}}\frac{1}{\eta}f(\eta). \tag{4.20}$$

Obviously, the above similarity transformations satisfy the continuity equation identically and their utilization in Eq. (4.14) and Eqs. (4.17)—(4.19) enables one to obtain the following form:

$$\frac{1}{2}\left(\frac{f'}{\eta} + f''\right) + \left(\frac{f'}{\eta}\right)^2 - \frac{f}{\eta}\left(\frac{f''}{\eta} - \frac{f'}{\eta^2}\right) = \frac{1}{\eta}\frac{d}{d\eta}\left(\eta\frac{d}{d\eta}\left(\frac{f'}{\eta}\right)\right),\tag{4.21}$$

$$f' = Re_{R_0}, \qquad f = -\frac{d}{\sqrt{\alpha \nu}} Re_{R_0}, \qquad \text{at} \quad \eta = Re_{R_0}$$

$$f' = 0, \qquad \qquad \text{at} \quad \eta = \infty$$

$$(4.22)$$

Here it is interesting to note that the initial condition and the boundary condition referred in Eq. (4.17) and Eq. (4.19), are merged to a single one, i.e.,  $f'(\infty) = 0$ . With the aid of transformation  $\bar{\eta} = (\eta^2 - Re^2_{R_0})/(2Re_{R_0})$  as well as some appropriate scaling of the function (i.e.,  $\bar{f} = \kappa f$ ), the system of equations (4.21)–(4.22) can be converted in a more compatible form so that numerical solution becomes quite feasible. The above mentioned transformation not only reshapes the domain from  $[Re_{R_0}, \infty)$  to  $[0, \infty)$  but also models the Eqs. (4.21)–(4.22) to the form (after dropping the bars):

$$((1+2\kappa\eta)f'')' = f'(f'-1) - (\frac{1}{2k}(1+2\kappa\eta) + f)f'', \tag{4.23}$$

$$f'(0) = 1, f(0) = -S, f'(\infty) = 0,$$
 (4.24)

where  $\kappa = \frac{1}{Re_{R_0}}$ ;  $Re_{R_0} = \sqrt{\frac{aR_0^2}{v}}$  denotes the surface curvature parameter, and  $s = \frac{d}{\sqrt{av}}$  denotes the suction/injection parameter. The values S > 0 correspond to wall injection while the values S < 0 refer to wall suction situation. The small values of  $\kappa$  define larger radius while the greater values of  $\kappa$  represent the cylinder with small radius. Therefore, by considering the larger values of  $\kappa$  (i.  $e \kappa > 1$ ) an exact understanding of the effects of surface curvature can be achieved.

#### 4.2.2 Numerical solution

The goal of current study has achieved, by solving the system of Eqs. (4.23)—(4.24) with the aid of Runge-Kutta shooting method. The results captured during the present analysis are given in Tables 4.7—4.8 and are also displayed graphically in Figs. 4.12—4.15.

**Table 4.9:** Values of -f''(0) as a function of S at various values of  $\kappa$ .

S	K =	0.25	ĸ=	0.5	K =	0.75	K =	1.0	K =	1.5
	1st sol.	2 <sup>nd</sup> sol.	1ª sol.	2 <sup>nd</sup> sol	1ª sol.	2 <sup>nd</sup> sol.	1sol.	2ªd sol.	1ª sol.	2 <sup>nd</sup> sol.
-10.0	12.0842	156.8071	11.0939	95.1697	10.7659	70.0250	10.6034	56.1938	10.4443	41.5483
-9.0	12.0842	127.4717	10.1035	77.1900	9.7766	57.1571	9.6151	46.1532	9.4577	34.4830
-8.0	10.1009	101.9822	9.11522	61.4704	8.7899	45.8007	8.6297	37.2398	8.4747	28.1710
-7.0	9.1121	80.1185	8.1298	47.9521	7.8067	35.9506	7.6483	22.80.42	7.4969	22.6201
-6.0	8.1259	61.6415	7.1485	36.5430	6.8286	27.5750	6.6729	22.80.42	6.5267	17.8264
-5.0	7.1435	46.2945	6.1733	27.1190	5.8581	20.6134	5.7064	17.2314	5.5683	13.7715
-4.0	6.1665	33.8051	5.2072	19.5262	4.8995	14.9753	4.7544	12.6874	4.6292	10.4190
-3.0	5.1979	23.8854	4.2561	13.5842	3.9608	10.5425	3.8266	9.0844	3.7220	7.7138
-2.0	4.2427	16.2356	3.3307	9.0899	3.0567	7.1709	2.9407	6.3134	2.8683	5.5824
-1.0	3.3103	10.5436	2.4515	5.8207	2.2143	4.6958	2.1271	4.2461	2.0994	3.9366
0.0	2.4194	6.4881	1.6563	3.5407	1.4767	1.7299	1.4281	2.7427	1.4497	2.6857
1.0	1.6064	3.7411	1.0000	2.0150	0.8958	1.7299	0.8820	1.6772	0.9422	1.7537
2.0	0.9311	1.9804	0.5291	1.0434	0.4849	0.9367	0.5000	0.9545	0.5768	1.0851
3.0	0.4540	0.9259	0.2434	0.4776	0.2367	0.4587	0.2605	0.5004	0.3333	0.6330
4.0	0.1820	0.3652	0.0972	0.1906	0.1043	0.2024	0.1251	0.2413	0.1822	0.3483
5.0	0.0593	0.1181	0.0338	0.0662	0.0415	0.0806	0.0557	0.1075	0.0945	01815
9.2493	0.0000	0.0000	0.0000	0.0001	0.0003	0.0006	0.0008	0.0016	0.0034	0.0067
9.6204			0.0000	0.0000	0.0001	0.0003	0.0005	0.0010	0.0025	0.0048
10.5683					0.0000	0.0000	0.0001	0.0003	0.0010	0.0020
11.6210							0.0000	0.0000	0.0004	0.0008
13.7621									0.0000	0.0000

**Table 4.10:** Values of -f''(0) as a function of  $\kappa$  at various values of S.

	<b>S</b> =	2.0	<i>S</i> =	1.0	S =	= 0.0	<b>S</b> =	-1.0	<b>S</b> =	-2.0
K	1ª Sol.	2 <sup>nd</sup> Sol.	1 <sup>st</sup> Sol.	2ª Sol	1ª SoL	2 <sup>nd</sup> Sol.	1ª Sol	2 <sup>nd</sup> Sol.	1 <sup>st</sup> Sol.	2 <sup>nd</sup> Sol.
0.009	53.5742	11551.16	54.5738	12165.573	55.5735	12800.9569	56.5732	13457.600	57.5729	14135.850
0.010	48.0208	8493.222	49.0204	8006.4913	50.0199	9518.8541	51.0196	10060.609	52.0192	10622.116
0.025	18.0554	578.7834	19.0524	667.0329	20.0498	763.7360	21.0475	869.2564	22.0453	983.9553
0.050	8.1229	76.9417	9.1097	100.6221	10.0990	128.8128	11.0902	161.8987	12.0828	200.2598
0.075	4.8709	24.8957	5.8376	36.0585	6.8134	50.3174	7.7951	68.0626	8.7807	89.6781
0.100	3.2989	11.8384	4.2351	18.5316	5.1927	27.5855	6.1627	39.3875	7.1406	54.3186
0.25	0.9311	1.9804	1.6064	3.7311	2.4194	6.4881	3.3103	10.5436	4.2427	16.2356
0.5	0.4983	1.0435	1.0000	2.0150	1.6563	3.5408	2.4516	5.8207	3.3307	9.0898
1.0	0.5000	0.9546	0.8820	1.6771	1.4281	2.7427	2.1271	4.2460	2.9407	6.3134
2.0	0.6727	1.2527	1.0355	1.9031	1.5243	2.7717	2.1429	3.8951_	2.8778	5.3231
3.0	0.8775	1.6114	1.2451	2.2520	1.7167	3.0591	2.2976	4.0518	2.9834	5.2555
4.0	1.0846	1.9716	1.4591	2.6118	1.9231	3.3885	2.4818	4.3135	3.1339	5.4016
5.0	1.2896	2.3262	1.6705	2.9682	2.1308	3.7268	2.6746	4.6100	3.3022	5.627
6.0	1.4917	2.6751	1.8784	3.3199	2.3365	4.0668	2.8700	4.921	3.4789	5.891
7.0	1.6912	3.0205	2.0830	3.668	2.5401	4.408	3.0655	5.243	3.6603	6.179
8.0	1.8886	3.3663	2.2852	4.018	2.741	4.753				
9.0	2.084	3.715	2.485	4.372	2.942				-	
10	2.280	4.071	2.685							

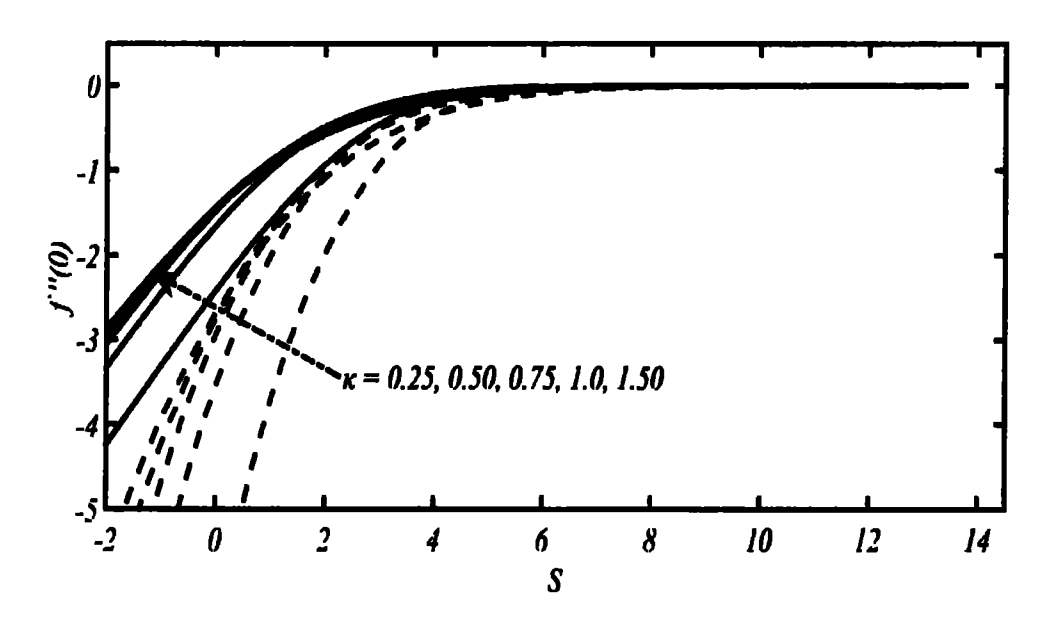


Fig. 4.14: Dual solutions domain of f''(0) for different values of curvature parameter  $\kappa$  as function of suction/injection parameter S.

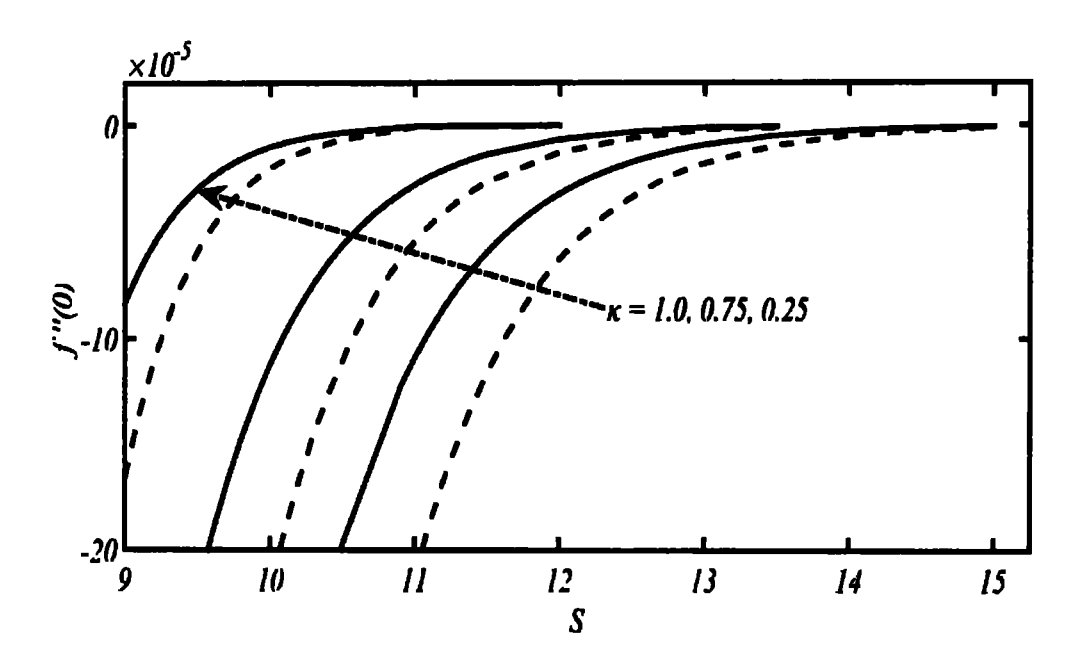


Fig. 4.15: A zoom-in portion of Fig. 4.14 showing the convergence of both solutions.

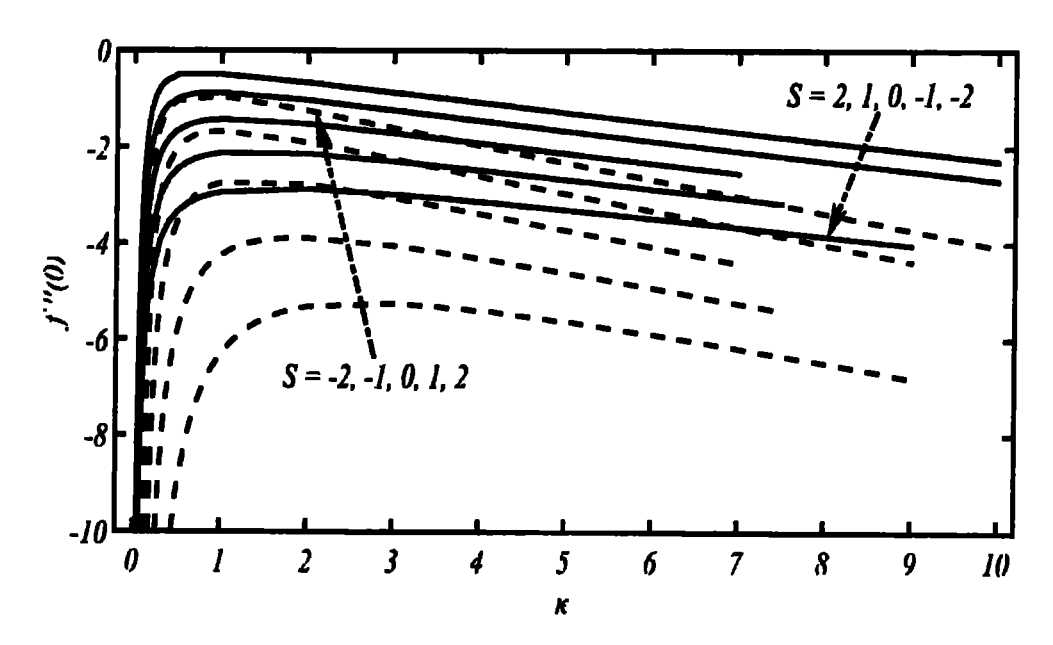


Fig. 4.16: Dual solutions domain of f''(0) for different values of suction/injection parameter against curvature parameter  $\kappa$ .

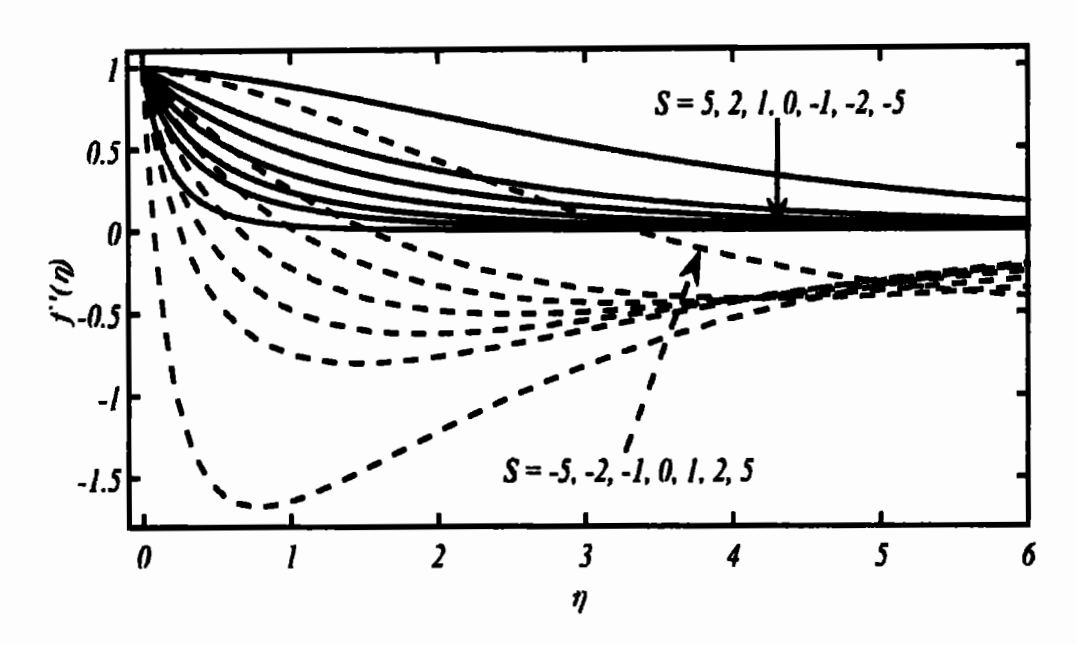


Fig. 4.17: Velocity profile under different values of suction/injection parameter at  $\kappa = 1$ .

#### 4.2.3 Results and discussion

The present study also highlights the effects of surface curvature as well as suction/injection parameters upon the flow caused by unsteady stretching cylinder. During the analysis, it is noted that the solution is possible for all values of  $\kappa$  i.e.,  $\kappa \geq 0$ . Further, for suction/injection parameter, the solution is not possible for all values of S (i.e.  $S \in R$ ) and exists only for certain ranges of S, which are calculated for some chosen values of  $\kappa$ . The numerical results are presented in tabular form and portrayed graphically in the upcoming figures, where solid lines correspond to first solution and broken lines represent the second solution. Fig. 4.14 is plotted against S for some selected values of curvature parameter,  $\kappa$ , where it is clearly observed that, for both branches the magnitude of skin-friction coefficient, f''(0), becomes higher and higher with the increasing values of  $\kappa$ . The effects of curvature parameter are more prominent for second

solution. To illustrate it more clearly Fig. 4.15 is drawn, which is a zoom-in part of Fig. 4.14, wherein it is also depicted that the dual solutions exist not only for suction velocity but also under the injection effects. Interesting character of the injection velocity is also highlighted in Fig. 4.15, wherein the situation has become more visible. With the increasing effects of injection, the two branches of solution come closer and closer and exhibit minor variations. The situation becomes more interesting when, for a particular value of  $\kappa$ , both solutions get converged at some critical point  $(S_c)$  and present a unique solution, no further solution is possible for  $|S| > |S_c|$ . The critical values, at which both solutions overlap to each other, are obtained with due care and presented in Table 4.9. It is also noted that as surface curvature increases more injection is required for achieving the critical point. It is observed that, by increasing the surface curvature effects, the flow separation can be delayed to some extent; however, both solutions ultimately overlap and dual solution ceases to exist under further increasing effects of wall injection. Similar findings were also reported by Tabassum et al. [82]. From the results presented in Table 4.10, it is revealed that there are less variations between the solutions for the case of injection; however, for suction domain the difference between the two branches becomes wider and significant. Figs. 4.14-4.15 portray these aspects with concrete visibility. Furthermore, the magnitudes of both solutions are amplified as the effects of suction become stronger and stronger. However, as the values of surface curvature parameter increase the magnitudes of both solutions are reduced accordingly.

Due to dominant role of the surface curvature, its effects are also investigated at some selected values of S, and the corresponding results are mentioned in Table 4.10 and are displayed in Fig. 4.16. It is realized that for some fixed value of S the magnitude of

f''(0) decreases with the increasing value of surface curvature. In case of suction, this situation is seen to happen much earlier than injection case. A more valuable finding of the current study is the existence of dual solutions in the absence of suction/injection parameter. The presence of dual solution for S=0, is a unique feature of this investigation, as, it is commonly believed that a sufficient amount of suction is mandatory for the existence of dual solutions. During the entire study it is well perceived that although the magnitude of f''(0) approaches to zero as  $S \to S_c$  but it never become positive. With further enhancement of injection effects, the boundary-layer thickness becomes too smaller and ultimately resulted in disappearance of boundary-layer flow.

To complete the understanding of flow behavior, velocity profiles are plotted against  $\eta$  for some selected values of S in Fig. 4.17. It is clearly observed that with the enhancement of the injection velocity the boundary-layer thickness magnifies to a great extent. Although, a prominent increment in boundary-layer thickness is noted for both branches of solution, however the second solution branch shows magnificent change in its behavior. It is depicted that, within the boundary-layer the second solution shows the presence of reverse flow for every value of S. Further, the existence of reverse flow begins from the lower-half and, with the increasing effects of suction it tends to be closer to the stretching boundary.

#### 4.3 Conclusion

Dual solutions found during this study are a unique feature of the current analysis which contradicts the well-established fact that the multiple solutions exist for shrinking surface flows only. The current study also discloses that the presence of suction/injection

velocity is not necessary for the occurrence of dual solutions. It is also shown that the dual solutions are also possible in the case of wall injection velocity. The outcomes of this investigation are expected to inspire the researchers in this area to further explore the hidden aspects of the boundary-layer flows of this nature. Numerical data reported in number of Tables is believed to serve as a good reference for further studies in this direction. On the basis of current results it is justified to state that the duality/multiplicity of solution of boundary-layer flows induced by continuous surfaces is neither a unique feature of shrinking surface flows, nor it can be attributed to the wall suction velocity, only. Hence, duality/multiplicity of solution is possible for shrinking surface flows as well as for the stretching surface flows, equally. This can possibly appear in the presence of wall suction; or wall injection, or even in the absence of wall suction/injection velocity.

In the case of unsteady stretching cylinder flow, the presence of non-unique solution is a unique feature of this study. It is a fact that the existing literature on the stretching surface flows did not experience the existence of dual solution. However, there is bulk of studies which openly neglect any possibility of dual solutions for the flows stimulated by stretching surfaces. In view of above this study is expected to serve as a mile stone in further refining the investigation of boundary-layer flows caused by axisymmetric stretching surfaces.

# Chapter 5

# Existence of multiple solutions for a shrinking cylinder flow

It has already been discussed in the planner case that the multiplicity/duality of solution is not confined to shrinking surfaces only and the provision of suction/injection is not obligatory for the existence of such solutions. In the current chapter, we shall focus to investigate the axisymmetric steady/unsteady flow phenomenon caused by shrinking cylinder and the possibility of dual solutions therein. Similar to planner case of self-similar flows caused by the shrinking surfaces, the axisymmetric flow is also studied under the consideration of various physical features. In the study of axisymmetric flows too, non-linear (power-law) wall velocity has been considered for the steady case and linear wall velocity is in the unsteady case. In both cases duality of solution has been witnessed under various circumstances.

## 5.1 Steady boundary-layer flow over a shrinking cylinder

The purpose of this investigation is the steady flow due to a permeable shrinking cylinder using the correct mathematical formulation proposed by Mehmood [56]. The effects of the shrinking parameter as well as the suction and curvature parameters are studied. As usual, similarity transformations are used to convert the governing partial differential equations to a set of nonlinear ordinary (similarity) differential equations which are then solved numerically by using the shooting method for various values of the involved parameters. It is observed that both the unique and multiple (dual) solutions are present for the flow phenomenon induced by a shrinking cylinder.

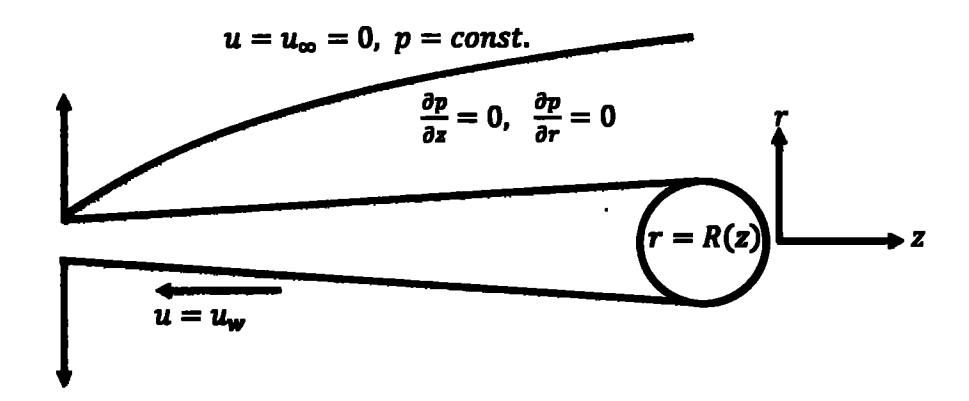


Fig. 5.1: Schematic of the axisymmetric flow and the associated coordinate system.

#### 5.1.1 Mathematical formulation

Consider a steady, incompressible viscous fluid flow caused by a continuous cylinder of radius R(z). It is supposed that the flow phenomenon, under consideration, experiences no circular rotation and has symmetry about z—axis. It is also assumed that there are no body forces as well as no pressure-gradient, therein. The governing system of this flow is the same as was for the stretching cylinder case given by Eqs. (4.1)—(4.2). Moreover, the similarity criterion for the shrinking wall velocity is also the same as for the stretching wall velocity. The only difference between these two flows is the opposite sign of wall velocities. For this case the similarity transformations are defined as

$$\eta = \sqrt{\frac{\bar{a}}{\nu}} z^{\frac{m-1}{2}} r$$
,  $u = \frac{\bar{a}z^m}{\eta} f'(\eta)$ ,  $v = \sqrt{\bar{a}v} z^{\frac{m-1}{2}} (\frac{f}{\eta} + \frac{m-1}{2} f')$ , (5.1)

due to which the equation of continuity (4.1) is satisfied identically and the momentum boundary-layer equation (4.2) and the boundary data are transformed as

$$\frac{f}{\eta} \left( \frac{f''}{\eta} - \frac{f'}{\eta^2} \right) - m \left( \frac{f'}{\eta} \right)^2 = \frac{1}{\eta} \frac{d}{d\eta} \left( \eta \frac{d}{d\eta} \left( \frac{f'}{\eta} \right) \right), \tag{5.2}$$

$$f' = Re_{R_0}, f = \frac{2S}{m+1}Re_{R_0}, at \eta = Re_{R_0}$$
  
 $f' = 0, at \eta = \infty$ 
(5.3)

where  $\Psi$  is the dimensionless stream function, given by

$$\Psi = \frac{-\sqrt{\bar{a}x^{m+1}\nu}}{n} rf(\eta). \tag{5.4}$$

In above system  $Re_{R_0} = \sqrt{\frac{\bar{a}R_0^2}{\nu}}$  is the Reynolds number based on the reference radius  $R_0$ ,  $\kappa = 1/Re_{R_0}$  is regarded as the surface transverse curvature parameter, and  $S = \frac{d}{\sqrt{\bar{a}\nu}}$  is the dimensionless suction/injection parameter: S > 0 corresponds to wall injection and S < 0 corresponds to wall suction velocity. To comply with the self-similarity criterion of this flow the wall suction velocity is chosen of the form  $v_w(z) = dz^{\frac{m-1}{2}}$ . During the study of flow phenomenon caused by shrinking surface, the shrinking rate is taken as  $a = -\bar{a}$  where  $\bar{a} > 0$  is the constant stretching rate. Eqs. (5.8) and (5.9) can be simplify by eliminating the involved variable  $\eta$  therein and the Reynolds number  $Re_{R_0}$  from the boundary conditions by using the following new variables

$$\bar{\eta} = \frac{\eta^2 - Re^2_{R_0}}{2Re_{R_0}}, \qquad f = \bar{f}Re_{R_0}.$$
 (5.5)

After dropping the bars the resulting equations can be presented as:

$$ff'' - mf'^2 = ((1 + 2\kappa\eta)f'')',$$
 (5.6)

$$f'(0) = 1,$$
  $f(0) = \frac{2S}{m+1},$   $f'(\infty) = 0.$  (5.7)

**Table 5.1:** Numerical values of -f''(0) against S for various values of  $\kappa$  at m=1.

S	κ =	0.10	$\kappa = 0.25$		$\kappa = 0.50$		$\kappa = 0.75$		$\kappa = 1.0$	
	1ª Sol.	2ª Sol	1 Sol	2ª Sol.	1ª Sol.	2ª Sol	1ª Sol.	2ª Sol	1" Sol.	2 <sup>nd</sup> Sol.
-2.4	1.8111	1.7881								
-2.5	1.9589	1.9350	1.8645	1.8256						
-3.0	2.5989	2.5651	2.5647	2.5259	2.4807	2.4176				
-3.5	3.1743	3.1255	3.1544	3.1026	3.1131	3.0480	3.0543	2.9615		
-4.0	3.7238	3.6557	3.7103	3.6408	3.6841	3.6036	3.6510	3.5522	3.6071	3.4794
-5.0	4.7865	4.6652	4.7789	4.6607	4.7649	4.6382	4.7488	4.6072	4.7299	4.5681
-6.0	5.8252	5.628	5.8203	5.6338	5.8115	5.6198	5.8016	5.5961	5.7905	5.5664
-8.0	7.8712	7.434	7.8687	7.474	7.8641	7.479	7.8592	7.464	7.8539	7.441
-10	9.8979	9.067	9.8963	9.173	9.8935	9.213	9.8905	9.212	9.8874	9.196

**Table 5.2:** Numerical values of -f''(0) against S for various values of  $\kappa$  at m=2.

	κ =	0.10	κ =	0.25	κ =	0.50	κ =	0.75	$\kappa = 1.0$	
S	I" Sol	2nd Sol	1ª SoL	2nd Sol	1ª Sol.	2 <sup>nd</sup> Sol.	1" Sol.	2 <sup>nd</sup> Sol.	I" Sol.	2 <sup>nd</sup> Sol.
-3.7	1.4189	0.7771								
-4.0	1.8494	0.4237	1.6434	-1.1758						
-5.0	2.7867	-0.7345	2.7438	-2.6406	2.6423	2.5428	1			
-5.5	3.1888	-1.6317	3.1589	-3.0234	3.0956	2.9899	3.0001	2.8579		
-6.0	3.5737	-2.8205	3.5511	-3.3731	3.5060	3.3814	3.4462	3.3125	3.3558	3.1718
-7.0	4.3138	-6.2046	4.2993	-4.0001	4.2719	4.0894	4.2391	4.0709	4.1982	4.0175
-8.0	5.0311	-11.123	5.0209	-4.5386	5.0020	4.7364	4.9804	4.7527	4.9552	4.7305
-10	6.4306	-26.475	6.4246	-5.3002	6.4139	5.8879	6.4021	5.9900	6.3890	6.0141

**Table 5.3:** Numerical values of f''(0) against S for various values of  $\kappa$  at m=1.

	S =	-3.0	S =	-4.0	S = -5.0		
K	1ª SoL	2 <sup>nd</sup> Sol.	1" Sol.	2 <sup>nd</sup> SoL	1ª Sol.	2 <sup>nd</sup> Sol.	
0.01	-2.6162	-2.5791	-3.7312	-3.6504	-4.7908	-4.6380	
0.05	-2.6087	-2.5749	-3.7280	-3.6573	-4.7889	-4.6606	
0.10	-2.5989	-2.5651	-3.7238	-3.6556	-4.7865	-4.6652	
0.20	-2.5770	-2.5404	-3.7150	-3.6467	-4.7815	-4.6635	
0.30	-2.5513	-2.5098	-3.7055	-3.6344	-4.7763	<b>-4.6571</b>	
0.40	-2.5203	-2.4710	-3.6953	-3.6200	-4.7708	-4.6484	
0.50	-2.4807	-2.4176	-3.6841	-3.6036	-4.7649	-4.6382	
0.60	-2.4238	-2.3308	-3.6719	-3.5850	-4.7588	-4.6267	
0.70			-3.658 <del>4</del>	-3.5639	-4.7522	-4.6140	
1.00			-3.6070	-3.4794	-4.7299	-4.5681	
1.25					-4.7074	<b>-4.519</b>	

**Table 5.4:** Numerical values of f''(0) against S for various values of  $\kappa$  at m=2.

	S =	-4.0	S =	<b>-5.0</b>	S = -6.0		
K	1" Sol.	2 <sup>nd</sup> SoL	1ª Sol.	2 <sup>nd</sup> Sol.	1ª Sol	2 <sup>nd</sup> Sol.	
0.01	-1.9144	0.1408	-2.8086	1.8261	-3.5859	4.5973	
0.05	-1.8879	-0.1243	<b>-2.7991</b>	1.3275	-3.5806	3.7990	
0.10	-1.8494	-0.4237	-2.7867	0.7345	-3.5737	2.8205	
0.20	-1.7402	-0.9336	-2.7591	-0.4810	3.5590	0.6329	
0.25	-1.6434	-1.1758	-2.7438	-2.6406	-3.5511	-3.3731	
0.30			-2.7272	-2.6325	-3.5430	-3.3880	
0.50			-2.6423	-2.5428	-3.5060	-3.3814	
0.60					-3.4844	-3.3604	
1.00					-3.3558	-3.1718	

**Table 5.5:** Numerical values of f''(0) as a function of S for various values of m at  $\kappa = 0.25$ .

S	m = -2.0		m = -3.0		m = -4.0		m = -5.0		m = -6.0	
	1st sol.	2nd sol	1st sol.	2nd sol.	1st sol.	2nd sol.	1st sol.	2nd sol.	1st sol.	2nd sol.
1	-2.2857		-1.8668	-1.8668	-1.9312	-1.9312	-2.0572	-	-2.1947	
2	-4.1333		-2.5154	-36.3802	-2.2800	-2.2804	-2.2951	-2.2951	-2.3756	-2.3756
3	-6.0869		-3.3481	-149.057	-2.7141	-9.1835	-2.5717	-2.5734	-2.5776	-2.5778
4	-8.0645		-4.2604	-386.22	-3.2259	-25.4071	-2.8919	-5.0285	-2.8033	-2.8114
5	-10.0512		-5.2074	<b>-794.81</b>	-3.7885	-53.7569	-3.2532	-10.6390	-3.0546	-3.8911
6	-12.0425		-6.1721	-1421.6	-4.3820	-97.820	-3.6467	-19.4413	-3.3304	-6.4974
7	-14.0364		-7.1470	-2313.6	-4.9951	-161.166	-4.0641	-32.1386	-3.6276	-10.4715
8	-16.0318		-8.1283	-3517.5	-5.6210	-247.36	-4.4988	-49.4734	-3.9423	-15.9480
9	-18.0283		-9.1138	-5079	-6.2557	-359.95	-4.9463	-72.1952	-4.2711	-23.1412
10	-20.0255		-10.1022	<b>-7048</b>	-6.8967	-502.52	-5.4034	-101.054	-4.6113	-32.2857

**Table 5.6:** Numerical values of f''(0) as a function of S for various values of m at  $\kappa = 0.50$ .

S	m = -2.0		m = -3.0		m = -4.0		m = -5.0		m = -6.0	
	1 <sup>st</sup> Sol.	2 <sup>nd</sup> Sol	1ª Sol.	2 Sol.	1ª Sol	2 <sup>nd</sup> Sol.	1ª Sol	2 <sup>nd</sup> Sol.	1" SoL	2nd Sol
1	-2.3334	1	<b>-1.95</b> 75	-1.9576	-2.0247	-2.0247	-2.1514	-2.1514	-2.2892	-2.2892
2	-4.1428		-2.5770	-17.7262	-2.3678	-2.3684	-2.3880	-2.3882	-2.4700	-2.4701
3	-6.0909	1	-3.3789	-98.888	-2.7834	-3.5187	-2.6584	-2.6593	-2.6697	-2.6700
4	-8.0666	1	-4.2778	-288.57	-3.2741	-14.5722	-2.9664	-2.9743	-2.8900	-2.8912
5	-10.0526		-5.2185	-633.85	-3.8220	-35.4921	-3.3130	-5.6588	-3.1326	-3.1381
6	-12.0434		-6.1797	-1181.5	-4.4062	-70.076	-3.6939	-11.7676	-3.3981	-3.7798
7	-14.0370		-7.1526	-1978.6	-5.0131	-121.90	-4.1014	-21.1969	-3.6851	-6.1601
8	-16.0322		-8.1325	-3071	-5.6349	-194.55	-4.5287	-34.6606	-3.9908	-9.9950
9	-18.0285		-9.1171	<b>-4507</b>	-6.2667	-291.57	-4.9707	-52.903	-4.3122	-15.3366
10	-20.0256		-10.1048	-6333	-6.9056	-416.52	-5.4235	-76.674	-4.6462	-22.3866

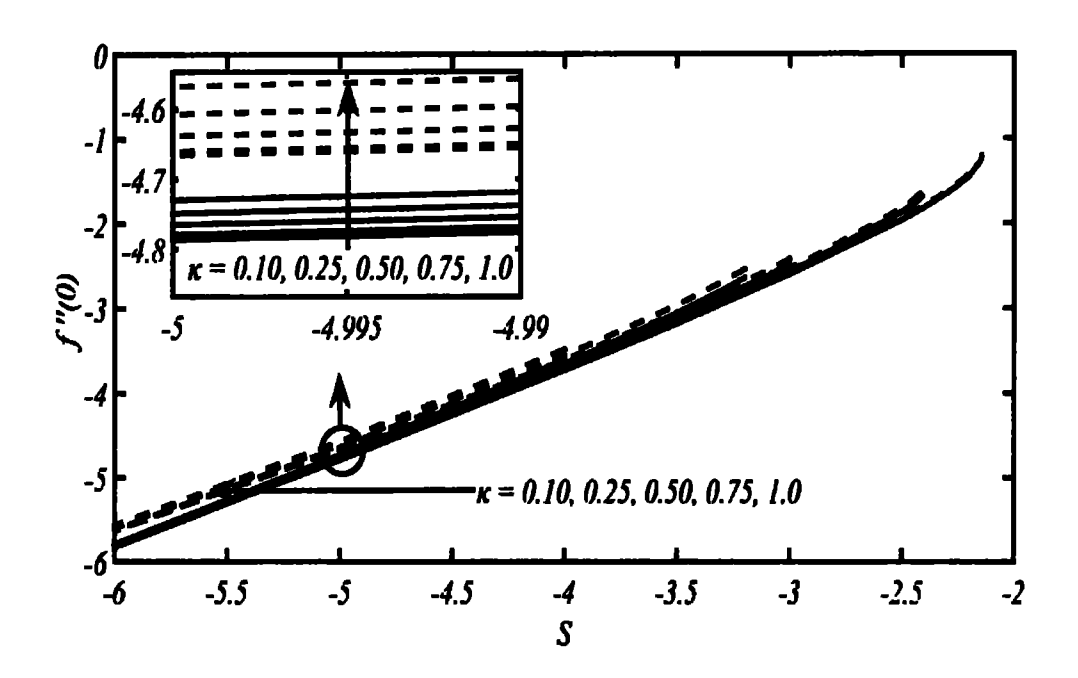


Fig. 5.2: Dual solutions domain of f''(0) for some selected values of curvature parameter  $\kappa$  as function of suction parameter S at m=1.

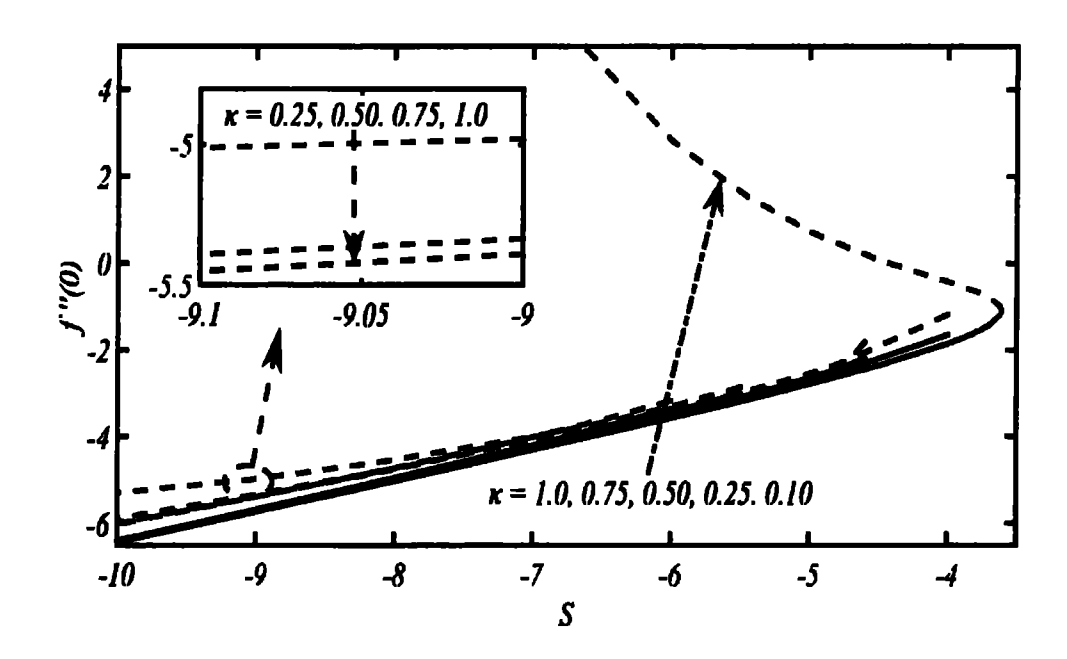


Fig. 5.3: Dual solutions domain of f''(0) for some selected values of curvature parameter  $\kappa$  as function of suction parameter S at m=2.

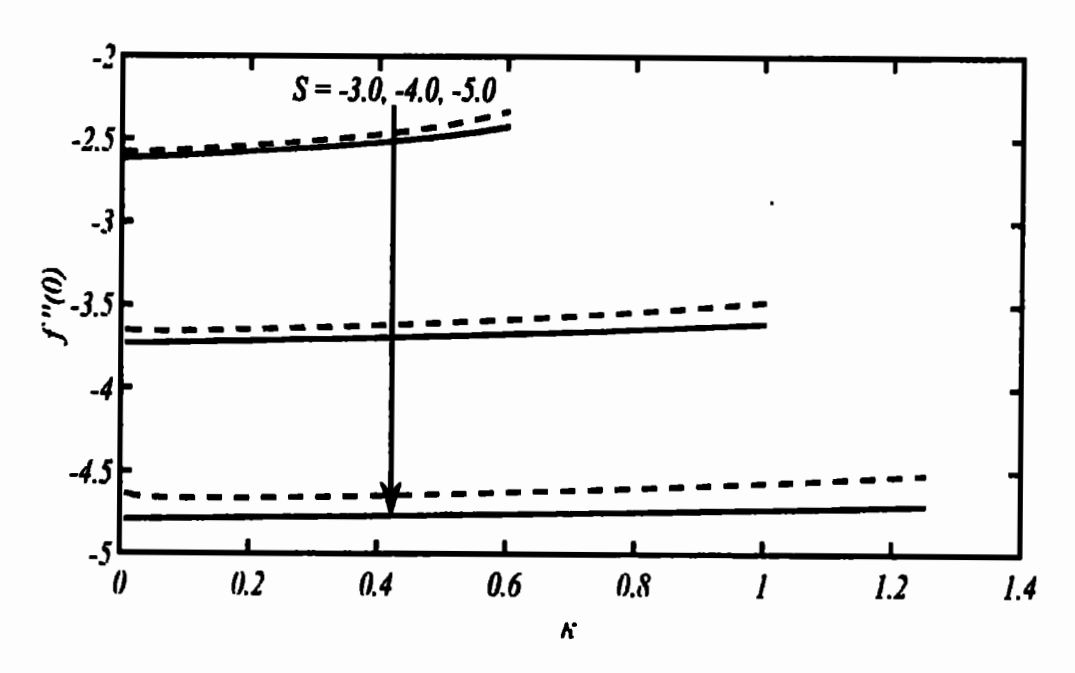


Fig. 5.4: Dual solutions domain of f''(0) for some selected values of suction parameter S as function of curvature parameter  $\kappa$  at m=1.

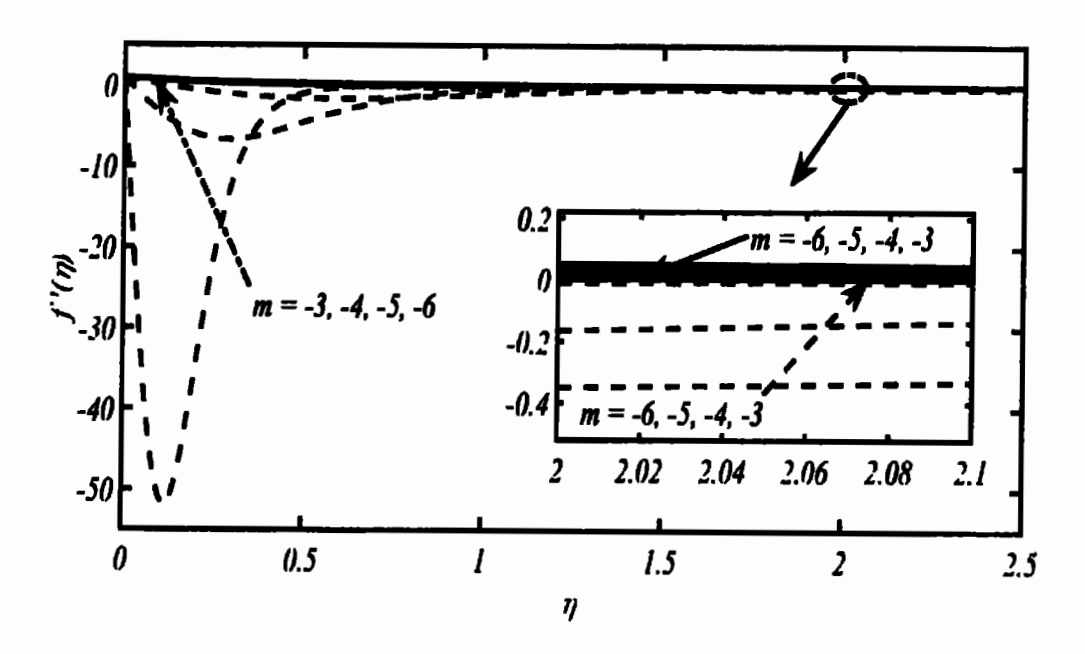


Fig. 5.5: Velocity profile for some selected values of m at  $\kappa = 0.25$  for S = 5.

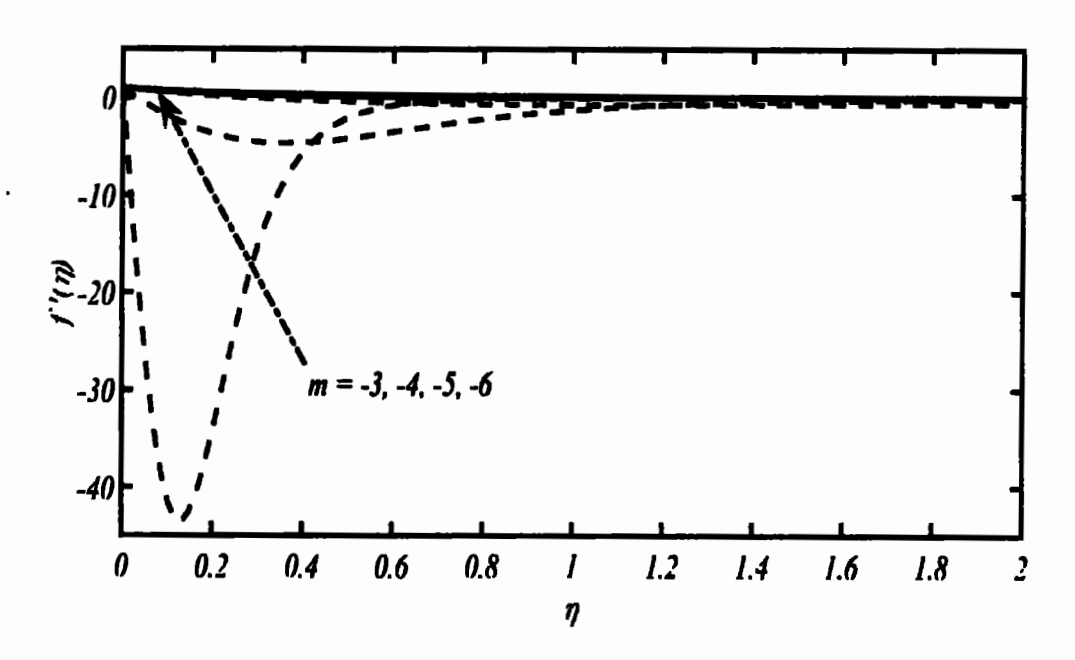


Fig. 5.6: Velocity profile for some selected values of m at  $\kappa = 0.50$  for S = 5.

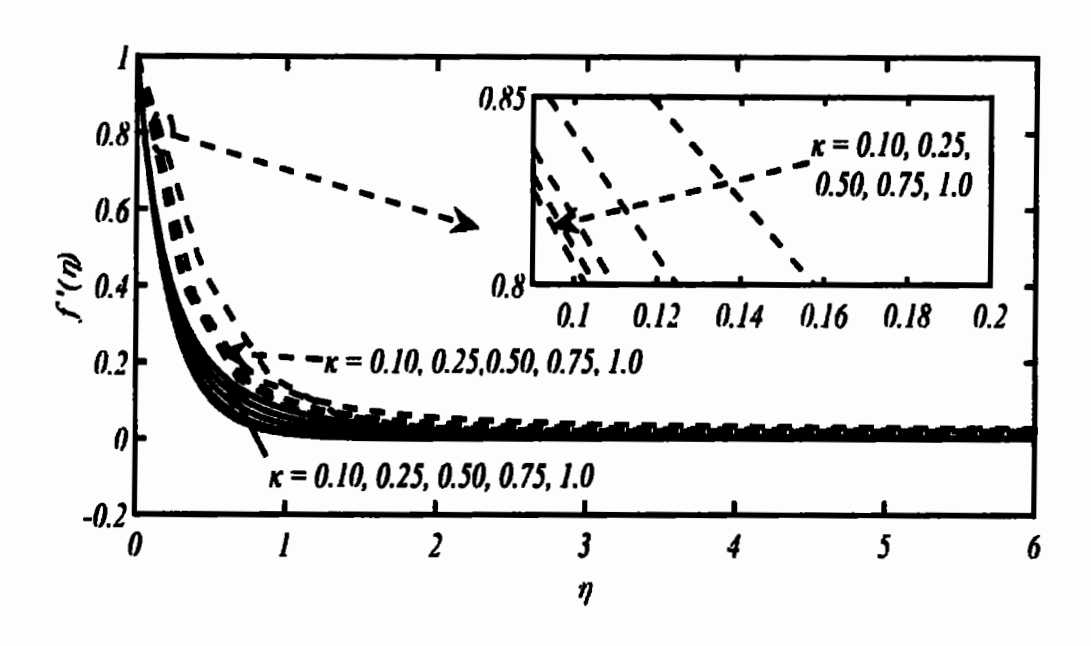


Fig. 5.7: Velocity profile for different values of curvature parameter at S=-5 for linear wall velocity.

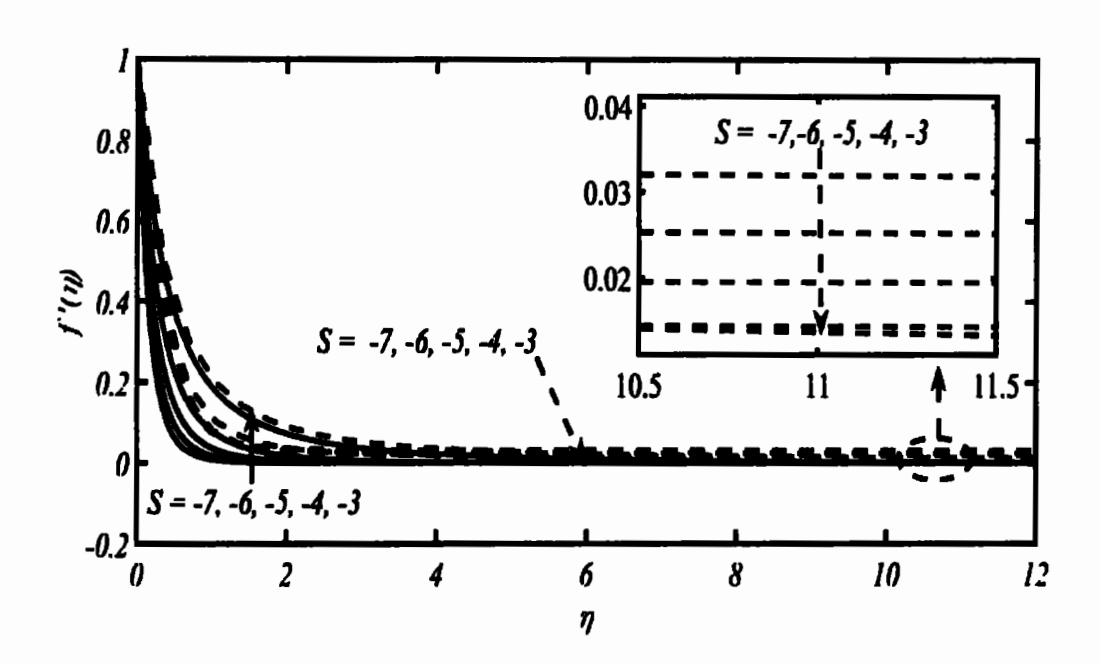


Fig. 5.8: Velocity profile for different values of suction parameter at  $\kappa = 0.25$  for linear case (m = 1).

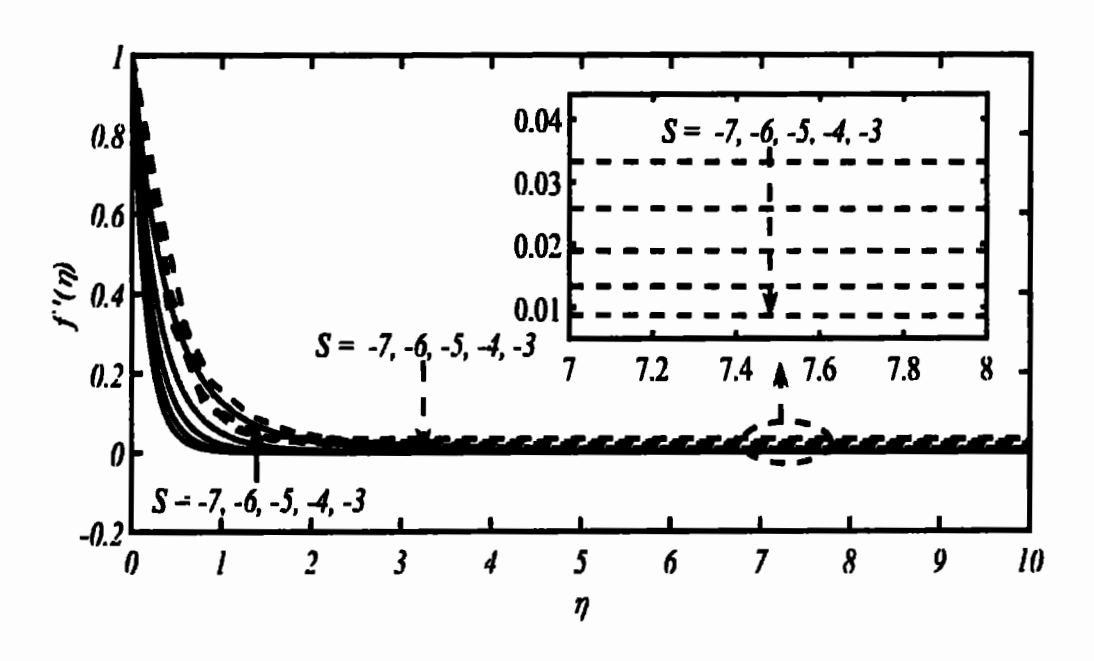


Fig. 5.9: Velocity profile for different values of suction parameter at  $\kappa = 0.50$  for linear case (m = 1).

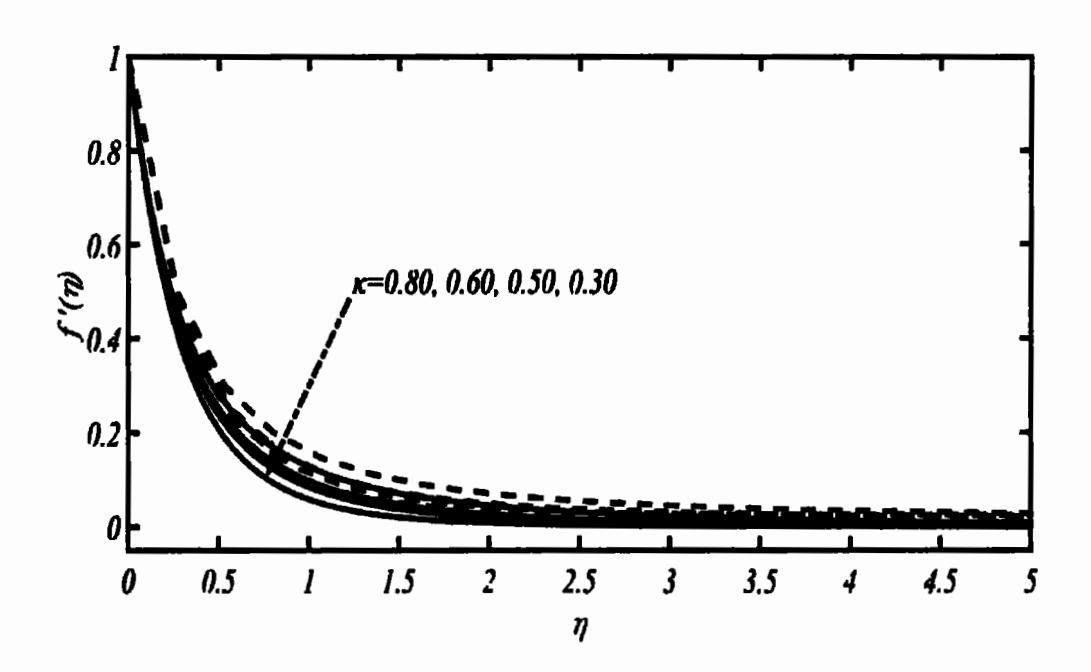


Fig. 5.10: Velocity profile for different values of curvature parameter at S=-6 for m=2.

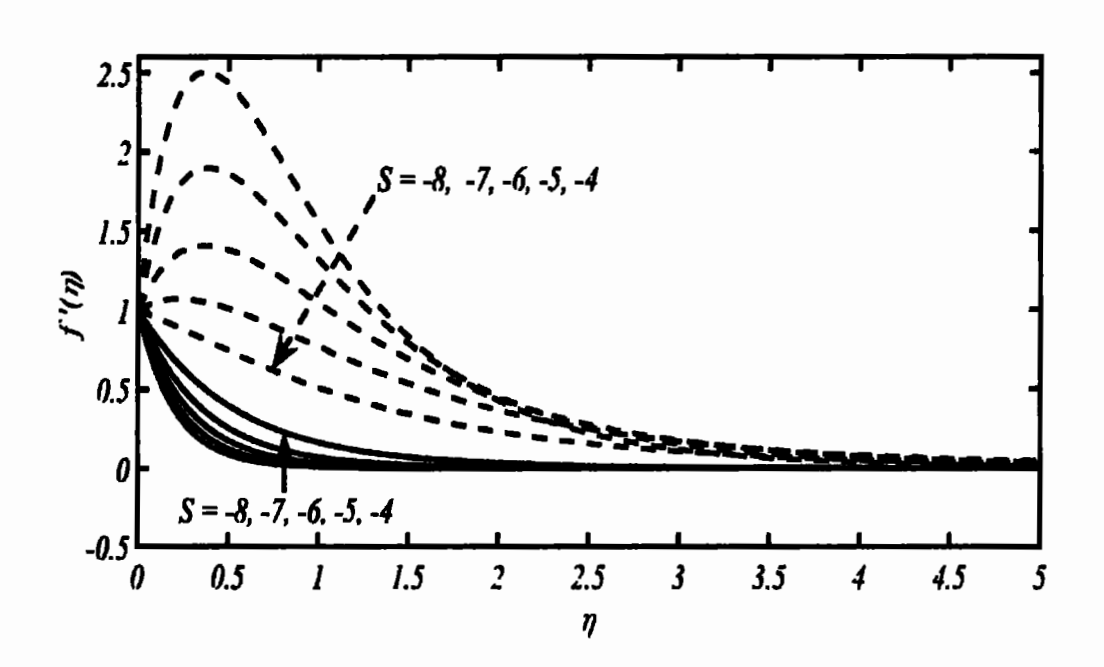


Fig. 5.11: Velocity profile for some selected values of S at  $\kappa = 0.10$  for m = 2.

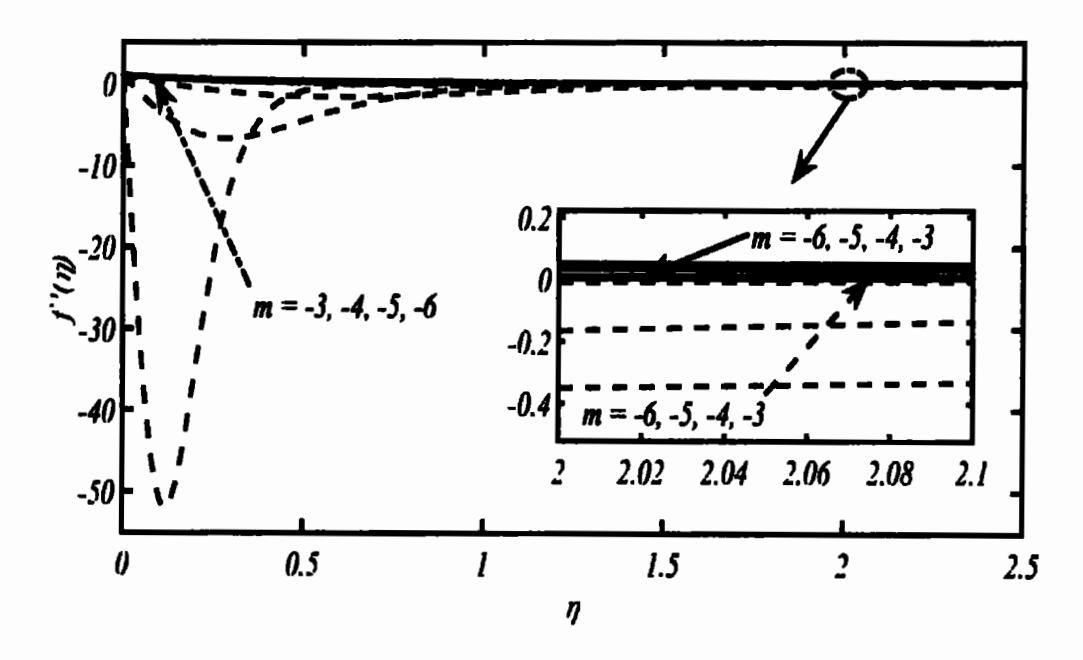


Fig. 5. 12: Velocity profile for some selected values of m at  $\kappa = 0.25$  for S = 5.

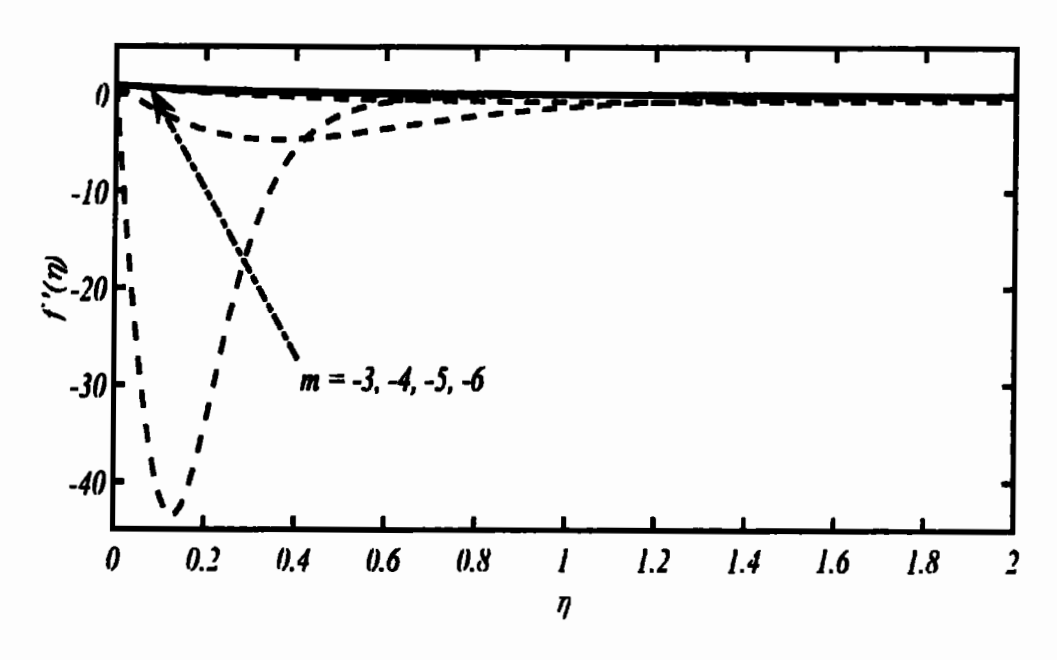


Fig. 5.13: Velocity profile for some selected values of m at  $\kappa = 0.50$  for S = 5.

#### 5.1.2 Results and discussion

The system (5.6)—(5.7) has been solved numerically with the aid of RK-shooting technique similar to the previous chapters. During current analysis the results captured for linear and non-linear wall velocities under the influence of different involved physical parameters are displayed in tabulated form (Tables 5.1-5.6) and also presented graphically in Figs. 5.2-5.13. Fig. 5.2 represents the impact of surface transverse curvature on the wall skin-friction, for linear case, when plotted against the suction parameter. It is depicted that at some chosen values of curvature parameter the dual solutions prevail for higher magnitudes of S and these solutions disappear as the suction effects become weaker and weaker. Fig. 5.3 is drawn to analyze the impact of curvature parameter for the case of non-linear shrinking velocity (m = 2). It is observed that for higher values of  $\kappa$ , almost similar pattern is noticed, i.e., with the provision of sufficient wall suction dual solutions are sighted and the occurrence of any solution tends to disappear during the weaker effects of suction. However, one aspect seems prominent here that at  $\kappa = 0.10$ , for higher suction effects, dual solutions show wider difference among the two branches and this gap becomes narrow with the reduction of suction. Here, it is a worth mentioning fact that (in this case) both first & second solutions don't get converged, however, they come closer and closer and ultimately reach the values -1.0828 & -1.0823, respectively, at a critical point "S = -3.61121432". However, this is not the case with every couple of solution, as is evident from Figs. 5.2-5.3. From these figures, it is clear that although dual solutions exist therein but, despite the tedious efforts, no critical points were observed at which both the solutions could overlap. To trace out the wall skin-friction distribution against  $\kappa$ , Fig. 5.4 is drawn at some specific

values of S. From the Fig. 5.4 it can be observed that at smaller values of suction parameter dual solutions do exist under the smaller curvature impacts and the solutions disappear as the curvature influences are strengthened. Resultantly, sufficient amount of suction is observed mandatory to capture the solution there.

In above discussion, it is clearly described that the dual solution is possible for decelerated wall velocity with the provision of sufficient wall suction velocity. To see the role of accelerated wall velocity, Figs. 5.5 & 5.6 are plotted and numerical data is presented in Tables 5.5 & 5.6, accordingly, wherein it is observed that dual solutions are only possible for injection wall velocity, while, the presence of wall suction does not guarantee for the existence of any kind of solution. Although, it is a well known fact that the wall suction supports the blowing boundary-layer while the wall injection velocity cause the boundary-layer to blow, in contrast. But such an opposite behavior has appeared due to the occurrence of a factor m + 1 in the denominator of second boundary condition at  $\eta = 0$ . During the analysis, it is noticed that for larger injection effects, both branches of solution show more and more differences and by reducing the injection effects the both solutions come closer and closer and ultimately get converged. The convergence of both solutions, in this case, is a unique aspect as this type of findings is not observed for the case of decelerated nature of wall velocity.

For further understanding the dual nature of solution, the velocity profiles for linear as well as non-linear shrinking velocities are displayed in the Figs. 5.7-5.11, wherein, it is clear that both the solution branches unanimously satisfy the far field boundary conditions, asymptotically. Velocity profile for the case of linear wall velocity, at different values of  $\kappa$ , and S are presented in Figs. 5.7-5.9, whereas smooth and

uniform variations are observed for both solutions therein. All figures describe that the effects of curvature parameter and wall suction velocity are opposite on both the solutions. The effects of curvature and suction parameters in the case of non-linear wall velocity (m = 2) are plotted in Figs. 5.10-5.11. Fig. 5.10 indicates the impact of different values of curvature parameter on the velocity profile at S = -6, while Fig. 5.11 shows the variation due to some chosen values of S at  $\kappa = 0.10$ . From these figures, the dual nature of the solution is also sighted which is obvious for power-law wall velocity. Almost similar behavior of flow phenomenon is noted as it occurred in the case of linear wall velocity. However, convergence of both solutions can be obtained more quickly as compared to linear wall velocity case. It is also observed that with the increment in the impact of suction parameter the boundary-layer thickness is boosted up accordingly. It is noticed that the presence of dual solution is possible only for decelerated wall velocities under the impacts of involved physical parameter. The velocity profiles for accelerated nature of wall velocity have been depicted in Figs. 5.12 & 5.13 for  $\kappa = 0.25$  and  $\kappa = 0.5$ , respectively. It is noticed that, as usual, first solution branches exhibit smooth variations while second solution branches portray an abrupt an unusual behavior.

### 5.2 Unsteady boundary-layer flow over a shrinking cylinder

In this section the steady aspects of shrinking cylinder are extended towards unsteady circumstances. Since, the appearance of an attractive concept about multiplicity/duality of solution in the field of shrinking surfaces flow, literature regarding these flows has become voluminous due to numbers of publications rendered by the involved researchers. A valuable literature can be cited in [68]–[78], wherein flows caused by the axisymmetric shrinking cylinder have been studied under the consideration

of different circumstances. In view of available literature, it is concluded that the existence of multiple/dual solutions is linked with the provision of sufficient wall suction or some other supporting internal/external ingredients. It is also noticed that almost, not a single fruitful effort has been carried out, so far, in connection to the existence of dual solutions in the absence of wall suction or even in the presence of wall injection. However, the existence of dual solutions cannot be connected, particularly, to the provision of suction/injection or other agents. During the current investigation, it is reported with strong evidences that the condition of provision of sufficient wall suction seems unnecessary for the existence of dual solutions as it is noted that dual solutions are also possible in the absence of wall suction or even in the presence of wall injection velocity. During the current analysis it is reflected that for the existence of duality of solution there is no need of any wall suction. Such kind of findings regarding dual nature of solution in context to a shrinking surface flow without the provision of wall suction or even in the presence of wall injection can be regarded as impressive outcomes in this domain of flows. It is also observed that the transverse surface curvature of the cylinder's surface paid a supporting role for the existence of dual solutions.

### 5.2.1 Mathematical formulation

Consider a continuous slim cylinder of infinite length, having a uniform cross-section. The cylinder is placed horizontally in a viscous, incompressible fluid so that no body force is acting there. There is no pressure-gradient therein and the cylinder is initially supposed to be at rest. The flow in the stationary fluid is caused by the impulsive start of the cylinder's motion (unsteady shrinking). In view of above assumptions, the continuity equation for the present case is the same as referred in Eq. (4.1), while the

governing equation of motion with the addition of an extra term (due to unsteadiness) to the L.H.S of Eq. (4.2), takes the following form:

$$\frac{\partial u}{\partial t} + u \frac{\partial u}{\partial x} + v \frac{\partial u}{\partial r} = v \frac{1}{r} \frac{\partial}{\partial r} (r \frac{\partial u}{\partial r}). \tag{5.8}$$

Since, the cylinder is supposed initially at rest, so that the ICs are read as

$$t \le 0, \quad u = v = 0, \quad \forall (r, z). \tag{5.9}$$

To allow for the normal wall velocity, the cylinder is supposed to be porous and with the passage of time (t > 0) it is set into motion (shrinking towards origin, i.e., z = 0) with some suitable velocity. As a result of this sudden motion, there develops a boundary-layer flow in the vicinity of shrinking cylinder. Therefore, the suitable boundary conditions for such an impulsive motion (t > 0) of the cylinder are taken of the form:

$$u = u_w(z, t), \quad v = v_w(z, t), \quad \text{at} \quad r = R(t)$$

$$u \to 0, \quad \text{as} \quad r \to \infty$$
(5.10)

Due to the unsteady nature of the current flow, the wall velocities  $u_w$  and  $v_w$  are supposed to be free to vary in z and t, while the radius of the cylinder is considered as uniform but to depend upon time. The nature of considered flow requires that the ambient fluid outside the boundary-layer remains at rest for all time ( $-\infty < t < \infty$ ). A detailed similarity criterion for the wall velocities  $u_w$ ,  $v_w$  and radius R(t) can be seen in [56], according to which (for a shrinking cylinder case):

$$u_w(z,t) = -\frac{\bar{a}z}{\tau}, \quad v_w(z,\tau) = d\tau^{-1/2}, \quad R(t) = R_0\tau^{1/2}; \quad \tau = \bar{a}t, \quad t > 0,$$
 (5.11)

where  $\bar{a}$  determines the constant shrinking rate, d stands for constant reference suction/injection velocity, while  $R_o$  refers to the constant reference radius of the shrinking cylinder. A more significant fact is that the cylinder, under consideration, is

swallowing in time and for the sake of self-similarity of the solution both the wall velocities  $(u_w \text{ and } v_w)$  decay in time as the cylinder swallows. It is necessary to understand that the above stated forms of the functions  $u_w$ ,  $v_w$ , and R are essential for similarity solution to exist. Further, the similarity variables in case of an unsteady shrinking cylinder, as reported by Mehmood [56], are of the forms:

$$\eta = \sqrt{\frac{\bar{a}}{v\tau}}r, \quad u = \frac{u_w}{\eta}f'(\eta), \quad v = \sqrt{\frac{\bar{a}v}{\tau}}\frac{1}{\eta}f(\eta).$$
(5.12)

The above similarity variables obviously satisfy the continuity equation (Eq. (4.1)), identically and Eqs. (5.8)—(5.10) are transformed as

$$\frac{f}{\eta} \left( \frac{f''}{\eta} - \frac{f'}{\eta^2} \right) - \left( \frac{f'}{\eta} \right)^2 - \frac{1}{2} \left( f'' + \frac{f'}{\eta} \right) = \frac{1}{\eta} \frac{d}{d\eta} \left( \eta \frac{d}{d\eta} \left( \frac{f'}{\eta} \right) \right), \tag{5.13}$$

$$f' = Re_{R_0}, \qquad f = \frac{d}{\sqrt{dv}} Re_{R_0}, \qquad \text{at} \quad \eta = Re_{R_0}$$

$$f' \to 0, \qquad \qquad \text{as} \quad \eta \to \infty$$

$$(5.14)$$

Here f represents the dimensionless stream function and 'refers the differentiation w.r.t.  $\eta$ , where  $Re_{R_0} = \sqrt{\frac{a{R_0}^2}{\nu}}$  is the Reynolds' number based upon the cylinder's reference radius,  $R_0$ . Although, the system (5.13)–(5.14) is in self-similar form which is ready to solve, however, to assist the numerical computations more efficiently, the equations can be made mathematically more compact by using

$$\bar{\eta} = \frac{\eta^2 - Re^2_{R_0}}{2Re_{R_0}}, \quad \text{and} \quad \bar{f} = \kappa f. \tag{5.15}$$

By the utilization of Eq. (5.15) the current domain of interest  $[Re_{R_0}, \infty)$  also leads to  $[0, \infty)$ . Consequently, the system (5.17)—(5.18) simply takes the form, after certain algebraic manipulations, as

$$(f - \frac{1}{2k}(1 + 2\kappa\eta))f'' - f'(1 + f') = ((1 + 2\kappa\eta)f'')', \tag{5.16}$$

$$f'(0) = 1, f(0) = S, f'(\infty) = 0,$$
 (5.17)

where  $\kappa = 1/Re_{R_0}$  is termed as curvature parameter, and  $S = \frac{d}{\sqrt{av}}$  designates the suction/injection parameter. The values of S > 0 correspond to the wall injection while the values S < 0 are referred to wall suction scenario.

**Table 5.5:** Numerical values of f''(0) at various values of  $\kappa$  and S.

S	$\kappa = 0.25$		$\kappa = 0.5$		κ = (	D. 75	$\kappa = 1.0$		
	1st sol.	2 <sup>nd</sup> soL	1st sol.	2 <sup>nd</sup> sol.	1 <sup>st</sup> sol.	2 <sup>nd</sup> sol.	1st sol.	2 <sup>nd</sup> sol.	
0.3	-0.4995	-0.0651	_						
0.1	-1.0935	0.6266							
0.0	-1.2775	0.8760							
-1.0	-2.6086	3.5646	-1.0000	-0.0845					
-2.0	-3.7232	7.5848	-2.5632	2.1469	-2.0538	0.5435	-1.5715	-0.4999	
<b>-3.0</b>	-4.7846	13.4546	-3.7020	5.0638	-3.3028	2.5432	-3.0673	1.2227	
<b>-4.0</b>	-5.8234	21.5343	-4.7721	9.2820	-4.4030	5.3481	-4.2030	3.2900	
-5.0	-6.8502	32.1456	-5.8151	15.0690	-5.4591	9.2353	-5.2725	6.1359	
-6.0	-7.8698	45.5876	-6.8443	22.6324	-6.4952	14.3667	-6.3153	9.9074	
<b>-7.0</b>	-8.8849	62.1401	<b>-7.8654</b>	32.1413	-7.5206	20.8549	-7.3 <del>444</del>	14.6944	
-8.0	-9.8968	82.0642	-8.8815	43.7291	-8.5393	28.7748	-8.3655	20.5504	
-9.0	-10.9065	105.6026	-9.8941	57.4942	-9.5538	38.1681	-9.3815	27.5011	
-10.0	-11.9145	132.9775	-10.9043	73.5001	-10.5653	49.0480	-10.3941	35.5511	

**Table 5.6:** Numerical values of f''(0) at various values of  $\kappa$  and S.

κ	S = -1		S = -0.5		S = 0		S = 0.5		S = 1.0	
	1st sol.	2 <sup>nd</sup> sol.	1 <sup>st</sup> sol.	2 <sup>nd</sup> sol.						
0.01	-50.980	9958.0	-50.480	9686.0	-49.979	9418.0	-49.479	9156	-48.979	8898
0.05	-10.908	139.5873	-10.403	123.3884	-9.8989	108.4592	-9.3935	94.7520	-8.8875	82.2185
0.10	-5.8280	26.8649	-5.3115	21.5357	-4.7914	16.9322	-4.2665	13.0042	-3.7345	9.6998
0.15	-4.0870	10.9250	-3.5510	8.0281	-3.0019	5.6457	-2.4302	3.7190	-1.8124	2.1732
0.20	-3.1816	5.8554	-2.6166	3.9236	-2.0135	2.3687	-1.3101	1.0785		
0.25	-2.6086	3.5646	-2.0000	2.1071	-1.2775	0.8760				
0.30	-2.1981	2.2914	-1.5178	1.0728						
0.35	-1.8742	1.4730	-1.0455	0.3094						
0.40	-1.5943	0.8803								
0.45	-1.3239	0.3957								
0.50	-1.0000	-0.0845								

**Table 5.7:** The critical values of suction parameter S calculated for some chosen values of curvature parameter.

к	Sc	1st sol.	2 <sup>nd</sup> sol.
0.25	0.3157822504	-0.2853	-0.2853
0.50	-0.926035063	- 0.5490	-0.5490
0.75	-1.493430711	-0.7960	-0.7960
1.0	-1.887497733	-1.0301	-1.0301

**Table 5.8:** The critical values of curvature parameter  $\kappa$  calculated for some chosen values of suction parameter.

S	κ <sub>c</sub>	1st sol.	2 <sup>nd</sup> sol.
1.0	0.190451504	-0.2197	-0.2197
0.5	0.2309048468	-0.2643	-0.2643
0.0	0.2900951501	-0.3289	-0.3289
-0.5	0.381082792	-0.4259	-0.4259
-1.0	0.525946169	-0.5753	-0.5753

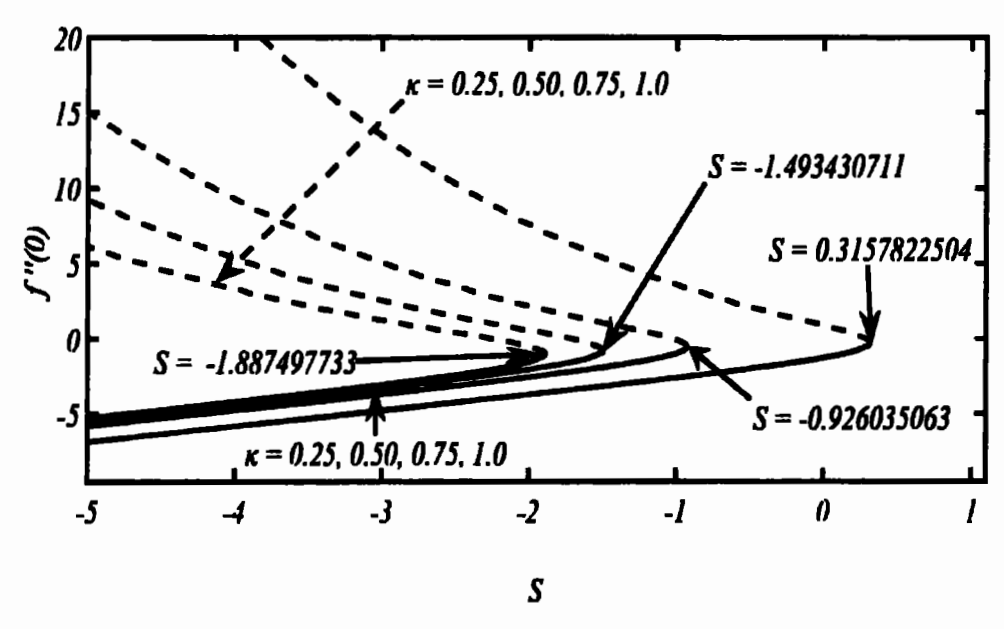


Fig. 5.11: Dual solution of f''(0) for different values of surface curvature parameter  $\kappa$  as a function of a suction/injection parameter S.

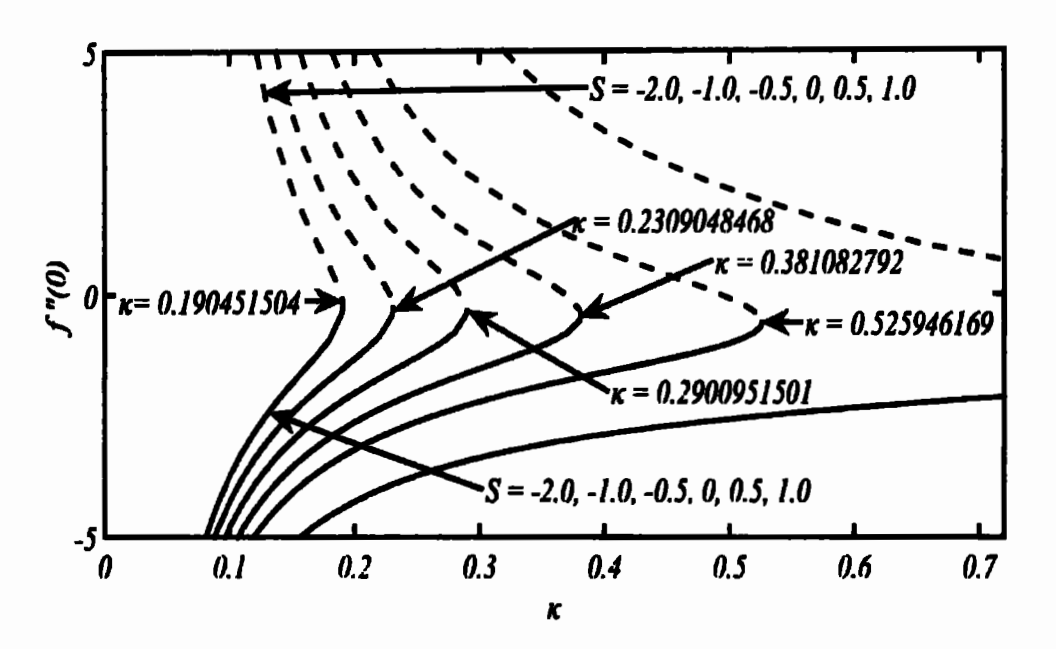


Fig. 5.12: Dual solution of f''(0) for different values of suction/injection parameter plotted against curvature parameter  $\kappa$ .

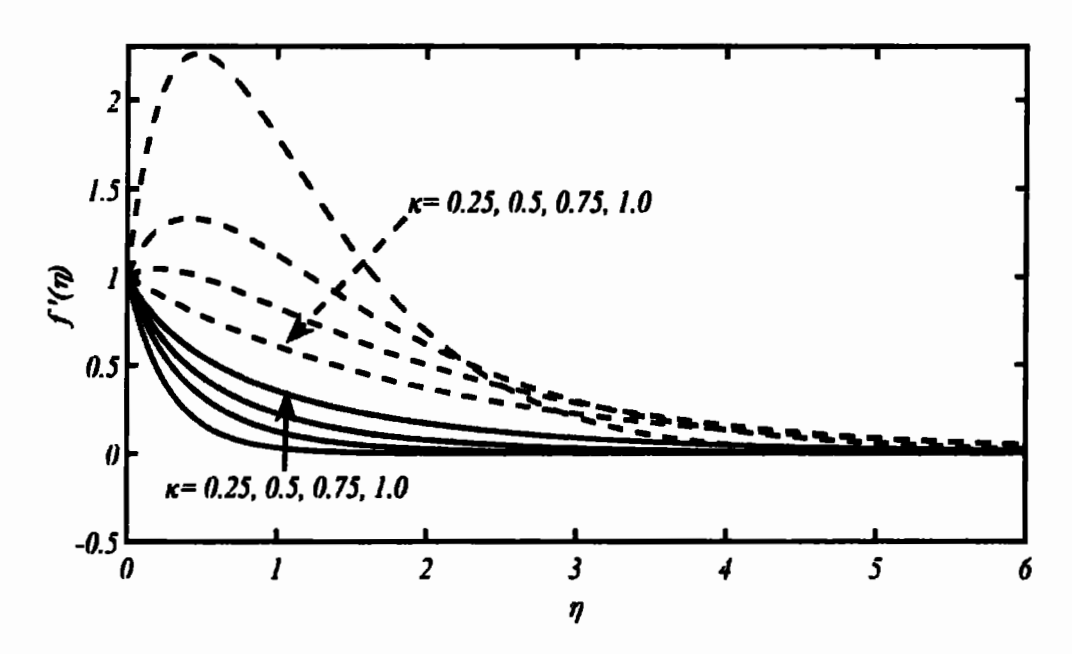


Fig. 5.13: Velocity profile for different values of curvature parameter at S=-2.

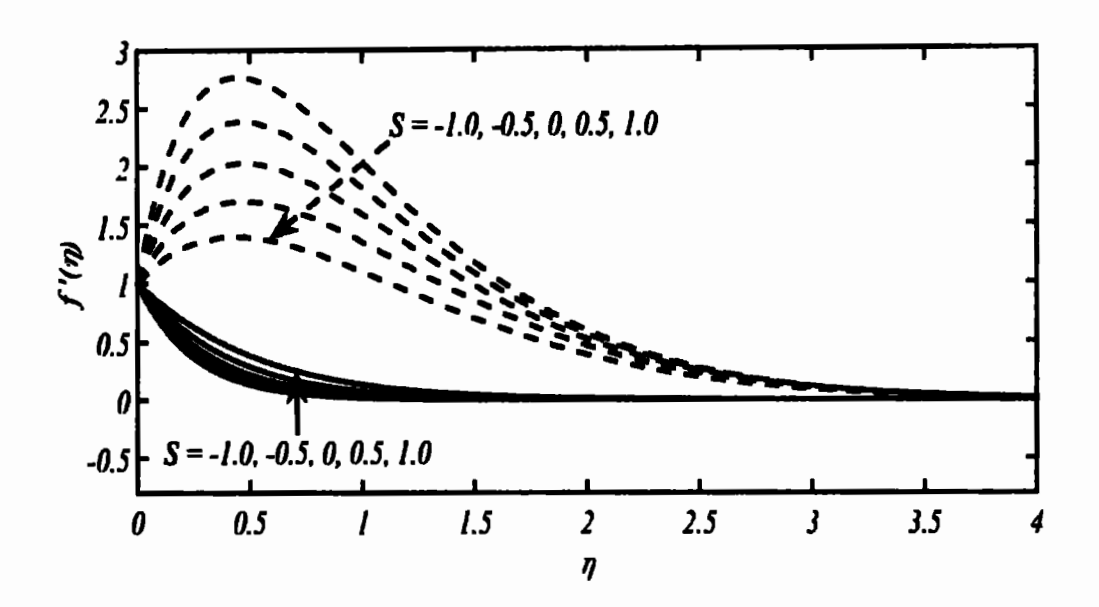


Fig. 5.14: Velocity profile for different values of suction/injection parameter at  $\kappa = 0.15$ .

### 5.2.2 Results and discussion

The self-similar system of Eqs. 5.16-5.17, obtained as a result of mathematical formulation carried out during the current analysis, is solved with the aid of a compatible numerical method that is known as  $4^{th}$  order Runge-Kutta shooting method. By utilizing this numerical technique, it becomes possible to capture dual solutions for various values of curvature parameter,  $\kappa$ , and suction/injection parameter, S, which are reported in tabular form as well as presented in the graphical form, where the first solution is shown by solid lines while broken lines designate the second solution.

Fig. 5.11 is drawn for the numerical data captured in context of skin-friction coefficient, f''(0), at various values of  $\kappa$  against S. From the graphical representation, it can be seen easily that dual solutions are possible, in the presence of wall suction, for all

assumed values of  $\kappa$ . As far as the nature of first solution is concerned, it remains negative throughout the process and its magnitude increases as the suction effects are amplified. However, the behavior of second branch of solution remains almost positive but changes its behavior for a while for smaller values of S. These facts can be realized more clearly for small values of  $\kappa$  ( $\kappa = 0.25$ ), where the solution is reported not only without suction but also for injection parameter, too, Further, with the increasing effects of injection the second solution changes its behavior from positive to negative. It is also noted that as the influence of curvature is enlarged the existence of dual solutions becomes impossible to shorten the character of suction parameter. Such type of information can be seen in Table 5.5. It is also noted that, with the increasing magnitude of S, the first solution slightly differs while the second solution exhibits prominent variations therein. Further, as the effects of suction parameter are reduced both the branches of solution tend to converge. With reducing the magnitude of S, we reach a point,  $S = S_c$ , where both the solutions ultimately get overlapped and on overlapping solution is obtained. It is also learned that the dual solution is possible only for  $S < S_c$ and no solution is observed beyond the critical point i.e.,  $S > S_c$ . To explore the point of convergence (critical point), time taking efforts have been made and ultimately we succeeded to trace out the relevant critical points which are also shown in the Fig. 5.11 as well as given in a tabulated form in Table 5.7. It is an interesting fact that the Fig. 5.11 is a mirror image of the results reported by Zaimi et al. [69] where the authors [69] utilized wrong self-similar formulation.

To explore the curvature effects, numerical data is collected for some selected values of S, which is referred in Table 5.6 and is also depicted in Fig. 5.12. From the

graphical representation, it is clearly noticed that the variation in the second solution is more visible in contrast to the first solution. At some specific values of curvature parameter, the magnitude of skin-friction coefficient increases with the increment in suction effects, but decreases with the increment of injection parameter. Further, it is revealed that the reduction in the magnitude of f''(0) remains to continue with the increment in curvature parameter. The magnitude of the first solution stayed negative throughout the process, while the second solution almost persisted a positive outlook, however, for higher values of  $\kappa$ , at S = -1.0, it changes its behavior from positive to negative. However, such types of findings are observed for suction scenario, only. By enhancing the curvature effects, the solution disappears more rapidly as the domain of solution shifts from suction to injection regime. It is worth mentioning that the solution is also reported without suction (S = 0). Here, it is noticed that the both solutions come closer and closer as the effect of surface curvature is intensified. Ultimately, for every assumed value of S, a critical point  $(\kappa_c)$  is figured out, accordingly. It is a fact that no solution is possible beyond the critical point (i.e.,  $\kappa > \kappa_c$ ). No doubt, such critical points are explored after a great deal of plenteous efforts and exercise. The critical values of  $\kappa$ for some chosen values of S are pertained in Table 5.8 and Fig. 5.12 is also ornamented with them, accordingly.

For complete understanding of the flow phenomenon, the velocity profile,  $f'(\eta)$ , is drawn in Figs. 5.13-5.14, where Fig. 5.13 is plotted for some chosen values of  $\kappa$  by choosing S as fixed (i.e., S=-2.0) and Fig. 5.14 is portrayed for some selected values of S, by taking curvature parameter as fixed (i.e.,  $\kappa=0.15$ ). Here, it is obvious that the two branches of the solution completely agree with the far field boundary

conditions, asymptotically. It is illuminated from Fig. 5.13 that the boundary-layer thickness is boosted as the curvature parameter is enlarged. It is also obvious, that the second solution bears wider span of boundary-layer, whereas, under the same circumstances, the first solution displays comparatively small variations in the boundarylayer thickness. The role of suction/injection parameter, at  $\kappa = 0.15$ , in the pattern of velocity profile is described in Fig. 5.14. It is observed that suction/injection parameter plays opposite role on the velocity profiles, i.e., by increasing the suction effects boundary-layer thickness decreases, however, it boosts up as the injection effects are magnified. Another important fact is that the solution is also noted without the provision of suction wall velocity. Capturing the solutions in the absence of wall suction or even in the presence of wall injection, is definitely a big achievement of the current study, as the existing literature seems quite in this regards. Infact, the findings of current study negate the well-established claims made about the existence of dual solutions. Now, it became crystal clear reality that the solution can be figured out with and without suction/injection influence. During the current study, it is also observed that the solution pattern portrayed in Figs. 5.13 & 5,14, is the reflection of the results displayed in Figs. 3 & 4 by the authors [69]. The outcomes of the present study are perceived to serve a helping tool to explore the hidden aspects of the multiple nature of solution for moving continuous surfaces.

#### 5.3 Conclusion

During the current investigation, the possibility of dual solutions is sorted out, for linear as well as non-linear shrinking wall velocity. The presence of sufficient amount of wall suction provided an assistive role regarding the existence of these solutions. Further, the impact of surface curvature for soliciting the non-unique solution is well noticed

during the analysis. These outcomes are the important features of this study and are the valuable findings for this flow. A comprehensive numerical data has been captured regarding dual solutions of this flow and presented in tabular form, which is definitely expected to help as most suitable reference for future studies. The outcomes of the present study shall definitely inspire the researchers to further disclose the hidden features of the boundary-layer flows, of this nature.

During the current study dual nature of solutions for unsteady viscous flow stimulated by an impulsively started shrinking cylinder has been analyzed. The present analysis exposes various fascinating unique conclusions, particularly related to the topic of shrinking surface flows. The prime feature of the current investigation is the existence of dual solution not only in the case of wall suction but also for the cases of wall injection as well as in the absence of wall suction, too. It is also noted that the dual solutions are possible even for sufficiently weak injection velocities. These two outcomes are definitely innovative and unique which have never been reported in the literature, previously. Definitely, such a unique outcome will stimulate the scientists to scrutinize the multiplicity/duality of solution for shrinking surface flows in the absence of wall suction and in the presence of wall injection velocity.

# Chapter 6

## Duality of solution for a stretching disk flow

In the current chapter we intend to deal with steady/unsteady characteristics of the self-similar boundary-layer flow caused by a flat circular disk of infinite radius. The disk is assumed to be non-rotating and of flexible nature and stretching in the radial direction. The literature available in the realm of stretching disk is mostly related to the circular motion whereas its non-rotational perspectives are rarely investigated. The axisymmetric surface flows were also studied for the exploration of a new type of solution, called multiple/dual solution. The current study is devoted to explore the possibility of dual solutions for the flow phenomenon initiated by a stretching disk, in the absence of any circular motion. Both the steady and unsteady aspects of a stretching disk flow are considered in this chapter for the exploration of duality of solution. The governing equations, obtained for the flow under consideration, are solved numerically with the aid of a trustworthy shooting technique. During the present study, dual solutions are captured for involved parameters.

### 6.1 Steady boundary-layer flow due to a stretching disk

In the family of axisymmetric flows the circular disk geometry is considered as the next of circular cylindrical geometry. The axisymmetric boundary-layer flow due to a radially stretching disk was first studied by Fang [79]. The author [79] utilized a linearly varying stretching wall velocity for this flow. Consequently, an exact self-similar solution was reported. A quick literature survey reveals that though the stretching disk flow has been investigated by a huge number of researchers but the stretching wall velocity had

strictly been limited to a linear form. Recently, Mehmood [56] determined a similarity criterion for the stretching wall velocity for the disk case and reported the possibility of a power-law (non-linear) wall velocity, also. This section intends to consider the said power-law (non-linear) form of radially stretching wall velocity to sort out the possibilities with regard to the existence of non-unique solution.

### 6.1.1 Statement of the problem

Consider a flat circular disk of infinite radius whose flexible surface is being stretched with variable velocity in radially outward direction. A schematic of the flow is shown in Fig. 6.1 with the associated system of coordinates. Such a stretching disk induces a two-dimensional boundary-layer flow for which the governing equation are given by

$$\frac{\partial(ru)}{\partial r} + \frac{\partial(rw)}{\partial z} = 0, \tag{6.1}$$

$$u\frac{\partial u}{\partial r} + w\frac{\partial u}{\partial z} = v\frac{\partial^2 u}{\partial z^2},\tag{6.2}$$

subject to the boundary conditions

$$u = u_{\mathbf{w}}(r), \qquad w = w_{\mathbf{w}}(r), \qquad \text{at } z = 0, \\ u = 0, \qquad \text{at } z = \infty$$
 (6.3)

where u and w are the velocity components taken along the radial (r-) and the axial (z-) directions, respectively, and v is termed as kinematic viscosity. Mehmood [56] determined that the above system admits an exact similarity solution if the wall velocities follow a form given

$$u_w(r) = ar^m, w_w(r) = dr^{\frac{m-1}{2}}, (6.4)$$

where a > 0 denotes a uniform stretching rate, and d is a constant such that: d > 0 correspond to wall injection velocity, and d < 0 correspond to wall suction velocity. Mehmood [56] introduced the following similarity transformations:

$$\eta = \sqrt{\frac{a}{\nu}} r^{\frac{m-1}{2}} z, \quad u = a r^m f'(\eta), \quad w = -\sqrt{a \nu} r^{\frac{m-1}{2}} (\frac{m+3}{2} f + \frac{m-1}{2} \eta f'), \quad (6.5)$$

due to which Eq. (6.1) is satisfied identically, while the system (6.2)-(6.3) transforms as:

$$f''' = mf'^2 - (\frac{m+3}{2})ff'', \tag{6.6}$$

$$f'(0) = 1,$$
  $f(0) = -\frac{2S}{m+3},$   $f'(\infty) = 0,$  (6.7)

where  $S = \frac{d}{\sqrt{av}}$  denotes dimensionless suction/injection: S > 0 correspond to wall injection while S < 0 correspond to wall suction.

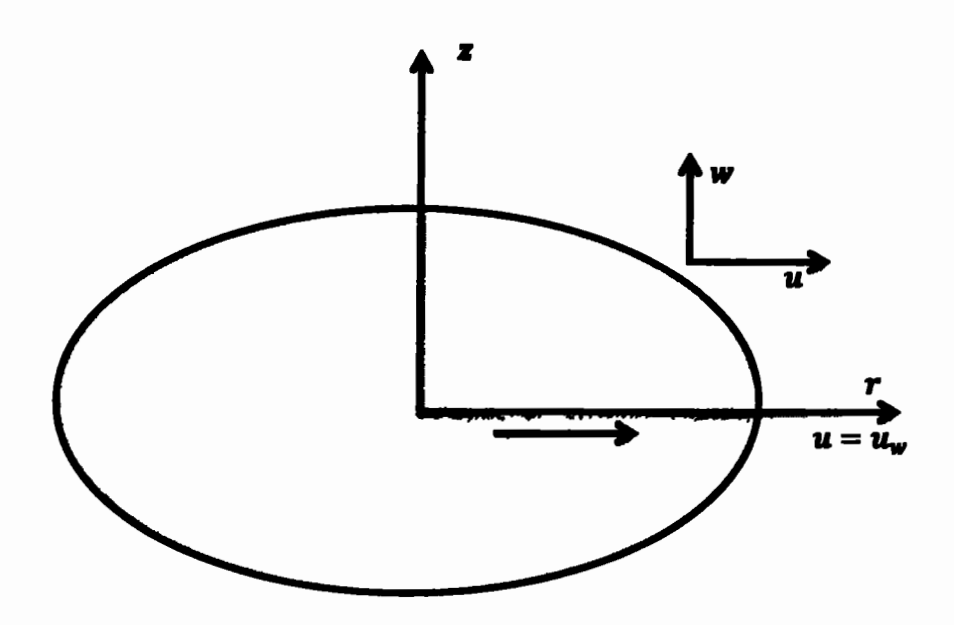


Fig. 6.1: Flow geometry and associated coordinates.

**Table 6.1:** A comparison of the data reported in [56] with the current results for some selected values of m at S=0.

	Two-dimensional	case	The disk case $-\left(\frac{m+3}{2}\right)^{-1/2}f''(0)$					
	$-\left(\frac{m+1}{2}\right)^{-1/2}f$	·"(0)						
m	Data reported in [56]	Present results	m	Data reported in [56]	Present results			
0	0.6276	0.6276	0	0.6276	0.6276			
1 1/5	0.7668	0.7668	3/5	0.7668	0.7668			
1/3	0.8299	0.8299	1	0.8299	0.8299			
1	1.0000	1.0000	3	1.0000	1.0000			
<b>A</b> 3	1.1484	1.1484	9	1.1484	1.1484			
-1/7	0.4645	0.4645	-3/7	0.4645	0.4645			
-1/5	0.3404	0.3404	-3/5	0.3404	0.3404			
-1/21	0.5816	0.5816	-1/7	0.5816	0.5816			

**Table 6.2:** Values of f''(0) against m for some selected values of S.

	S = 0.0		<b>S</b> =	1.0	<b>S</b> =	2.0	S = 3.0	
m	1st sol.	2 <sup>nd</sup> sol.	1st sol.	2 <sup>nd</sup> sol.	1st sol.	2 <sup>nd</sup> sol.	1 <sup>st</sup> sol.	2 <sup>nd</sup> sol.
-4	-2.3690	-2.3697	-3.4486	-4.0674	-4.9541	-11.113	-6.6906	-28.423
<b>–5</b>	-1.9025	-1.9047	-2.4060	-2.5186	-3.0567	-3.9421	-3.8224	-7.0049
-6	-1.7197	-1.7233	-2.0464	-2.0994	-2.4465	-2.7447	-2.9118	-3.9027
<b>-7</b>	-1.6208	-1.6254	-1.8625	-1.8976	-2.1478	-2.2982	-2.4743	-2.9217
-8	-1.5586	-1.5639	-1.7503	-1.7775	-1.9710	-2.0655	-2.2196	-2.4721
-9	-1.5158	-1.5217	-1.6747	-1.6976	-1.8541	-1.9219	-2.0537	-2.2183
-10	-1.4845	-1.4909	-1.6201	-1.6404	-1.7711	-1.8239	-1.9373	-2.0554

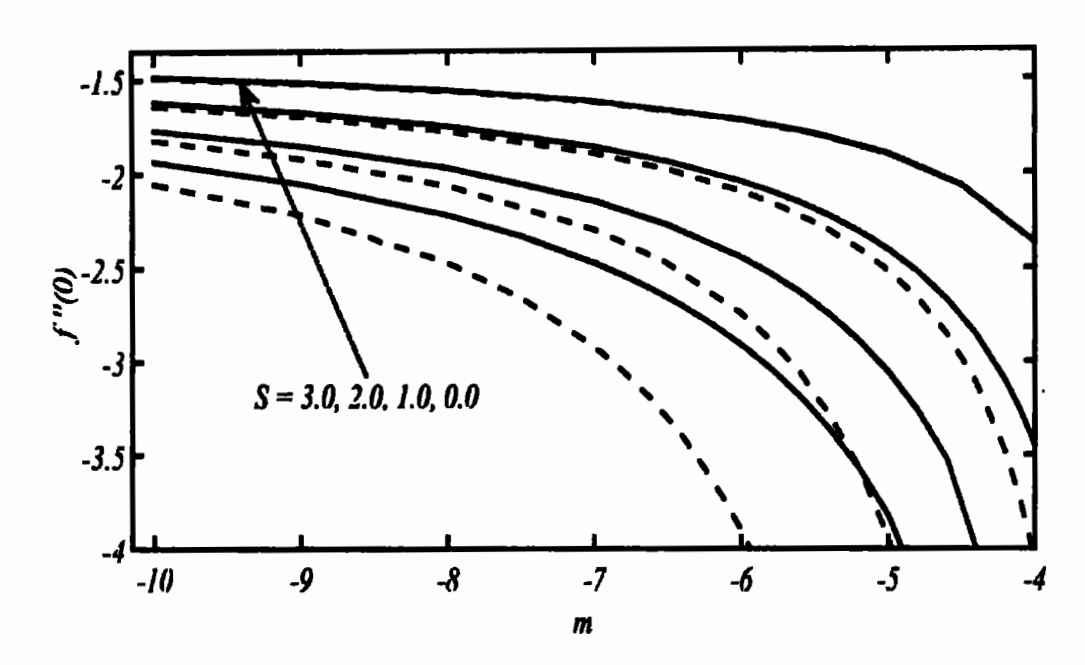


Fig. 6.2: Dual solutions shown by f''(0) for some selected values of S against m.

### 6.1.2 Duality of solution

An inspection of the systems (2.5)-(2.6) and (6.6)-(6.7) reveals that the boundary data of the two systems are identical while the self-similar equations of the two systems, namely, Eqs. (2.5) and (6.6) differ by little. A careful comparison of the two equations reveals that both the equations are inter-convertible. Particularly, Eq. (6.6) can simply be recovered by replacing "m" by "3m" in Eq. (2.5). This fact has also been explained by Mehmood [56] where the author recovered self-similar solution (in the accelerated case m > 0) for the disk from the self-similar solution of two-dimensional stretching sheet flow. This indicates the possibility of recovering a self-similar solution (in the decelerated case, m < 0) for the shrinking disk flow from that of the shrinking sheet solution, if available.

Interestingly, duality of solution for a shrinking sheet flow has already been reported by Mehmood and Usman [55]. Therefore, it is not necessary to solve the current problem, separately; rather the solution of the current problem can simply be recovered from that reported in [56] by replacing "m" by "3m" in the data of [56]. By doing so the results for a steady stretching disk flow have been reported in Tables 6.1–6.2 and Fig. 6.2. Obviously, duality of solution has been sorted for the case with m < 0, that is the decelerated case of stretching wall velocity. This fact ensures the presence of dual solutions in the case of stretching disk provided that the shrinking wall velocity is of decelerated nature.

### 6.2 Unsteady boundary-layer flow due to a stretching disk

The characteristics of flow phenomenon due to a moving continuous cylinder (stretching/shrinking) have been discussed in the preceding chapters (4<sup>th</sup> & 5<sup>th</sup>). Moreover, the steady flow due to a stretching circular disk has been presented in preceding section of this chapter with regard to the occurrence of dual solutions. The purpose of this section is to investigate the various aspects of unsteady flow due to a flat circular stretching disk for the existence of dual solutions. Here we are focused on the analysis of unsteady flow caused by a non-rotating flexible stretching disk. It is a fact that most of the literature on account of flows stimulated by stretching disk surface are related to rotational aspects, while non-rotational characteristics have been given a very few consideration. Further, with the appearance of multiple/dual solutions, there is a need to sort out the possibility about the occurrence of multiplicity/duality of the flow phenomenon initiated by a stretching disk surface. In this regards, the present effort is made to investigate the unsteady features of the self-similar boundary-layer flow

stimulated by stretching disk, particularly the existence of dual solutions has been given a prime focus.

### 6.2.1 Mathematical formulation

Consider a flexible flat circular disk of an infinite radius placed in an incompressible, stationary viscous fluid. The nature of the disk is supposed to be porous so that the normal wall velocity across the disk surface is permitted. Further, the pores are regarded as of uniform width and equally distributed on the disk surface. The disk is taken, initially, at rest and at time t > 0 a sudden motion/stretching is allowed (in radial direction) with a velocity  $u_w(r,t)$ . Such kind of wall velocity creates unsteady, two-dimensional, axisymmetric boundary-layer flow in the neighboring fluid. The stretching pattern and the associated coordinate system are presented in Fig. 1. In view of above assumptions the boundary-layer equation of continuity in this case remains unaltered (i.e., Eq. (6.1)), while the equation of motion referred in Eq. (6.2) takes the following form:

$$\frac{\partial u}{\partial t} + u \frac{\partial u}{\partial r} + w \frac{\partial u}{\partial z} = v \frac{\partial^2 u}{\partial z^2}. \tag{6.8}$$

As there is no circular motion therefore the angular component of velocity is chosen as zero. The most suitable initial and boundary conditions are taken as:

$$u = u_{w}(r, t), \qquad w = w_{w}(r, t), \qquad \text{at } z = 0, u = 0, \qquad \text{at } z = \infty$$

$$(6.9)$$

where u and w are the velocity components taken along the radial (r-) and the axial (z-) directions, respectively, and v is termed as kinematic viscosity. The disk is being stretched in the radial direction with the velocity of the form:

$$u_{\mathbf{w}}(r,t) = \frac{ar}{1-rt},\tag{6.10}$$

where a > 0 is a constant and is referred as a constant stretching rate. The wall velocity mentioned in Eq. (6.10) ensures for the existence of a self-similar solution. In view of the wall velocity (Eq. (6.10)) the following similarity transformations (in dimensionless form) are introduced as,

$$\eta = \sqrt{\frac{a}{\nu}} \frac{1}{\sqrt{1-\gamma t}} z, \qquad u = \frac{ar}{1-\gamma t} f'(\eta), \qquad and \quad w = -2\sqrt{\frac{a\nu}{1-\gamma t}} f(\eta), \tag{6.11}$$

where,  $\gamma$  is a parameter describing the unsteadiness of the flow phenomenon under consideration. Eq. (6.11) satisfies the continuity equation (i.e., Eq. (6.1)), identically, and transforms Eqs. (6.8)—(6.9) to the following set of equations:

$$f''' = f'^2 - 2ff'' + \beta(f' + \frac{\eta}{2}f'')$$
 (6.12)

$$f'(0) = 1, f(0) = -S, f'(\infty) = 0.$$
 (6.13)

Here,  $\beta = \frac{r}{a}$  is designated as unsteadiness parameter where its positive and negative values characterize the accelerated and decelerated cases, respectively. Further by taking  $\beta = -1$ , the above Eq. (6.12), recovers the form of Eq. 8.52 formulated by Mehmood [56] for unsteady stretching disk. For the present study, we suppose the decelerating stretching disk with  $\beta \leq 0$ . Furthermore, it is worth-mentioning that for the above mentioned self-similar system, the normal velocity must be of the form  $w_w(r,\tau) = \frac{d}{\sqrt{1-\gamma t}}$ , and it can be written in dimensionless form as  $\frac{d}{2\sqrt{av}}$  (= S). Positive values of S correspond to wall injection scenario while negative values of it refer to wall suction situation.

### 6.2.2 Numerical solution

A comparison of Eq. (6.12) with Eq. (2.10) reflects that the unsteady case of stretching disk cannot be recovered from the corresponding case of stretching sheet, different from the steady case. Therefore, the system (6.12)—(6.13) has been solved numerically with the aid of 4<sup>th</sup>-order Runge-Kutta shooting technique as did in previous chapters. Duality of solution has been captured in various situations.

**Table 6.3:** Numerical values for f''(0) for some selected values of  $\beta$  as a function of S.

S	$\beta = -3.0$		$\beta = -2.0$		$\beta = -1.0$		$\beta = 0.0$		$\beta = 1.0$	
٥	1ª Sol	2nd Sol	1ª Sol.	2nd Sol	1ª Sol	2nd Sol.	1st Sol	2 <sup>nd</sup> Sol	1st Sol	2 <sup>nd</sup> Sol
4.105	0.2642	0.2642	- <del>-</del>					1		
3.8	0.2905	0.2901	0.1398	0.1398						
3.0	0.3922	0.3863	0.1843	0.1834	-0.0001	-0.0001		+	1	
2.0	0.5819	0.5099	0.2677	0.2459	-0.0098	-0.0126	-0.2499		1	
1.0	0.5472	0.1483	0.1833	0.0010	-0.1603	-0.2098	-0.4766		1	
0.0	-0.3400	-1.6332	-0.6211	-1.4186	-0.8994	-1.2638	-1.1737		1	
-1.0	-2.0579	-5.7950	-2.2288	-4.9828	-2.3996	-4.1147	-2.5703			
-2.0	-4.0139	-13.6207	-4.1234	-11.7614	-4.2329	-9.5636	-4.3424		-4.4519	
-5.0	-10.0011	-65.6172	-10.0499	-55.7642	-10.0987	-41.7180	-10.1475		-10.196	
-6.0	-12.0006	-92.4302	-12.0416	-77.4122	-12.0826	-56.1223	-12.1235		-12.164	
-8.0	-16.0002	-157.097	-16.0312	-127.899	-16.0621	-88.8698	-16.0931		-16.124	
-10.0	-20.0001	-233.125	-20.0249	-186.27	-20.0498	-126.265	-20.0746		-20.099	

**Table 6.4:** Values of f''(0) as a function of  $\beta$  for some selected values of S.

Q	S = 2.0		S = 1.0		S = 0.0		S = -1.0		S = -2.0	
β	1ª Sol.	2ª Sol	1" SoL	2ª SoL	1ª Sol	2ª Sol	1 SoL	2ªd Sol.	1" Sol.	2ª Sol
0.1					-1.2008		-2.5873		-4.3435	
0.05	1		-0.4914		-1.1872		-2.5788		-4.3479	
0.0	-0.2499		-0.4766		-1.1737		-2.5703		-4.3424	
-0.0000	-0.2499		-0.4765	1	-1.1737	-1.1737	-2.5703		-4.3424	
-0.0002	-0.2498		-0.4765	-0.4765	-1.1731	-1.1786	-2.5702		-4.3424	
-0.001	-0.2496	1	-0.4763	-0.4764	-1.1734	-1.1768	-2.5701	-2.5933	-4.3423	
0.005	-0.2488	1	-0.4751	-0.4754	-1.1723	-1.1825	-2.5694	-2.6439	-4.3419	-4.5467
	-0.2275	-0.2275	-0.4465	-0.4485	-1.1465	-1.2033	-2.5532	-3.0529	-4.3315	-5.9059
-1.0	-0.0098	-0.0126	-0.1603	-0.2098	-0.8994	-1.2638	-2.3996	-4.1147	-4.2329	-9.5636
-2.0	0.2677	0.2459	0.1833	0.0010	-0.6211	-1.4186	-2.2288	-4.9828	-4.1234	-11.7614
-3.0	0.5819	0.5099	0.5472	0.1483	-0.3400	-1.6332	-2.0579	-5.7950	-4.0139	-13.6207
-4.0	0.9297	0.7654	0.9266	0.2360	-0.0567	-1.8844	-1.8868	-6.5794	-3.9044	-15.3217
-5.0	1.3074	1.0023	1.3185	0.2717	0.2283	-2.1591	-1.7157	-7.3456	-3.7949	-16.9257
-6.0	1.7116	1.2138	1.7208	0.2646	0.5149	-2.4493	-1.5445	-8.0984	-3.6853	-18.4623
-7.0	2.1392	1.3961	2.1319	0.2231	0.8028	-2.7500	-1.3732	-8.8406	-3.5758	-19.9484
-8.0	2.5876	1.5476	2.5506	0.1546	1.0918	-3.0582	-1.2019	-9.5740	-3.4662	-21.3950
-9.0	3.0546	1.6683	2.9758	0.0651	1.3818	-3.3717	-1.0305	-10.3000	-3.3567	-22.8093
-10.0	3.5383	1.7595	3.4068	-0.0405	1.6727	-3.6892	-0.8590	-11.0196	-3.2471	-24.1966

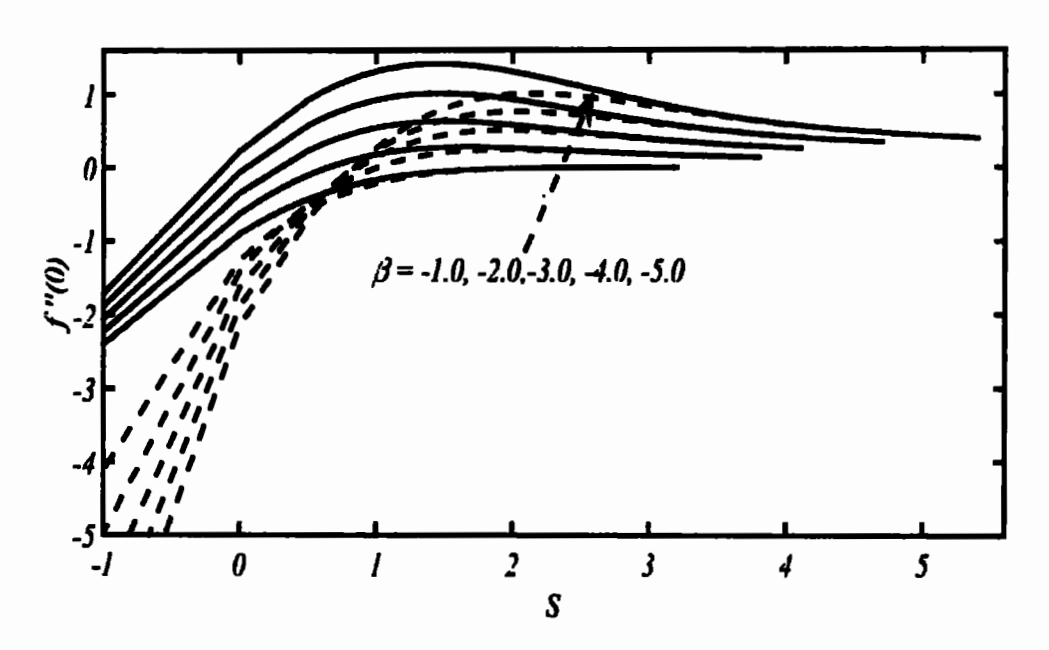


Fig. 6.3: Dual solutions shown by f''(0) for some selected values of  $\beta$  against suction/injection parameter S.

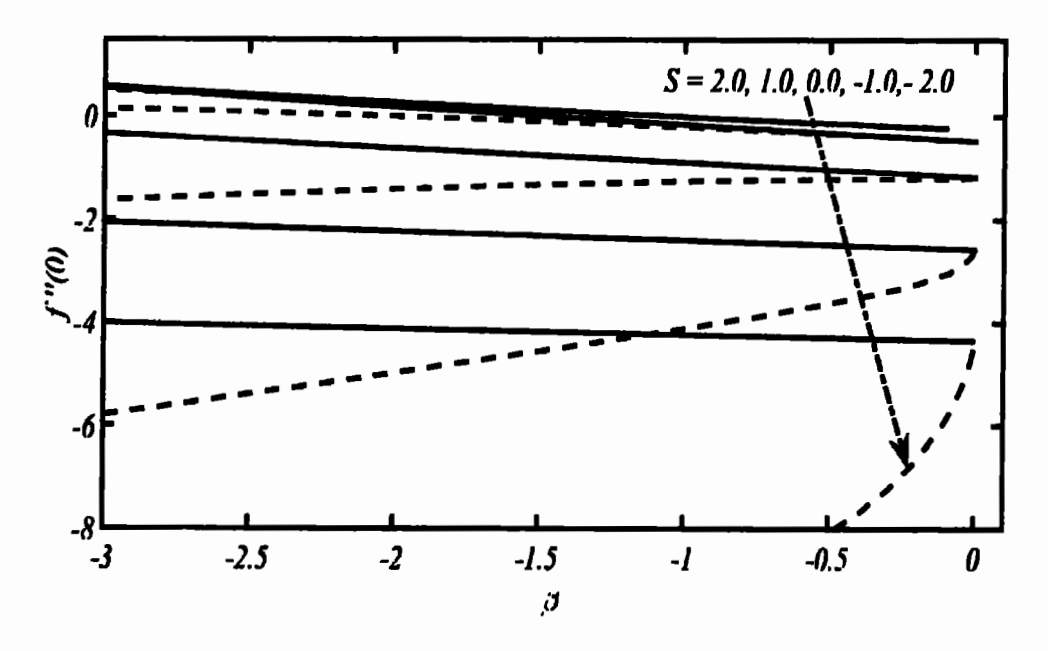


Fig. 6.4: Dual solutions shown by f''(0) for some selected values of suction/injection parameter S as a function of  $\beta$ .

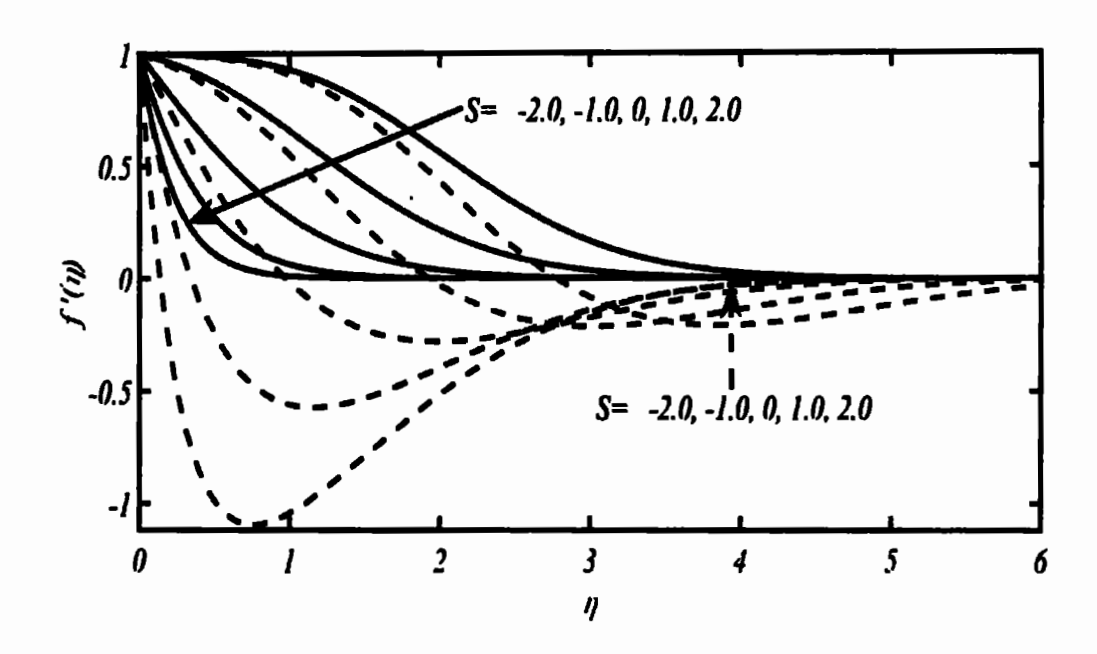


Fig. 6.5: Velocity profile for different values of S at  $\beta = -1$ .

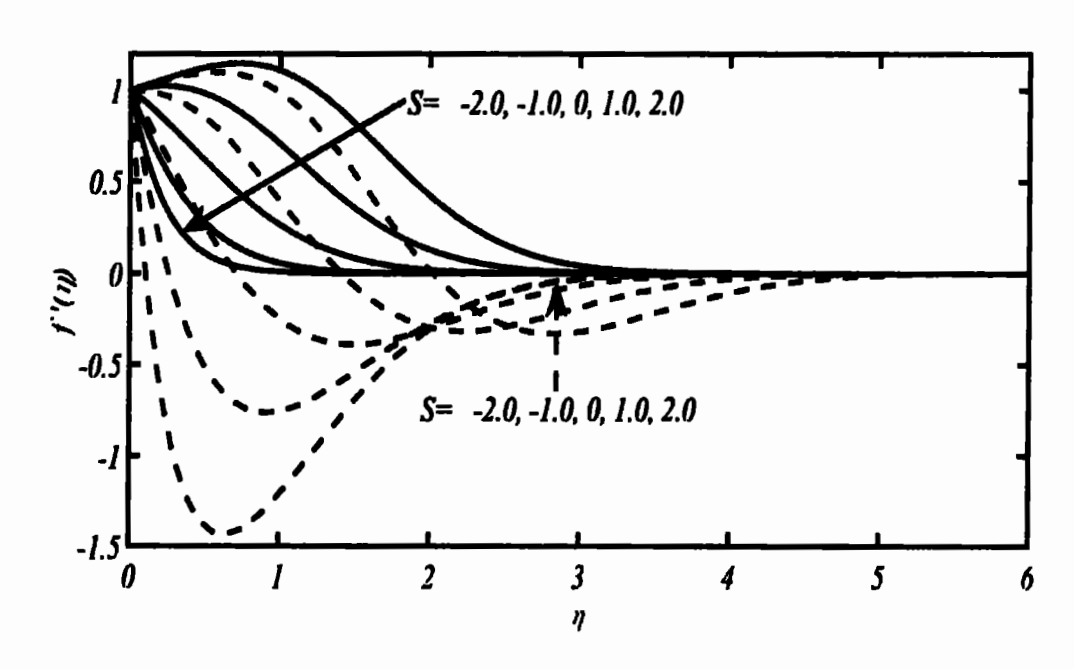


Fig. 6.6: Velocity profile for different values of S at  $\beta = -2$ .

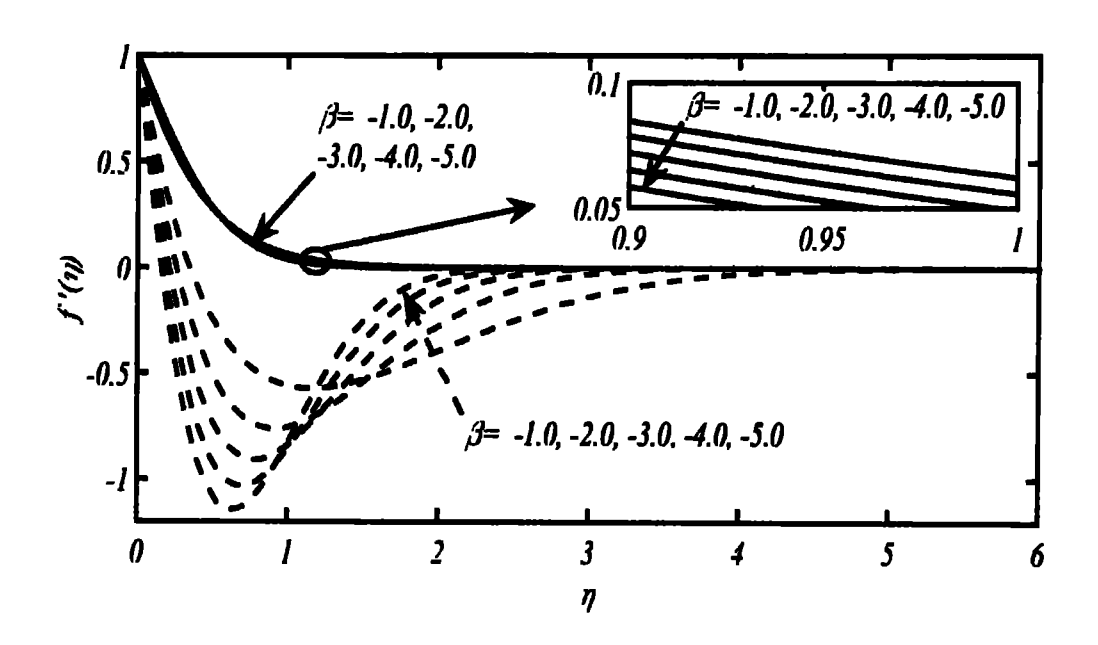


Fig. 6.7: Velocity profile for different values of  $\beta$  S at S=-1.

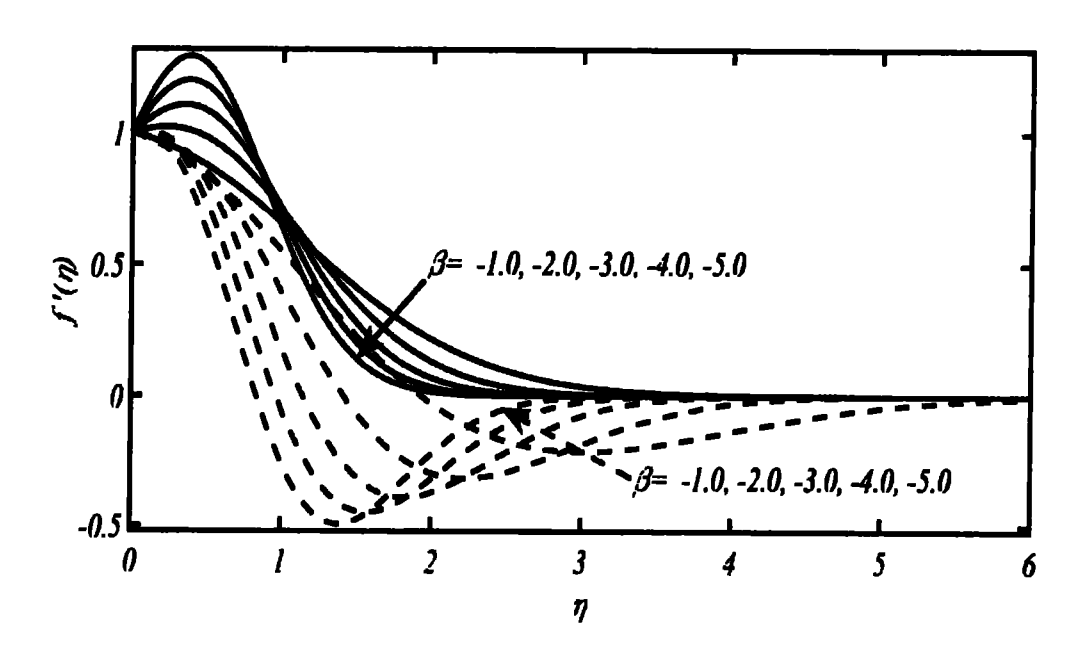


Fig. 6.8: Velocity profile for different values of  $\beta$  S at S=1.

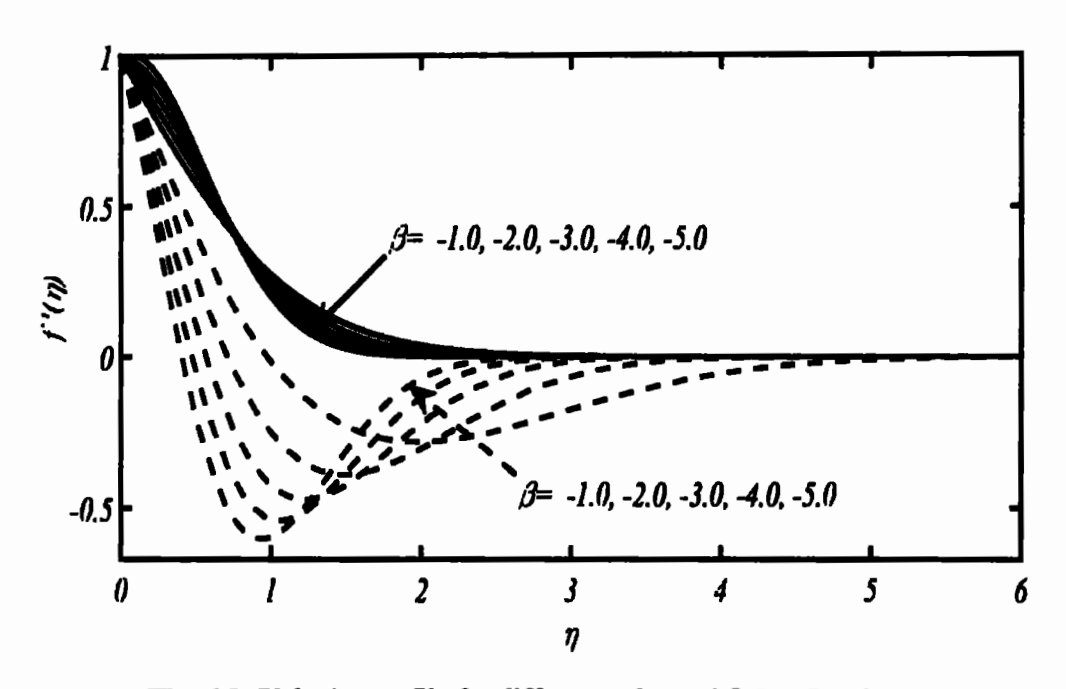


Fig. 6.9: Velocity profile for different values of  $\beta$  S at S=0.

### 6.2.3 Results and discussion

The information collected during the current analysis is prescribed in Tables 6.3-6.4 and is also illustrated through Figs. 6.3-6.9. Fig. 6.3 is plotted to analyze the role of unsteadiness parameter,  $\beta$ , against suction/injection parameter. From the graphical representation, it is depicted that the dual solution is possible not only for suction case, but also for injection case. Further, the solution is also sighted without the provision of suction/injection effects. It is noticed that with the increasing values of suction parameter the variation in the first solution is smaller as compared to the second solution. As the values of suction parameter are reduced both solutions express minor deviations with eachother. Resultantly, both solutions are overlapped at some critical points as shown in Fig. 6.3. It is worth mentioning that the second solution is possible for only decelerated case ( $\beta < 0$ ), while no second solution is reported for accelerated circumstances even

after utmost efforts. At a particular value of injection parameter, both the solutions get converged. Further, Fig. 6.4 is drawn at some chosen values of S, against  $\beta$ , wherein small variations are noted in the skin-friction coefficient (for instance see Table 6.4). Under the influence of suction parameter, both solutions comprise of negative values which increase as the flow becomes more and more retarded. However, as we enter in the domain of injection flow, both solutions attain positive attitude with the increasing magnitude of  $\beta$ . In the case of no suction effects, the second solution remains negative throughout the process while first solution changes its behavior from positive to negative as the magnitude of  $\beta$  decreases. These facts can be sighted in Table 6.4, wherein also noted that a unique solution exists for  $\beta = 0$ .

The velocity profiles for various values of  $\beta$  and S are drawn in Figs. 6.5–6.9, where dual solutions have been noted which obviously satisfy the far field boundary conditions, asymptotically. At some chosen values of S, the velocity profiles are presented in Figs. 6.5 & 6.6, for  $\beta=-1$  and  $\beta=-2$ , respectively, where almost similar behavior is depicted in both situations. The second solutions, in both circumstances, have more boundary-layer thickness as compared to first solution. Figs. 6.7 & 6.9 are plotted to see the effects of suction/injection parameter on velocity, while Fig. 6.9 expresses the velocity profile without the involvement of any suction influence. It is noticed that the boundary-layer thickness increases with the increment in the retarded nature of the flow. In all situations, the second solution has wider span as compared to the first solution.

#### 6.3 Conclusion

The two-dimensional, unsteady, self-similar boundary-layer flow due to a flat flexible stretching disk under the influences of wall suction/injection and unsteadiness parameter has been examined. During the course of current analysis following facts have been noticed:

- a) The dual solutions are possible not only in the presence of suction/injection parameter but also reported without provision of these ingredients.
- b) The retarded nature of flow has the potency to exhibit the dual solutions while accelerated flow doesn't express any duality and contains only single solution.
- c) The magnitude of skin-friction coefficient, f''(0), enhances as the suction effects magnify and similar behavior is observed for unsteadiness parameter, however, the magnitude of f''(0) becomes lower as the influence of injection increases.
- d) The velocity profiles for second solution, at higher values of suction and unsteadiness parameters, are boosted-up as compared to the first solution.

# Chapter 7

## Duality of solution for a shrinking disk flow

This chapter is devoted to scrutinize the steady as well as unsteady features of the self-similar boundary-layer flow caused by a flat flexible circular disk of infinite radius. The steady and unsteady cases of shrinking disk flow have been considered separately. Interesting findings with regard to the duality of solution have been reported.

This chapter is a continuation of the previous one where the duality of solution for the stretching disk flow has been sorted out for the steady and unsteady flow situations. Similar to the stretching disk case the shrinking disk flow has also not been explored completely. Particularly the power-law form of the shrinking wall has never been considered before, to the best of our knowledge. Moreover, most of the available studies on stretching/shrinking disk flow involve the consideration of rotational effects. Therefore, the prime aim of present analysis is to scrutinize the different characteristics of flat circular non-rotating shrinking disk for the presence of dual solutions. Due to the non-availability of sufficient literature regarding non-rotational character of shrinking disk flows, the present study seems to be a unique effort made to fill the existing gap. Since, the idea of multiple/dual solutions has provoked various fruitful attempts to figure out the multiplicity of the flow phenomenon originated by the shrinking disk surfaces. In this context, the current work is made to explore the steady and unsteady characteristics of the self-similar boundary-layer flow induced by shrinking disk; mainly the exploration of dual solutions is the key feature.

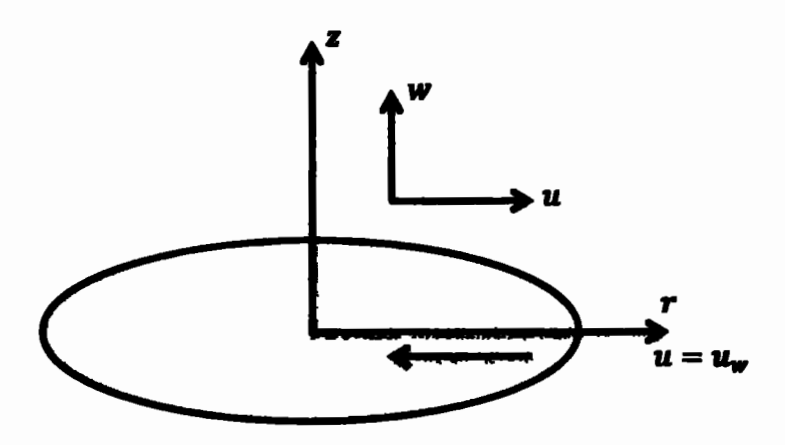


Fig. 7.1: Flow geometry and associated coordinates.

### 7.1 Steady boundary-layer flow due to a shrinking disk

In this section, nature of axisymmetric flows due to a steady shrinking disk is considered. Fang [79] was initiated the investigation of stretching disk flow by taking linearly varying stretching wall velocity and reported an exact self-similar. Like the stretching case of the disk flow, its shrinking features are studied for rotational effects of linearly varying wall velocities and non-rotational situations are rarely dealt. Fortunately, a similarity criterion for the power-law (non-linear) of shrinking wall velocity for the disk case was described by Mehmood [56] in his recently published monograph. In this section, the existence of dual solution has been analyzed for power-law (non-linear) form of radially shrinking wall velocity.

#### 7.1.1 Statement of the problem

Consider a non-rotating flexible circular disk which is shrinking in radially direction. In this case all the assumptions are same as being considered for the steady stretching prospective, except of the negative sign with the wall velocities, which is obvious. A schematic of the flow is shown in Fig. 7.1 with the associated system of

coordinates. Due to quite resemblances with stretching, the continuity equation and the equation are same as given in Eqs. (6.1)—(6.2), however, wall velocities (as introduced by Mehmood [56] for the under consideration problem) are of the form given by

$$u_w(r) = -ar^m,$$
  $w_w(r) = dr^{\frac{m-1}{2}},$  (7.1)

where a denotes a uniform shrinking rate, and d is a constant such that: d > 0 correspond to wall injection velocity and d < 0 correspond to wall suction velocity. Mehmood [56] introduced the following similarity transformations:

$$\eta = \sqrt{\frac{a}{\nu}} r^{\frac{m-1}{2}} z, \quad u = -ar^m f'(\eta), \quad w = \sqrt{a\nu} r^{\frac{m-1}{2}} (\frac{m+3}{2} f + \frac{m-3}{2} \eta f'), \quad (7.2)$$

due to which continuity equation (Eq. (6.1)) is satisfied identically, while the equation of motions along with boundary conditions (i.e., (6.2)–(6.3)) transform as:

$$f''' = \left(\frac{m+3}{2}\right) f f'' - m f'^2 \tag{7.3}$$

$$f'(0) = 1,$$
  $f(0) = \frac{2}{m+3}S,$   $f'(\infty) = 0,$  (7.4)

where  $S = \frac{d}{\sqrt{av}}$  denotes dimensionless suction/injection: S < 0 correspond to wall suction while S > 0 referred to wall injection.

A comparison of the systems (3.2)-(3.3) and (7.3)-(7.4) shows that the boundary data of the two systems are identical while the self-similar equations of the two systems, namely, Eqs. (3.2) and (7.3) with little bit variations therein. Again, here it is also noticed that Eq. (7.3) can easily recovered by replacing "m" by "3m" in Eq. (3.2). A detailed information can be seen in [56], where the author has given a consolidated criterion regarding recovering self-similar solution (in the accelerated case m > 0) for the disk from the self-similar solution of two-dimensional stretching sheet flow.

**Table 7.1:** Values of f''(0) against m for some selected values of S.

	S = ·	-7.0	<b>S</b> = -	-8.0	S = -	10.0	S = -	12.0
m	1st sol.	2nd sol.	1st sol.	2nd sol.	1st sol.	2nd sol.	1st sol.	2nd sol.
-10	-7.8725		-8.7797		-10.6404		-12.5419	
<b>-5</b>	-7.4098		-8.3622		-10.2933		-12.2460	
-1	-7.0000		-8.0000		-10.0000		-12.0000	
0	-6.8905		-7.9047		-9.9242		-11.9370	
1	-6.7778		-7.8073		-9.8474		-11.8735	
2	-6.6615		-7.7076		-9.7694		-11.8093	
3	-6.5413		-7.6055		-9.6904		-11.7445	
4	-6.4168	3.1457	-7.5008	6.5805	-9.6101	17.6026	-11.6791	35.1808
5	-6.2873	2.9059	-7.3932	6.1791	-9.5286	16.7238	-11.6129	33.5970
6	-6.1524	2.4278	-7.2825	5.4239	<b>-9.4457</b>	15.1533	-11.5461	30.8172
7	-6.0112	1.9247	-7.1685	4.6407	-9.3615	13.5335	-11.4786	27.9528
8	-5.8629	1.4489	-7.0508	3.9109	-9.2758	12.0263	-11.4103	25.2844
9	-5.7062	1.0105	-6.9290	3.2527	-9.1886	10.6696	-11.3412	22.8779
10	-5.5396	0.6064	-6.8027	2.6644	-9.0998	9.4619	-11.2714	20.7316

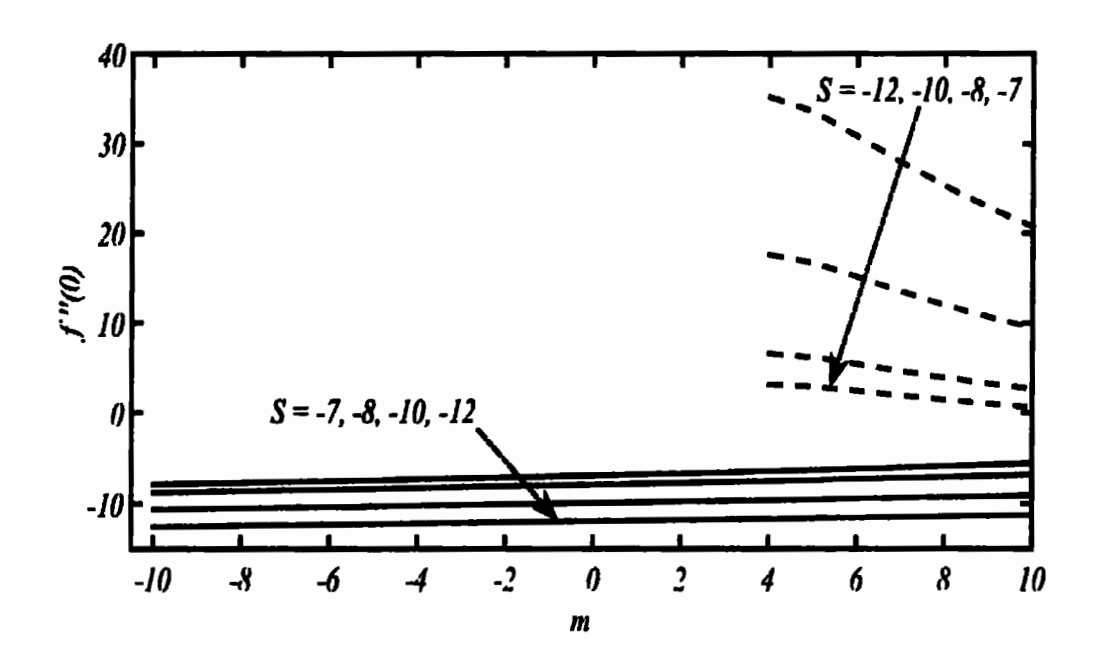


Fig. 7.2: Dual solutions shown by f''(0) for some selected values of S against Power-law index, m.

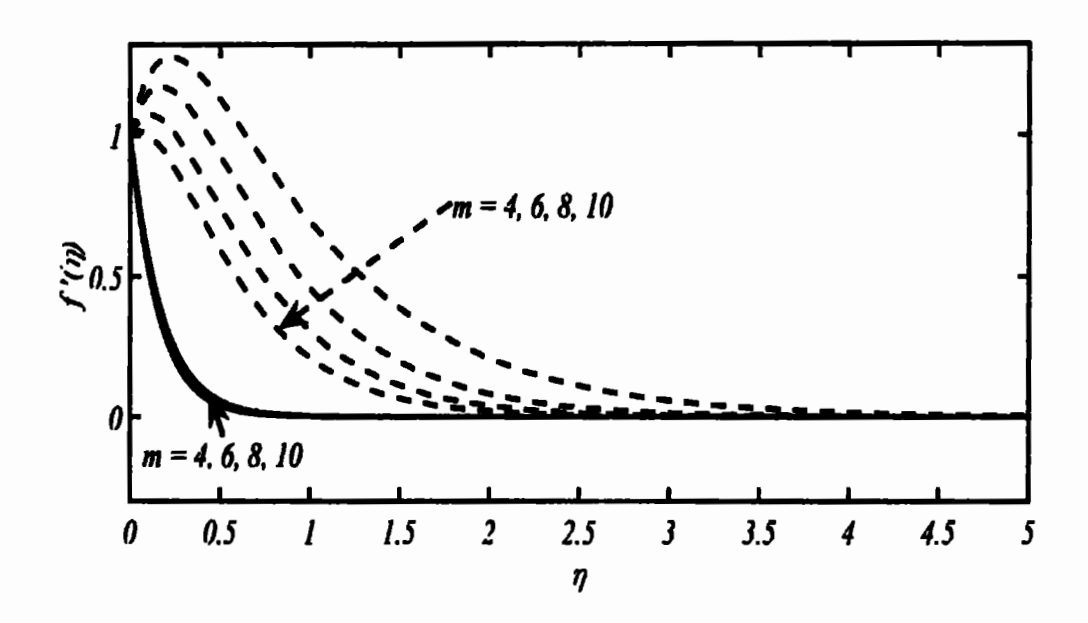


Fig. 7.3: Velocity profile for different values of power-law index, m at S=-7.

## 7.1.2 Duality of solution

Recently, Mehmood and Usman [55] provided comprehensive information regarding the existence of dual solutions for stretching/shrinking surface flows, wherein the authors [55], already reported the duality of solution for a shrinking sheet, therefore, it is not needed to explain the under consideration problem, separately; rather the solution of the present problem can easily be recovered from that presented in [56] by just replacing power-law index "m" by "3m" in the data of [56]. By following previous practice the outcomes found out for the case of steady shrinking disk flow are presented in Table 7.1, and displayed in Figs. 7.2–7.3. During the study, dual solutions have been figured out for m > 3, while after that a unique solution is sighted till m = -1. Further, it is also noted that the solution persist in the presence of adequate amount of suction velocity. The first branch of solutions reflects smooth but minor variations and having

negative values in entire domain of solution. However, the second branch of solutions has a different attitude that reported for first solution.

## 7.2 Unsteady boundary-layer flow due to a shrinking disk

Since regarding the existence of multiple solutions, bulk of literature has been produced by many authors towards shrinking surface flows. Meanwhile, ample efforts were made to analyze the fluid flow circumstances caused because of disk surfaces rotating with specific angular velocity. However, only few efforts were carried out to scrutinize the disk flow behavior in the absence of rotational motion. Therefore, the nonrotational shrinking disk flow is also required to be explored for the existence of dual solutions. The inspiration of the recent investigation is obtained from the contributions rendered by the author [56], wherein the wall velocity of the form  $u_w(r,t) = \frac{-\bar{a}r}{1-rt}$ ;  $\bar{a} > 0$ is suggested, in case of radially shrinking disk having infinite radius, for the existence of self-similar boundary-layer flow. The proposed retarded shrinking wall velocity  $(u_w(r,t) = \frac{-dr}{1-\gamma t})$  contributes to establish a retarded boundary-layer and enables one to figure out some meaningful solution with the provision of mass suction

#### 7.2.1 Mathematical formulation

For the mathematical modeling of the problem of unsteady shrinking disk flow, almost all assumptions are analogous as narrated in the case of unsteady stretching disk (sec 6.2), due to which the equation of continuity as well as the equation of motion remain the same as referred in Eq. (6.1) & Eq. (6.2). Therefore, there is no need to reproduce them, herein. The only difference is the choice of shrinking wall velocity of the

form  $u_w(r,\tau) = -\frac{\alpha r}{1-\gamma t}$ , which modifies the similarity transformation, given in Eq. (6.5), as under:

$$\eta = \sqrt{\frac{a}{\nu}} \frac{1}{\sqrt{1-\gamma t}} z, \qquad u = \frac{-ar}{1-\gamma t} f'(\eta), \qquad and \qquad w = 2\sqrt{\frac{a\nu}{1-\gamma t}} f(\eta). \tag{7.5}$$

Eq. (7.5), obviously satisfies the continuity equation (Eq. (6.1)), identically, and its utilization converts the equation of motion (Eq. (6.2)) and the associated boundary conditions to the following form:

$$f''' = 2ff'' - f'^2 + \beta(f' + \frac{\eta}{2}f''), \tag{7.6}$$

$$f'(0) = 1, f(0) = S, f'(\infty) = 0,$$
 (7.7)

where,  $\beta = \frac{\gamma}{a}$  is the unsteadiness parameter: whereas its positive and negative values categorize the accelerated and decelerated cases, respectively. Further, by choosing  $\beta = -1$ , the governing Eq. (7.6) yields the Eq. 8.52 framed by Mehmood [56] for unsteady shrinking disk. Furthermore, for the above mentioned self-similar system, the normal wall velocity must be of the form  $w_w(r,\tau) = \frac{d}{\sqrt{1-\gamma t}}$  and its dimensionless form reads as  $\frac{d}{2\sqrt{av}}$  (say S). A comparison of the two equations, namely Eq. (7.6) and Eq. (6.6) reflects that both are the same having opposite scalar coefficients. Moreover, Eq. (7.6) resembles to Eq. (3.14) by a lot involving a little difference in its constant coefficient. Therefore, all such problems are different from each other and have been given attention, separately.

**Table 7.2:** Numerical values of  $S_c$  for some selected values of the parameter  $\beta$ .

β	Sc	1st Sol	2 <sup>nd</sup> SoL
-1.0	-1.346886807	-1.1532	-1.1532
-2.0	-1.365284109	-0.7659	-0.7659
-3.0	-1.3781027822	-0.3812	-0.3812
-4.0	-1.3879697533	0.0000	0.0000
-5.0	-1.39598577367	0.3779	0.3779

**Table 7.3:** Numerical values of  $\beta_c$  for some selected values of suction parameter S.

S	βς	1 <sup>st</sup> Sol.	2 <sup>nd</sup> Sol.
-1.35	-1.1400095	-1.0990	-1.0990
-1.36	-1.66710229	-0.8947	-0.8947
-1.38	-3.17491743	-0.3142	-0.3142
-1.40	-5.5762158	0.594	0.594

**Table 7.4 (a-b):** Numerical values f''(0) for some selected values of  $\beta$  and S.

(7.4 a)

_							_		_						
-5.0	3mg 201	I	ŀ	ı	I	21.5388	35.3691	45.0050	52.8125	59.6118	65.7670	71.4706	76.8373	81.9410	86.8327
S = -5.0	1. Sot	-9.9500	-9.8987	-9.8730	-9.8474	-9.7961	-9.7447	-9.6934	-9.6421	-9.5908	-9.5395	-9.4882	-9.4369	-9.3856	-93343
-4.0	Jos	I	_	ı	1	12.6149	20.7323	26.5696	31,4614	35.8238	39.8410	43.6118	47.1960	50.6328	53.9495
S=-	1" SoL	ı	-7.8724	-7.8399	-7.8073	-7.7422	-7.6770	-7.6119	-7.5468	-7.4817	-7.4166	-7.3514	-7.2863	-7.2212	-7.1561
-3.0	JoS put	ı	ı	ı	-	2.6067	9.7837	12.9874	15.7756	18.3228	20.7085	22.9768	25.1547	27.2605	29.3068
S=-	705 ,1	ı	-5.8271	-5.7821	-5.7371	-5.6472	-5.5573	-5.4673	-5.3774	-5.2875	-5.1975	-5.1076	-5.0176	-4.9277	-4.8377
-2.0	7- Sol	ı	ı	1	1	1.0662	2.7301	4.1167	5.3748	6.5546	7.6804	8.7660	9.8200	10.8485	11.8558
S	705 7	ı	-3.7269	-3.6507	-3.5745	-3.4220	-3.2695	-3.1170	-2.9644	-2.8117	-2.6590	-2.5063	-2.3535	-2.2007	-2.0479
1.50	7m Sol.	1	ı	ı	1	-0.3596	0.3433	0.9640	1.5402	2.0867	2.6114	3.1189	3.6124	4.0941	4.5656
S = -1.50	705 ,1	Ī	ı	-24697	-23344	-2.0615	-1.7858	-1.5078	-1.2275	-0.9453	-0.6611	-0.3750	-0.0873	0.2020	0.4930
1.40	795 74	ı	ı	ı	-1.3491	-0.6980	-0.2448	0.1327	0.4455	9/9970	i	ı	1	ı	ı
S = -1.40	1. Sol	ı	ı	-2.1945	-2.0192	-1.6546	-1.2699	-0.8602	-0.4146	0.1021	****	1	1	ı	ı
1.38	705 12	1	ı	ı	-1.3404	-0.7937	-0.4323	-0.2351		1	i	1	-	1	1
S = -1.38	1ª Sol	ı	ı	١	-1.9458	-1.5422	-1.0927	-0.5243	1	١	1	ı	}	1	ı
1.36	75.72	ı	1	ı	-1.3464	-0.9258	1	1	1	1	ı	1	1	i	1
S = -1.36	I" Sol	ı	ł	ı	-1.8653	-1.3925	١	1		ı	1	1	-	ı	١
1.35	705 ,2	ı	_		-1.3554	-1.0414						•			i
S = -1.35	705 "I			1	-1.8210	-1.2678									
9	Ь	2.0	1.0	0.5	0.0	-1.0	-2.0	-3.0	-4.0	-5.0	-6.0	-7.0	-8.0	0.6-	-10.0

_			_	г	Г	Т	Т	Т	Т	Г				Г									Т
-30.0	705 p.L	ı	ł	ı	ı	ı	ı	I	ı	i	ı	l	ı	565.0	961.6	1296.7	1595.6	1869.4	2124.0	2363.3	2590.0	2805.8	
S	1.50	-60.0583	-60.0500	-60.0417	-60.0333	-60.0250	-60.0167	-60.0083	-60.0000	-59.9916	-59.9833	-59.9791	-60.0004	-59.9667	-59.9583	-59.9500	-59.9416	-59.933	-59.9249	-59.9166	-59.9082	-59.8999	
-25.0	7 Sol.	ı	ı	ı	ı	1	ı	1	1	ı	ı	ı	ı	31.9766	53.0935	67.9296	79.6999	89.7411	98.6831	106.8631	114,4811	121.6654	
N II	74.504	1	-50.0600	-50.0500	-50.0400	-50.0300	-50.0200	-50.0100	-50.0000	-49.9900	-49.9799	-49.9749	-49.9699	-49.9600	-49.9499	-49.9399	-49.9299	-49.9199	-49.9099	-49.8999	-49.8899	-49.8798	
-20.0	75.52	ı	1	ı	ı	ı	1	ı	ı	ı	ı	ı	ı	418.83	713.15	960.12	1179.42	1379.18	1564.16	1737.29	1900.5	2055.4	
  -	14.504	i	!	-40.0626	-40.0501	-40.0375	-40.0250	-40.0125	-40.0000	-39.9875	-39.9749	-39.9687	-39.9624	-39.9499	-39.9374	-39.9249	-39.9123	-39.8998	-39.8873	-39.8748	-39.8623	-39.8497	
-15.0	705 72	1	1	1	ļ	1	ı	ı	ı	ı	ı	ı	1	176.98	301.25	402.65	490.42	568.57	639.34	704.11	763.86	819.32	
S	1. Sol	ı	ı	i	1	i	-30.0334	-30.0167	-30.0000	-29.9833	-29.9666	-29.9582	-29.9499	-29.9332	-29.9164	-29.8997	-29.8830	-29.8663	-29.8496	-29.8329	-29.8162	-29.7995	
-10.0	74.504	1	1	1	1	ı	ı	ı	1	ı	1	ı	86.1829	146.1011	192.855	231,613	264.739	293.696	319,500	342.874	364.341	384.28	
S H	1.504	ı	ı	1	ı	ı	1	1	-20.0001	-19.9750	-19.9498	-19.9372	-19.9246	-19.8995	-19.8743	-19.8492	-19.8240	-19.7988	-19.7737	-19.7485	-19.7234	-19.6982	
-9.0	795 74	1	ı	ļ	ı	1	ı	ı	ı	1	ı	ı	1	70.9301	119.9742	157.544	188.172	214.064	236.596	256.679	274.926	291.752	
II	105,1	ł	I	ı	ı	1	1	1	-18.0002	-17.9722	-17.9442	-17.9302	-17.9162	-17.8882	-17.8602	-17.8322	-17.8042	-17.7762	-17.7482	-17.7202	-17.6922	-17.6642	
-8.0	2m Sal.	1	ı	ı	ı	ı	ı	1	ı	ı	1	ı	ı	56.7640	95.6739	124.7427	148.0244	167.5787	184.6192	199.8838	213.8380	226.7883	
. = S	1. 301	1	ı	ı	ı	1	ı	1	ı	-15.9687	-15.9371	-15.9214	-15.9056	-15.8740	-15.8425	-15.8109	-15.7793	-15.7478	-15.7162	-15.6847	-15.6531	-15.6215	
-7.0	3mg 204	1	ı	ı	ı	ı	ı	1	ı	1	1	١	1	43.7525	73.3171	94.7189	111.6540	-13.7110 125.9144	138.4428	-13.6386 149.7689	160.2125	169.9800	
- = S	I" SoL	1	Į	1	I	1	1	i	ı	-13.9642	-13.9281	-13.9100	-13.8919	-13.8557	-13.8195	-13.7833	-13.7472	-13.7110	-13.6748	-13.6386	-13.6024 160.2125	-13.5663 169.9800	
0.0	7m Sol	1			1	1	1	1	1	1	-	-	١	31.9766	53.0935	67.9296	79.6999	89.7411	98.6831	106.8631	114.4811	121.6654	
2 = 2	I" SoL	1	1	-	İ	-	ļ	-	1	-11.9583	-11.9159	-11.8947	-11.8735	-11.8311	-11.7886	-11.7462	-11.7038	-11.6614	-11.6190	-11.5766	-11.5342	-11.4918	
æ		10.0	9.0	8.0	7.0	0.9	5.0	4.0	3.0	2.0	1.0	0.5	0.0	-1.0	-2.0	-3.0	0.4	-5.0	-6.0	-7.0	9.0	-9.0	

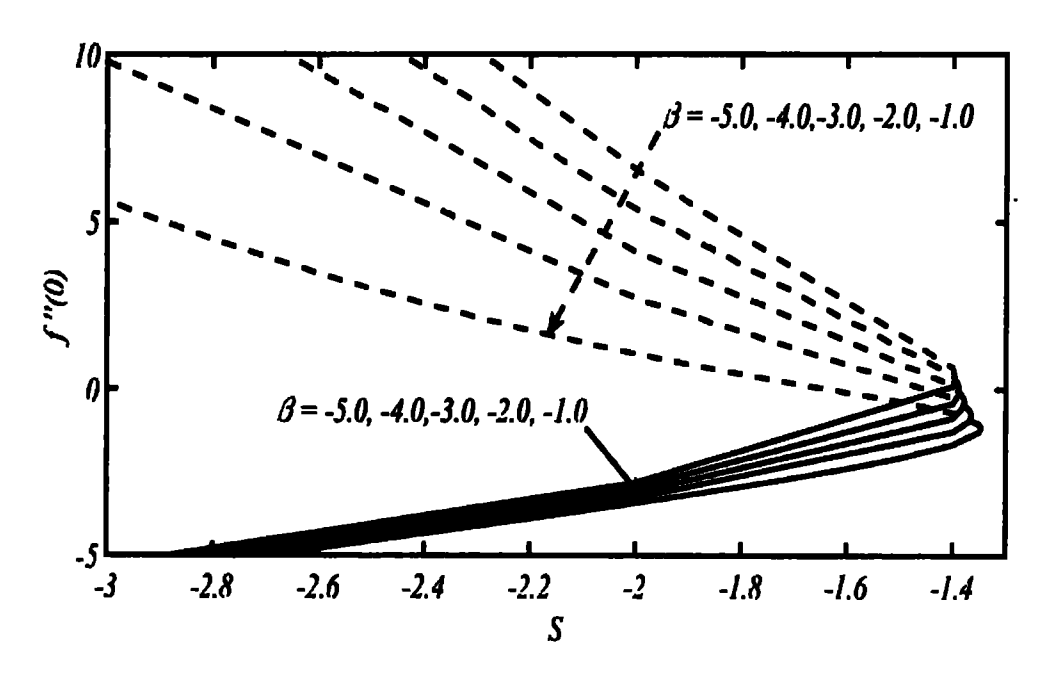


Fig. 7.4: Duality of solution shown through f''(0) against S at some selected values of unsteadiness parameter  $\beta$ .

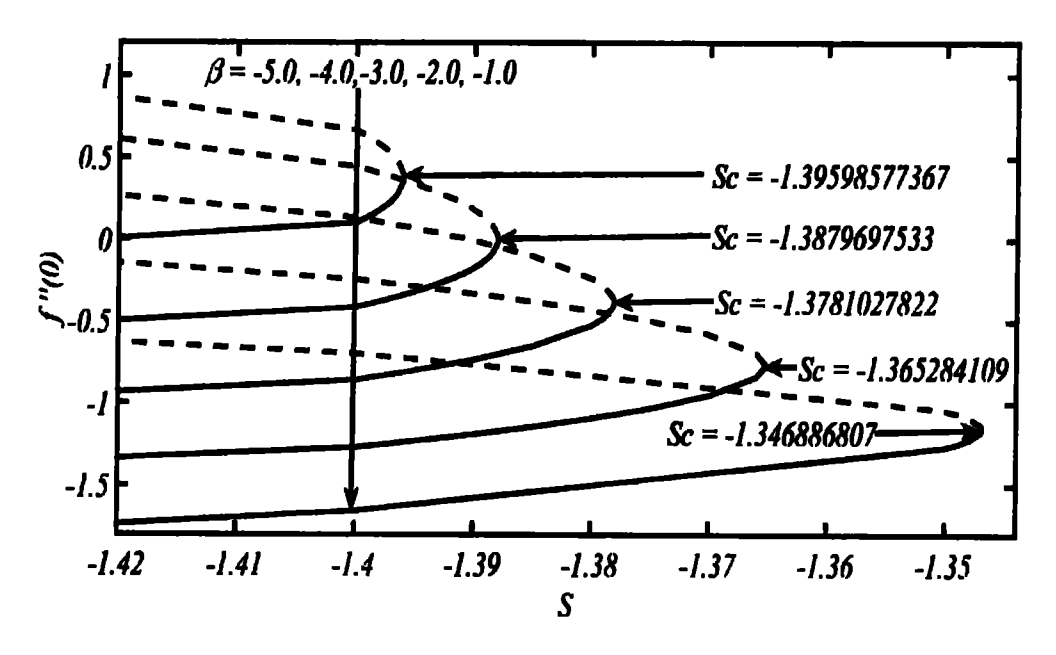


Fig. 7.5: A zoom-in portion of Fig. 7.4 showing the convergence of two solution branches.

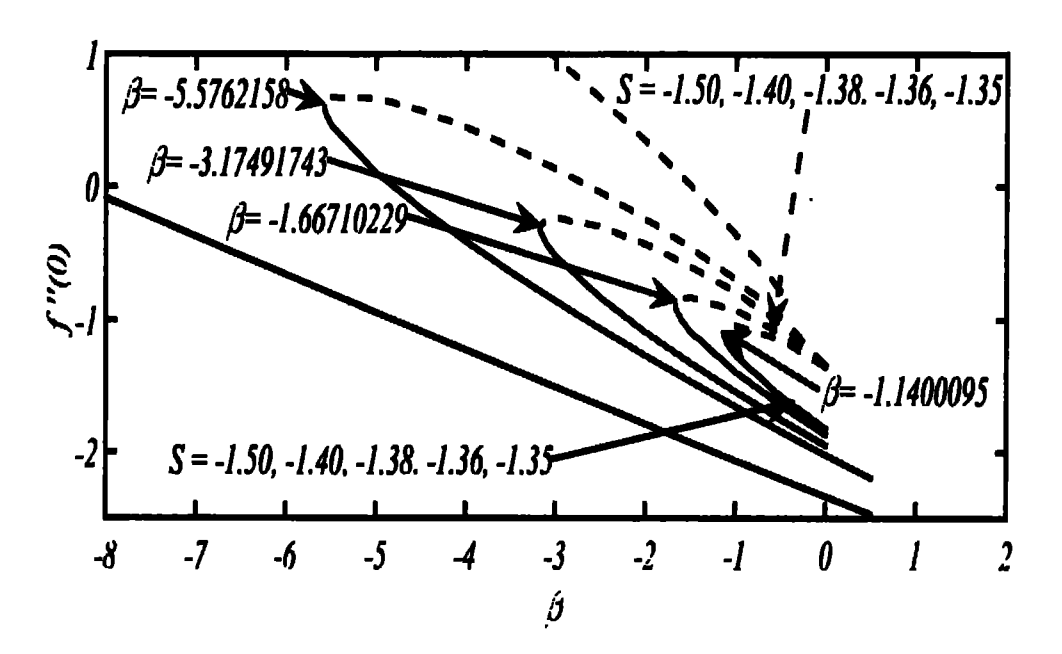


Fig. 7.6: Duality of solution shown through f''(0) plotted against  $\beta$  at some selected values of suction parameter S.

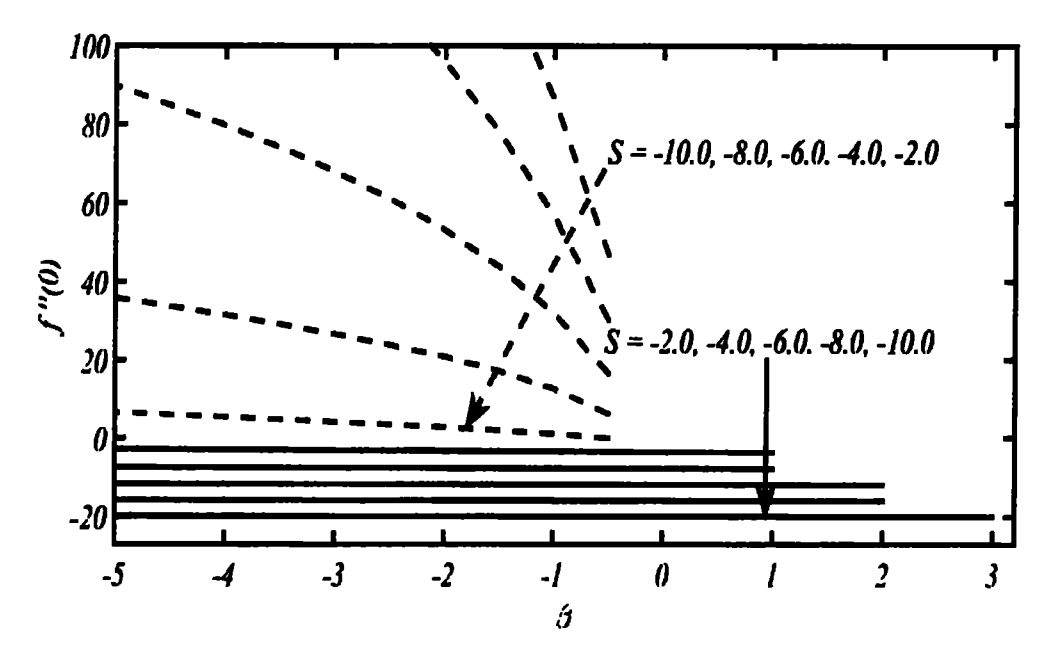


Fig. 7.7: Duality of solution shown through f''(0) plotted against  $\beta$  at some moderate values of S.

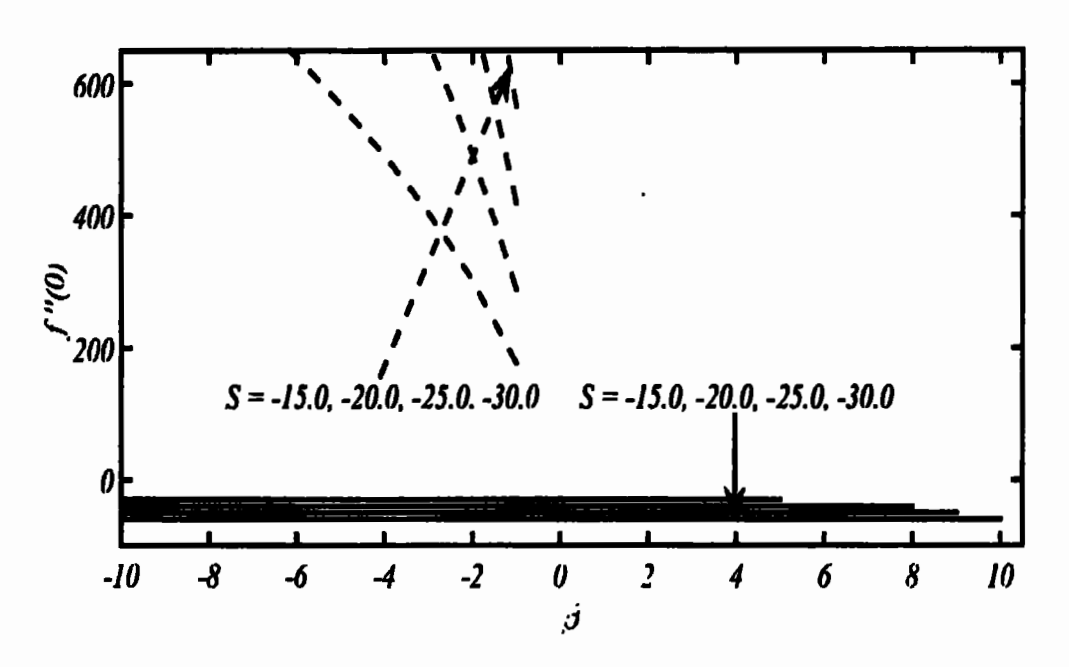


Fig. 7.8: Duality of solution shown through f''(0) plotted against  $\beta$  at some higher values of S.

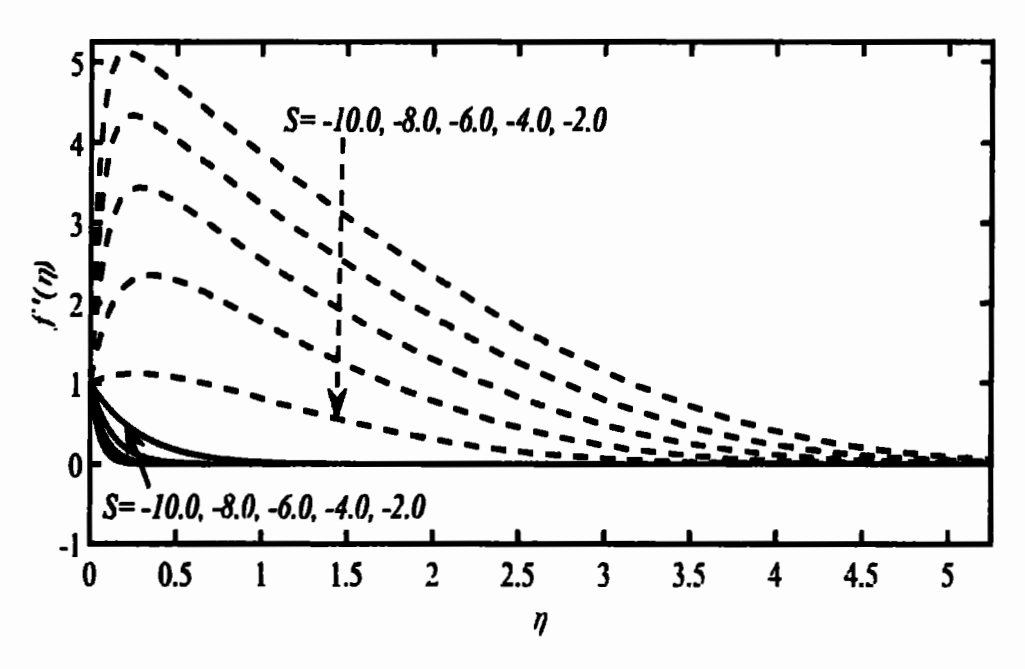


Fig. 7.9: Velocity profile for different values of suction parameter S at  $\beta = -1$ .

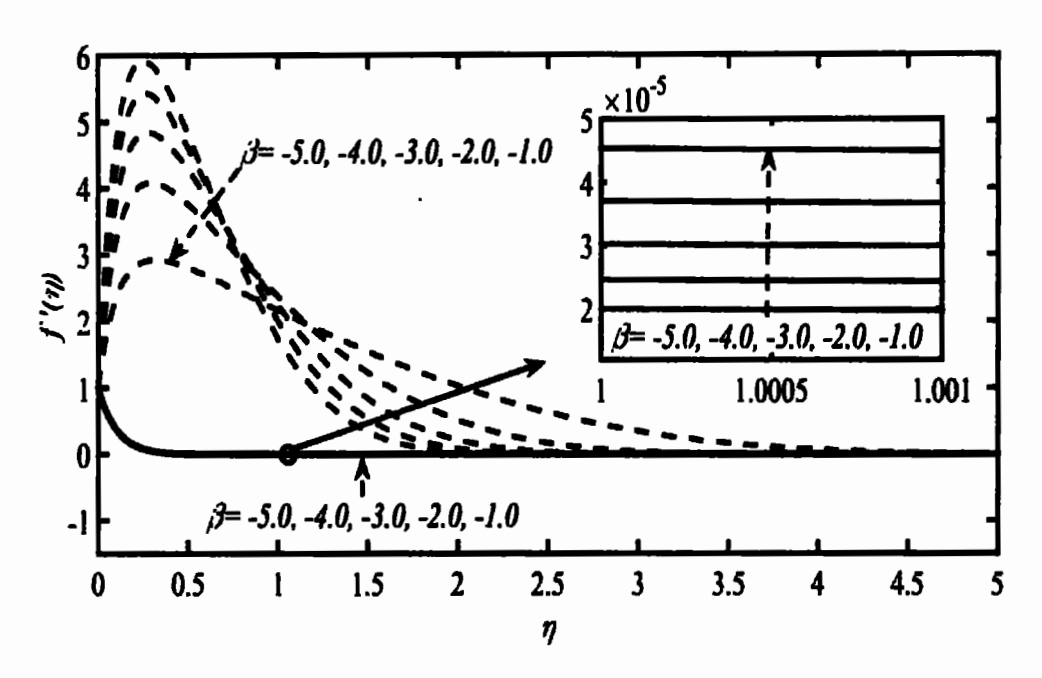


Fig. 7.10: Velocity profile for different values of  $\beta$  at S=-5.

#### 7.2.2 Results and discussion

The solution of the governing Eq. (7.6), subject to the boundary-condition given in Eq. (7.7), is chalked-out with the aid of an authentic numerical technique used in previous chapters. The outcomes of the present study are different with the findings reported (in **Chapter 6**) for unsteady stretching disk in the sense that here dual solutions are possible under the provision of sufficient wall suction only, while, presence of injection effects play no role in the existence of solution. Due to such kind of facts, the character of suction parameter is discussed in view of unsteadiness parameter ( $\beta$ ). It is noticed that, under the influence of wall suction, dual behavior of the solution is sighted only for retarded nature of flow  $\beta$ (< 0), while, inspite of utmost efforts, its accelerated scenario is see unable to contribute towards duality of the solution. The numerical data, for involved parameters, obtained during the course of present investigations, is presented

in graphical form in Figs. 7.4–7.8, and also displayed in tabular form in Table 7.2–7.4. The coefficient of wall skin-friction, f''(0), is plotted, against S at some selected values of  $\beta$ , in Fig. 7.4, whereas its zoom-in portion can be seen in Fig. 7.5. From Fig. 7.4, it is clearly observed that the existence of duality is only confined to retarded flow situation in the presence of suction effects. Meanwhile, after making persistent attempts, it is also perceived that there is no duality of solution for injection parameter as well as in the absence of suction effects. Further, the existence of dual solution, with the increasing effects of  $\beta$ , is totally dependent upon the presence of suction parameter and this fact can also be visualized in Figs. 7.4–7.5. The two solutions are seen to converge with the reduction of suction effects and ultimately an overlapping solution is observed at some critical value of S (see Fig. 7.5), whereas these critical values ( $S_c$ ) have been obtained with great devotion as well as after paying utmost efforts and are presented in Table 7.2.

Figs. 7.6–7.8 are drawn for various values of S against  $\beta$  and there have been experienced valuable outcomes. Fig. 7.6 is portrayed to represent the behavior of skin-friction coefficient; comparatively for smaller values of S, wherein it is depicted that the interval of  $\beta$  is expended with the increasing effects of suction parameter. Here it is also noted that for a specific/fixed value of S, the gap between both solutions becomes narrow and narrow as the magnitude of  $\beta$  reduces and as the process continues an overlapping solution is sighted. Fortunately, we were able to find out critical points against each selected values of S, whereas the information obtained for the critical points are enumerated in Table 7.3. Here, it is also a fact that the convergence of both solutions, as narrated in Fig. 7.6, is possible for smaller values of S while for the case of higher effects of suction parameter, the merging situations of both solutions could not be materialized

even at the cost of diligent attempts. The reason behind this fact is the leading role of suction parameter which enables the solution to be pertained for specific range of retarded flow. As the retarded nature of the flow exceeds from a certain limit (i.e., for higher values of  $\beta$ ) the solution disappears, accordingly. The critical values reported in Table 7.3 to clearly describe the range for which the solution is available. To see the effects of higher values of S, for decelerated/accelerated flow, Figs. 7.7-7.8 are plotted. wherein almost similar features have been noticed as observed in Fig. 7.6. However, some other interesting information about the existence/non-existence of solution is also experienced. For example, it is depicted that the dominant character of suction parameter results in the vanishing of second solution even for smaller values of  $\beta$ . This is the primary difference between the results reported for smaller values of S (Fig. 7.6) and outcomes figured out for larger values of S (Figs. 7.7-7.8). It is already described in Table 7.4, that for small values of S (i.e., S = -1.40, -1.38, -1.36, -1.35) the solution is possible for all  $\beta < 0$ , however the solution starts decaying for further higher values of S. From Table 7.4, it is noticed that at S = -1.50, the second solution disappears in the interval  $-1 < \beta < 0$ , however, the first solution is seen for some positive values of  $\beta$ . It is worth noting aspect that for the retarded nature of flow, the presence of dual solutions is linked with the provision of some external agents, i.e., suction/injection, pressuregradient or surface curvature etc. In the present analysis, the suction parameter plays a supporting role in the existence of dual solutions.

The behavior of velocity profile under the influence of S and  $\beta$  is presented in Figs. 7.9-7.10, wherein it is well noticed that the boundary-layer thickness reduces, in case of first solution, with the increasing effects of suction. Whereas, unsteadiness

parameter exerts almost insignificant affects herein. Such kind of information is agreed with the already reported findings. Comparatively, to the first branch of solution, the second solution experiences prominent changes in the boundary-layer character with the variations of both S and  $\beta$ .

#### 7.3 Conclusion

During the current analysis, unsteady flow stimulated by sudden motion of a shrinking disk is discussed. The analysis reveals that the duality of solution is not an essential feature of shrinking surface flows. During the course of present study, it is noticed that the existence of dual solutions could not be sighted for all values of  $\beta$ , even in the presence of sufficient wall suction. It is revealed that for the existence of dual solutions the flow should be of retarded nature, otherwise neither the shrinking surface nor the provision of sufficient wall suction guarantee for the existence of duality of solution. The flow phenomenon under consideration, is categorized in two phases, i.e., the accelerated flow situations ( $\beta > 0$ ) and the decelerated circumstances ( $\beta < 0$ ), whereas for  $\beta = 0$ , the steady character of the flow is achieved. It is clearly assessed that accelerated flow does not play any role in the existence of dual solutions and only a unique solution is obtained under the provision of sufficient wall suction. On the other hand, for the case of retarded flow, dual solutions exist with the assistance of sufficient wall suction velocity. Further, under the moderate effects of suction velocity, the solution is reported for all values of  $\beta$  < 0, whereas for higher values of suction the domain for the existence of solution reduces to  $\beta \leq -1$ . On the basis of above discussion, it has become clear that the retarded nature of flow is the key for the existence of dual/nonunique solution.

# **Chapter 8**

#### **Conclusions**

The current study analyzed the self-similar boundary-layer flows stimulated by continuous stretching/shrinking surfaces, particularly to search out the existence/non-existence of multiple solutions. With the appearance of a new concept regarding the non-unique nature of the shrinking surface flows, the topic of multiplicity of solution has attracted a number of researchers who did their best to investigate the viscous flows for the possibility of non-unique solution. However, there are some misinterpretations attributed to the existence of multiple solutions from very first day. That is, possibility of multiplicity is assumed for the shrinking surface flows under the provision of sufficient wall suction. That is why; very rare fruitful efforts were made to search out the non-unique solutions for the cases of stretching surface flows.

The steady/unsteady aspects of continuous stretching and shrinking sheet have been analyzed, for the existence/non-existence of dual solutions, in the presence as well as absence of wall suction/injection velocity. For a steady flow due to a stretching sheet when the wall velocity follows a (non-linear) power-law form the uniqueness and non-uniqueness of solution has equally been observed. The matter of fact is that such a stretching sheet flow admits a unique solution when the stretching wall velocity is of accelerated nature and admits multiple solutions when the wall velocity is of decelerated nature. Definitely, for the retarded nature of stretching wall velocity the blowing boundary-layer is assisted by the provision of sufficient amount of wall suction. Besides the steady flow due to a stretching sheet the unsteady aspects of the stretching sheet flow have also been given a full consideration. Important information is obtained in

connection to the duality of solution. The existence of non-unique solution is experienced not only in the presence of wall suction/injection velocity but is also figured-out in the absence of any of these. It is again a worth-mentioning fact that the duality of solution has been sighted for the decelerated nature of wall velocity. The outcomes of the investigation of steady/unsteady stretching sheet flow are exclusive in the context of well-established facts about the existence of multiple solutions in such flows. Earlier, the characteristic of non-uniqueness of solution had been assumed to be an integral part of the shrinking surface flows (only) under the provision of sufficient wall suction. However, the facts reported in this dissertation, with regard to the stretching surface flows, have simply neglected the well-established unrealistic facts and prestige of shrinking surface flows. Moreover, the provision of sufficient wall suction for the existence of dual solution has also been neglected as the dual solutions have been reported for the decelerated flow in the presence of suction/injection as well as in the absence of these ingredients. These facts clearly indicate that the occurrence of dual solution is just because of the retarded nature of the flow.

According to the massive literature on the duality of shrinking surface flows, the most attractive features of the shrinking surface flows are believed to be the existence of multiple solutions subject to the provision of adequate amount of wall suction velocity. Moreover, the shrinking surface flows are admitted to exhibit more non-linear phenomenon. On this basis the shrinking surface flows had been believed to be richer in physics than the stretching surface flows. This chapter offers a unique opportunity to compare the two flows (due to stretching and shrinking surfaces) in this regard. Similar to the stretching sheet flow, the steady and unsteady cases of the shrinking sheet flow have

also been investigated in full detail, in this dissertation. Our analysis reflects that there exists nothing especial or specific to the shrinking sheet flow. All the features, regarding the occurrence of dual solutions, observed in the stretching sheet flow have equally been observed in the shrinking sheet flow. For the shrinking sheet flow too, the duality is simply reported because of the decelerated nature of the wall velocity. For the accelerated nature of the wall velocity the shrinking sheet flow admits a unique solution, similar to the stretching sheet flow, which has never been realized. It is a matter of fact that neither the stretching sheet flows had been investigated for the existence of dual solutions nor the shrinking sheet flows had been investigated for the existence of unique solution. That is, in the produced literature, the topic of stretching sheet flow had always been studied for the accelerated case while the shrinking sheet flow had always been studied for the decelerated case. Consequently, non-unique solutions was assumed to be the salient feature of the shrinking sheet flow while the stretching sheet flow was believed to admit a unique solution.

Like the planner case of viscous flows due to stretching/shrinking surfaces, their axisymmetric aspects have also well inspiring motivations. In this regard the steady/unsteady cases of the flow due to a stretching cylinder have been considered in detail. The existence of non-unique solution for the case of two-dimensional stretching sheet gives a trivial motivation to investigate for the existence of dual solutions in axisymmetric case. During this analysis, it is noted that dual solutions are existent in the presence of suction/injection velocity. It is interesting to note that for stretching cylinder flow (when the wall velocity follows a power-law form) the duality has also been sighted in the accelerated case. This apparently seems to be the consequence of the involvement

of suction/injection velocity and the surface transverse curvature parameter which infact disturb the flow in a variety of ways. It is therefore reported that the case of stretching cylinder requires further careful analysis in order to develop a complete understanding of the associate flow phenomenon. It is also remarked that, to the best of our knowledge, the case of non-linear stretching cylinder has never been investigated for the existence of duality of solution. Similarly, the duality of solution has also been sighted for the unsteady stretching cylinder, not only due to the provision of wall suction velocity but also due to the provision of wall injection velocity, and more interestingly, in the absence of these two.

Similar to the case of stretching cylinder flow, duality has also been captured for the shrinking cylinder flow. Dual solutions have been observed for the decelerated nature of wall velocity in the steady and unsteady cases. Overall, duality of solution has been observed in the presence of wall suction/injection and even in the absence of these two. Moreover, the involvement of surface transverse curvature parameter also plays an interesting role regarding the manipulation of flow in view of the non-uniqueness of solution. Thus in this case too, it has been made evident that the duality of solution is not a unique feature of the shrinking surface flows. Moreover, the duality of solution is not simply connected to the provision of sufficient wall suction rather it can also be sighted for other scenarios, such as in the presence of wall injection or even in the absence of wall suction or injection velocity.

The axisymmetric surfaces are composed of cylindrical and disk geometries, whereby the involvement of surface curvature has dominant character in flow situations caused by the motion of continuous moving (stretching/shrinking) cylinder. The disk

surfaces, however, are free from the influence of surface curvature, though exhibiting an axisymmetric flow. The flow phenomenon caused by the continuous motion of steady and unsteady stretching disk has also been investigated for the possibility of dual solutions. In the steady cases of stretching or shrinking disk, availability of second solution has been witnessed for the retarded nature of the wall velocity. In these cases the solution can simply be recovered from the corresponding cases of two-dimensional stretching, or shrinking sheet flow. In the unsteady case of stretching or shrinking disk flow, dual solutions have also been figured out. In the unsteady case there appeared no possibility of recovering the solution from the corresponding two-dimensional flow. In all these cases the fundamental reason for the existence of a non-unique solution is the retarded nature of the corresponding boundary-layer flow.

The behavior of solution curves of unsteady shrinking disk case is quite different from that of unsteady stretching disk case. The dual solutions for shrinking disk flow are possible for decelerated flow only under the provision of sufficient wall suction amount, while for the stretching disk flow duality has also been captured in the presence of suction; in the presence of wall injection, and even in the absence of the two.

In this dissertation, three categories have, mainly, been investigated for the existence of non-unique solution, namely, the steady/unsteady two-dimensional planner case; the two-dimensional axisymmetric case involving circular cylinders; and the two dimensional axisymmetric case of non-rotating disk by considering stretching as well as the shrinking nature of the disk surface. Interestingly, duality of solution has equally been witnessed in all these six different flow situations. It is, overall, concluded that neither the existence of non-unique solution could be regarded as a unique feature of the shrinking

surface flows only, nor it could be solely attributed to the provision of sufficient wall suction velocity. The existence of duality of solution can, however, be attributed to the retarded nature of the on-going boundary-layer flow which is sometimes quite a weak and is supported with the provision of sufficient wall suction velocity or due to the surface transverse curvature; and which is sometimes not that weak and sustains against sufficiently strong wall injection too. In total the retarded boundary-layer is appeared to be a quite vulnerable of producing a non-unique solution. With these outcomes it is expected that most of the misconceptions about the existence of dual solutions for the shrinking surface flows have been cleared, now. In this regard, the current study and the data reported herein are expected to serve as a good reference for future studies.

## References

- [1] L. Prandtl, Über Flüssigkeits bewegung bei sehr kleiner Reibung, In Proceedings of 3rd International Mathematical Congress, Heidelberg, (1904) 484–491.
- [2] S. Goldstein, *Modern Developments in Fluid Dynamics*, Clarendon Press, Oxford, 1938.
- [3] G. K. Batchelor, *An Introduction to the Fluid Dynamics*, Cambridge University Press, 1967.
- [4] H. Schlichting, Boundary Layer Theory, McGraw Hill, New York, 1968.
- [5] H. Blasius, Grenzschichten in Flüssigkeiten mit Kleiner Reibung, ZAMP, 56 (1908) 1-37.
- [6] L. Bairstow, Skin friction, J. Roy. Aero. Soc., 19 (1925) 3.
- [7] S. Goldstein, Concerning some solutions of the boundary-layer equations in hydrodynamics, Proc. Cambr. Phil. Soc., 26 (1930) 1–30.
- [8] L. Howarth, On the solution of the laminar boundary layer equations, Proc. Roy. Soc., London, A 164 (1938) 547-579.
- [9] D. Meksyn, New Methods in Laminar Boundary-Layer Theory, London, 1961.
- [10] J. M. Burgers, In Proceedings of 1st International Congress Application Mechanism, Delft 1924.
- [11] V. M Falkner, S.W Skan, Some approximate solutions of the boundary-layer equations, Phil. Mag., 12 (1931) 865-896.
- [12] B. C. Sakiadis, Boundary-layer behavior on continuous solid surface: I. Boundary-layer equations for two-dimensional and axisymmetric flow, AIChE, 7 (1) (1961) 26-28.
- [13] B. C. Sakiadis, Boundary-layer behavior on continuous solid surfaces: II. The boundary-layer on a continuous flat surface, AIChE, 7 (2) (1961) 221–225.
- [14] F. K. Tsou. E. M. Sparrow, R. J. Glodstein, Flow and heat transfer in the boundary-layer on a continuous moving surface, Int. J. Heat Mass Trans, 10 (1967) 219-235.
- [15] L. J. Crane, Flow past a stretching sheet, ZAMP, 21 (1970) 645-647.
- [16] P. S. Gupta, A.S. Gupta, Heat and mass transfer on a stretching sheet with suction or blowing, Can. J. Chem. Eng., 55 (1977) 744-746.

- [17] A. Chakrabarti, A.S. Gupta, Hydromagnetic flow and heat transfer over a stretching sheet, Q. Appl. Math., 37 (1979) 73-78.
- [18] W. H. H. Banks, Similarity solution of the boundary-layer equations for a stretching wall, J. Mech. Theor. Appl., 2(3) (1983) 375-92.
- [19] E. Magyari and B. Keller, Heat and mass transfer in the boundary layers on an exponentially stretching continuous surface, J. Phys. D Appl. Phys., 32(5) (1999) 577-585.
- [20] K. R. Rajagopal, T. Y. Na and A. S. Gupta, Flow of a viscoelastic fluid over a stretching sheet, Rheol. Acta, 23 (1984) 213-5.
- [21] P. Carragher, L. J. Crane, Heat transfer on a continuous stretching sheet, ZAMM, 62 (1982) 564-5.
- [22] L. J. Grubka, K. M. Bobba, Heat transfer characteristics of a continuous stretching surface with variable temperature, ASME J. Heat Trans., 107 (1985) 248-250.
- [23] M. E. Ali, Heat transfer characteristics of a continuous stretching surface, Wärme Stoffübertrag, 29 (1994) 227–234.
- [24] E. Magyari, B. Keller, Exact solutions for self-similar boundary-layer flows induced by permeable stretching wall, Eur. J. Mech. B-Fluids, 19 (2000) 109–122.
- [25] T. Fang, Similarity solution for a moving flat plate thermal boundary-layer, Acta Mech., 163 (2003) 161-172.
- [26] T. Fang, Further study on a moving wall boundary-layer problem with mass transfer, Acta Mech., 163 (2003) 183-188.
- [27] C. Y. Wang, The three dimensional flow due to stretching surface, Phys. Fluids, 27 (1984) 1915–7.
- [28] W. J. McCroskey, Some current research in unsteady fluid dynamics the 1976 freeman scholar lecture, ASME J. Fluid Eng., 99 (1977) 8-39.
- [29] C. D. Surma Devi, H. S. Takhar and G. Nath, Unsteady three-dimensional boundary-layer flow due to a stretching surface. Int. J. Heat Mass Trans, 29 (1986) 1996–1999.
- [30] C. Y. Wang, Liquid film on an unsteady stretching surface, Q. Appl. Math. 48 (1990) 601–610.
- [31] S. H. Smith, An exact solution of the unsteady Navier-Stokes equations resulting from a stretching surface, ASME J. Appl. Mech., 61 (1994) 629-633.

- [32] I. Pop, T. Y. Na, Unsteady flow past a stretching sheet, Mech. Res. Comm., 23 (1996) 413-422.
- [33] H. I. Andersson, J. B. Aarseth, B. S. Dandapat, Heat transfer in a liquid film on an unsteady stretching surface, Int. J. Heat Mass Trans., 43 (2000) 69-74.
- [34] E. M. A. Elbashbeshy, M. A. A. Bazid, Heat transfer over an unsteady stretching surface, Int. J. Heat Mass Trans., 41 (2004) 1-4.
- [35] Sharidan, T. Mahmood, I. Pop, Similarity solutions for the unsteady boundary layer flow and heat transfer due to a stretching sheet, Int. J. Appl. Mech. Eng., 11 (2006) 647-654.
- [36] A. Mehmood, A. Ali, Unsteady boundary-layer flow due to an impulsively started moving plate, Proc. IMechE Part G: J. Aerospace Eng., 221 (2007) 385–390.
- [37] A. Mehmood, A. Ali, T. Shah, Unsteady boundary-layer viscous flow due to an impulsively started porous plate, Can. J. Phys., 86 (2008) 1079-1082.
- [38] R. Tsai, K. H. Huang, J. S. Huang, Flow and heat transfer over an unsteady stretching surface with a non-uniform heat source, Int. Comm. Heat Mass Trans., 35 (2008) 1340–1343.
- [39] S. Mukhopadhyay, Heat transfer analysis of unsteady flow over a porous stretching surface embedded in a porous medium in presence of thermal radiation, Acta. Tech., 56 (2011) 115–124.
- [40] M. Miklavcic, C. Y. Wang, Viscous flow due to a shrinking sheet, Quart. Appl. Math., 64(2) (2006) 283–290.
- [41] T. Fang, Boundary layer flow over a shrinking sheet with power-law velocity, Int. J. Heat Mass Trans., 51(25/26) (2008) 5838-5843.
- [42] T. Fang, W. Liang, C. F Lee, A new solution branch for the Blasius equation— a shrinking sheet problem, Comput. Math Appl., 56(12) (2008) 3088-3095.
- [43] T. Fang and J. Zhang, Closed-form exact solutions of MHD viscous flow over a shrinking sheet, Commun. Nonlinear Sci. Numer. Simulat, 14(7) (2009) 2853–2857.
- [44] T. Fang and J. Zhang. Thermal boundary layers over a shrinking sheet: an analytical solution, Acta. Mech., 209 (2010) 325-343.

- [45] H. Rosali, A. Ishak, I. Pop, Stagnation point flow and heat transfer over a stretching/shrinking sheet in a porous medium, Int. Comm. Heat Mass Trans., 38 (2011) 1029–1032.
- [46] N. A. Yacob, A. Ishak, I. Pop, Melting heat transfer in boundary—layer stagnation point flow towards a stretching/shrinking sheet in a micropolar fluid, Computers and Fluids, 47 (2011) 16–21.
- [47] N. C. Rosca, T. Grason, I. Pop, Stagnation-point flow and mass transfer with chemical reaction past a permeable stretching/shrinking sheet in a nanofluid, Sains Malaysiana, 41 (2012) 1271–1279.
- [48] Y. Y. Lok, A. Ishak, I. Pop. MHD stagnation-point flow towards a shrinking sheet, Int. J. Numer., Methods Heat Fluid Flow, 21(1) (2011) 61-72.
- [49] T. Fang, J. Zhang, S. Yao, Viscous flow over an unsteady shrinking sheet with mass transfer, Chin. Phys. Lett., 26(1) (2009) 0147031-4.
- [50] N. A. Yacob, A. Ishak, I. Pop, Unsteady flow of a power-law fluid past a shrinking sheet with mass transfer, Z. Naturforsch, 67 (2012) 65-69.
- [51] A. M. Rohni, S. Ahmad, I. Pop, Flow and heat transfer over an unsteady shrinking sheet with suction in a nanofluids, Int. J. Heat Mass Trans., 55 (2012) 1888–1895.
- [52] M. Sualia, N. M. A. Nik Longa, A. Ishak, Unsteady stagnation point flow and heat transfer over a stretching/shrinking sheet with prescribed surface heat flux, App. Math. Comp. Intel., 1 (2012) 1–11.
- [53] A. M. Rohni, S. Ahmad, A. I. M. Ismail, I. Pop, Flow and heat transfer over an unsteady shrinking sheet with suction in a nanofluids using Buongiorno's model. Int. J. Heat Mass Trans., 43 (2013) 75–80.
- [54] S. K. Nandy, T. R. Mahapatra, Effects of slip and heat generation/absorption on MHD stagnation point flow of nanofluid past a stretching/shrinking surface, Int. J. Heat Mass Trans., 64 (2013) 1091–1100.
- [55] A. Mehmood, M. Usman, Fascination of the shrinking sheet flow: a reality or a misconception, J. Appl. Mech. Tech. Phy., 60(3) (2019) 483-490.
- [56] A. Mehmood, Viscous Flows: Stretching and Shrinking of Surfaces, Springer, 2017.
- [57] R. F. Probbstein, D. Elliot, The transverse curvature effect in compressible axially symmetric laminar boundary-layer flow, J. Aero Sci., 23 (1956) 208-214.

- [58] B. C. Sakiadis, Boundary-layer behavior on continuous solid surfaces: III. The boundary-layer on a continuous cylindrical surface, AIChE, 7 (3) (1961) 467-472.
- [59] L. J. Crane, Boundary-layer flow due to a stretching cylinder, ZAMP, 26 (1975) 619-622.
- [60] C. Y. Wang, Fluid flow due to a stretching cylinder, Phys. Fluids, 31(3) (1988) 466–468.
- [61] H. I. Burde, On the motion of fluid near stretching circular cylinder, J. Appl. Math. Mech., 53(2) (1989) 271-273.
- [62] A. Ishak, R. Nazar, I. Pop, Uniform suction/blowing effect on flow and heat transfer due to a stretching cylinder, Appl. Math. Model., 32 (2008) 2059–2060.
- [63] A. Ishak, R. Nazar, Laminar boundary layer flow along a stretching cylinder. Eur. J. Sci. Res., 36(1) (2009) 22-29.
- [64] T. Fang, S. Yao, Viscous swirling flow over a stretching cylinder, Chin. Phys. Lett., 28(11) (2011) 1147021-4.
- [65] S. Mukhopadhyay, MHD boundary layer slip flow along a stretching cylinder, Ain Shams Eng. J., 4 (2013) 317–324.
- [66] A. Mehmood, M. Usman, TVC effects on flow separation on slender cylinders, Thermophys. Aeromech., 25 (2018) 507-514.
- [67] T. G. Fang, J. Zhang, Z. Y. Fang, and T. Hua, Unsteady viscous flow over an expanding stretching cylinder, Chinese Phys. Lett., 28 (12) (2011) 1247071-4.
- [68] Y. Y. Lok, I. Pop, Wang's shrinking cylinder problem with suction near a stagnation point, Phys. Fluids, 23 (2011) 0831021-8.
- [69] W. M. K. A. W. Zaimi, A. Ishak, I. Pop, Unsteady viscous flow over a shrinking cylinder, J. of King Saud University Science, 25(2) (2013) 143-8.
- [70] K. Zaimi, A. Ishak, I. Pop, Unsteady flow due to a contracting cylinder in a nanofluid using Buongiorno's model, Int. J. Heat Mass Trans., 68 (2014) 509-13.
- [71] U. Mishra, G. Singh, Dual solutions of mixed convection flow with momentum and thermal slip flow 0ver a permeable shrinking cylinder, Comput. Fluids, 93 (2014) 107–115.

- [72] V. Marinca, R.D. Ene, Dual approximate solutions of the unsteady viscous flow over a shrinking cylinder with optimal homotopy asymptotic method, Adv. Math. Phys., (2014) 417643-54.
- [73] Z. Abbas, S. Rasool, M. M. Rashidi, T. Javed, Heat transfer analysis due to an unsteady stretching/shrinking cylinder with partial slip condition and suction, Ain Shams Eng. J., 6 (2015) 939-945.
- [74] N. Najib, N. Bachok, N.M Arifin, Stability of dual solutions in boundary-layer flow and heat transfer over an exponentially shrinking cylinder, Indian J. Sci. Technol., 9 (48) (2016) 97740-5.
- [75] A. Ali, D. N. K. Marwat, S. Asghar, Viscous flow over a stretching (shrinking) and porous cylinder of non-uniform radius, Adv. Mech. Eng., 11(9) (2019) 1-9.
- [76] N. C. Roşca, A. V. Roşca, I. Pop, J. H. Merkin, Nanofluid flow by a permeable stretching/shrinking cylinder, Int. J. Heat Mass Trans., (2019) 1-11.
- [77] I. S. Awaludina, R. Ahmad, A. Ishak, On the stability of the flow over a shrinking cylinder with prescribed surface heat flux, Propul. Power Res., 9(2) (2020) 181-187.
- [78] N. S. Khashi'ie, I. Waini, N. A. Zainal, K. Hamzah, A. R. M. Kasim, Hybrid nanofluid flow past a shrinking cylinder with prescribed surface heat flux, Symmetry, 12 (2020) 1-18.
- [79] T. Fang, Flow over a stretchable disk, Phys. Fluids, 19 (2007) 128051-4.
- [80] S. Hussain, F. Ahmad, M. Shafique, Numerical solution for the flow over a stretchable disk, APJMR, 1 (2013) 51-61.
- [81] A. Mehmood, G. D. Tabassum, M. Usman, A. Dar, Unsteady self-similar flow over an impulsively started shrinking sheet: Flow augmentation with no separation, Int. J. Nonlinear Sci. Numer. Simul., (2020) 1–7.
- [82] G. D. Tabassum, A. Mehmood, M. Usman, A. Dar, Multiple solutions for an unsteady stretching cylinder, J. Appl. Mech. Tech. Phy., 61 (2020) 439-446.
- [83] A. Mehmood, G. D. Tabassum, M. Usman, Existence of multiple solutions for a shrinking surface flow subjected to no wall suction/injection, Eur. J. Mech. B. Fluids, 81 (2020) 124–128.

